BERICHTE
aus dem Fachbereich Geowissenschaften
der Universität Bremen

No. 138

Wenzhöfer, F.

BIOGEOCHEMICAL PROCESSES AT THE SEDIMENT WATER INTERFACE AND QUANTIFICATION OF METABOLICALLY DRIVEN CALCITE DISSOLUTION IN DEEP SEA SEDIMENTS

Berichte, Fachbereich Geowissenschaften, Universität Bremen, No. 138,
103 pages, Bremen 1999

ISSN 0931-0800

The "Berichte aus dem Fachbereich Geowissenschaften" are produced at irregular intervals by the Department of Geosciences, Bremen University.

They serve for the publication of experimental works, Ph.D.-theses and scientific contributions made by members of the department.

Reports can be ordered from:

Gisela Boelen

Sonderforschungsbereich 261

Universität Bremen

Postfach 330 440

D 28334 BREMEN

Phone: (49) 421 218-4124

Fax: (49) 421 218-3116

e-mail: eggerich@uni-bremen.de

Citation:

Wenzhöfer, F.

Biogeochemical processes at the sediment water interface and quantification of metabolically driven calcite dissolution in deep sea sediments.

Berichte, Fachbereich Geowissenschaften, Universität Bremen, No. 138, 103 pages, Bremen, 1999.

ISSN 0931-0800

Biogeochemical processes at the sediment water interface and quantification of metabolically driven calcite dissolution in deep sea sediments

DISSERTATION

zur Erlangung des Doktorgrades der Naturwissenschaften

- Dr. rer. nat. -

im Fachbereich 5

der Universität Bremen

vorgelegt von

Frank Wenzhöfer

Bremen

April 1999

Tag des Kolloquiums: 23. April 1999

Gutachter:

Prof. Dr. Bo B. Jørgensen

Prof. Dr. Horst D. Schulz

Prüfer:

Prof. Dr. H. Willems

Prof. Dr. C. Devey

Preface

This work is submitted as a dissertation and has been supervised by Prof. Dr. Bo B. Jørgensen and Prof. Dr. Horst D. Schulz. The study was conducted as part of the Special Research Project 261 "The South Atlantic in the Late Quaternary: Reconstruction of Material Budget and Current Systems" at the University of Bremen funded by the German Research Foundation. Part of this study was also conducted in the European Union project "Hydrothermal Fluxes and Biological Production in the Aegean Sea (No. MAS3-CT 95-0021).

The thesis consists of seven separate studies in which I was directly involved. Four of these studies are printed as manuscripts (Chap. 2 - 5), while the other three manuscripts are summarized in the Overview of Research. All manuscripts have either been submitted or will be submitted for publication in international journals. The thematic context as well as a general introduction into the study of biogeochemical processes at the sediment water interface is outlined in an introduction chapter. A summary at the end of the thesis presents the main results as well as an outlook of further research topics.

Manuscript No. I (Deep penetrating oxygen profiles measured *in situ* by oxygen optodes) consists of my own investigations. Dr. O. Holby assisted with the lander deployments during the cruise and Dr. O. Kohls was involved in the sensor development. Manuscript No. II (Calcite dissolution driven by benthic mineralization in the deep sea: *In situ* measurements of Ca^{2+}, O_2, pH , pCO_2 is based mainly on my own profiling data. The contribution of the other Co-authors consists of providing chamber lander data and helpful discussions (Dr. S. Boehme) and adding bulk sediment analyses (B. Strotmann). M. Adler together with Dr. C. Hensen developed the model and we discussed the modeling of my profiling data. Manuscript No. III (*In situ* microsensor studies of a hydrothermal vent at Milos, Greece) is based on my data. H. Nielsen and Dr. O. Holby provided the temperature transect data and handled the lander during the deployments. Data from Dr. R. Glud (photosynthesis) were of substantial importance for describing the area. My own contribution to manuscript IV (Carbon oxidation in sediments of Gotland basin, Baltic Sea, measured *in situ* by use of benthic landers) consist of diffusive oxygen measurements, data processing and authorship. Manuscript V (Sulfate reduction in Black Sea sediments, *in situ* and laboratory radiotracer measurements from the shelf to 2000 m) contains my data for calculation of diffusive oxygen fluxes, and I was also involved in the discussion of the data. To manuscript VI (Importance of mussel covered shelf sediments for remineralization processes in the Black Sea: *In situ* measurements with a free

falling benthic chamber lander) my oxygen flux measurements were added to interpret the chamber lander data. Manuscript VII (*In situ* measurements of respiration and metabolism of the deep sea shrimp Heterocarpus grimaldii (Pandalidae) - a case study) contains substantial amount of my data.

Table of contents

Chapter 1

Chapter 2

Deep penetrating oxygen profiles measured *in situ* by oxygen optodes

Chapter 3

Calcite dissolution driven by benthic mineralization in the deep sea: *In situ* measurements of Ca^{2+}, pH, pCO_2, O_2

Chapter 4

In situ microsensor studies of a hydrothermal vent at Milos (Greece)

Chapter 5

Carbon oxidation in sediments of Gotland Basin, Baltic Sea, measured *in situ* by use of benthic landers

Chapter 6

Danksagung

Chapter 1

Introduction

The complex interplay of biological, geological and chemical processes by which materials and energy are exchanged and reused at the Earth's surface are known as biogeochemical cycles. These intermeshed processes operate on timescales of microseconds to eons and occur within a size range from a living cell to the entire land-atmosphere-ocean system (Hedges, 1992; Wollast et al., 1990). To understand these cycles is crucial to protect our natural environment and to ensure a sustainable use of their sources. The first step to resolve the global interactions is to study the single processes and learn how they function.

The oceans cover most of the earth's surface and it is well known that they play a major role in the biogeochemical cycles, and act as a regulator in the global carbonate system (sink or source of atmospheric CO_2) (Fig. 1). Marine sediments play a major role in the oceanic carbon cycle as the main site processes such as remineralization and reoxidation take place (Jørgensen, 1983; Santschi et al., 1990; Canfield, 1993; Rowe et al., 1994; Jahnke, 1996).

Global Carbon Cycle

One of the most important global cycles is the carbon cycle (Berner, 1982, 1989). Carbon is the major energy source for living organisms and also an end metabolite of respiration. As can be seen in Fig. 1 the ocean stores the highest amount of carbon in the deep sea (Berner, 1989; Siegenthaler and Sarmiento, 1993). Across the water atmosphere boundary the ocean carbonate pool is linked to the pCO_2 present in the atmosphere, resulting in a net uptake of pCO_2 by the modern oceans (Sundquist, 1993).

The dissolved carbonate in the photic zone of surface waters is the main source for biological fixation of carbon either as $CaCO_3$ or organic matter. Since most of the organic matter is effectively recycled in the surface waters ("microbial food loop") only very little organic material reaches the seafloor (1 - 10 %; Suess, 1980; Deming and Baross, 1993; Martin et al., 1987). The mechanisms for transport of carbon to the seafloor are either physical transport ("physical carbon pump") as a component of a water mass that is eventually

subducted to the deep sea or transport of biological produced $CaCO_3$ and organic material as biogenic particles/snow ("biological carbon pump") (Fig. 1). At the sediment surface a second high rate of recycling of carbon take places. Remineralization is by far the most common fate of recently biosynthesized carbon and thus is the dominant sink term in the global organic carbon balance. The efficiency of the recycling of organic matter in the oceans is demonstrated by the small fraction (0.2 %) of the marine primary production preserved in marine sediments (Hedges, 1992; Berner, 1989). One of the most striking features of the global carbon cycle is the low rate of organic burial in marine sediments compared with the corresponding fluxes of organic materials into the ocean.

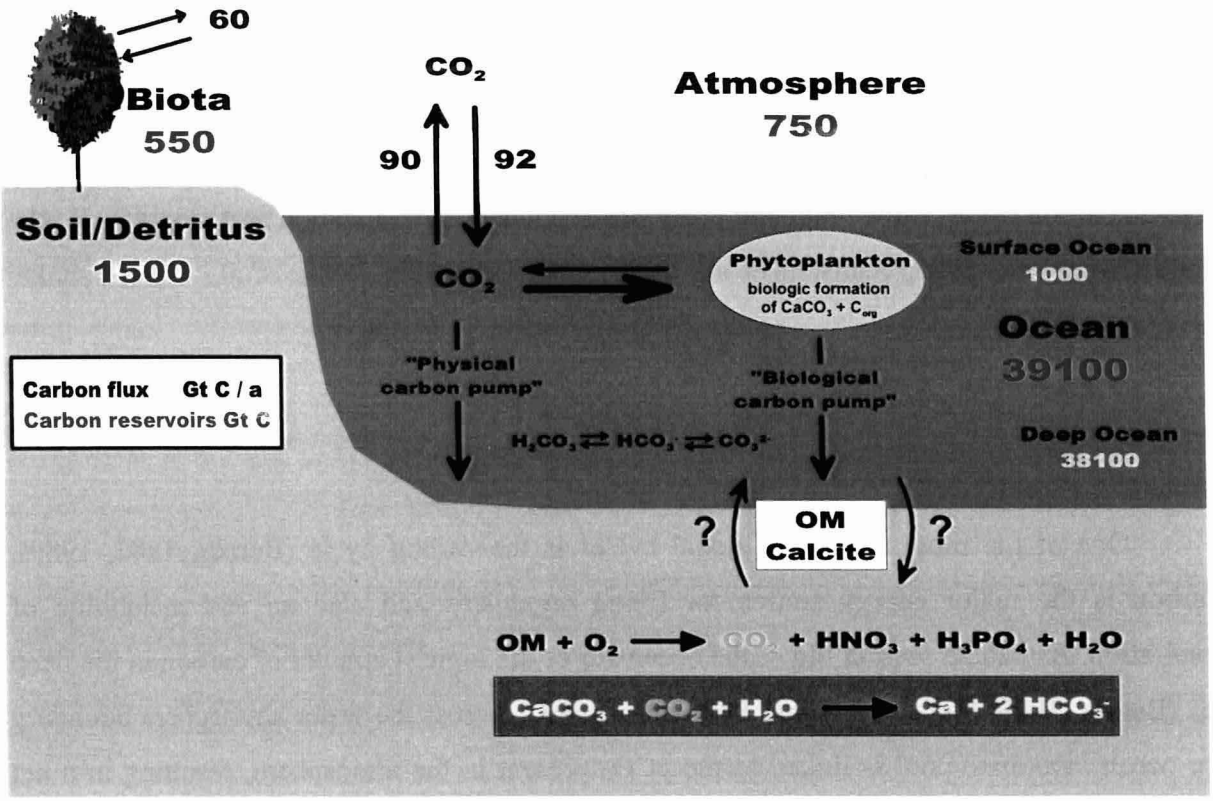

Fig. 1: Illustration of the global carbon cycle. Sources (red numbers) and fluxes (black arrows) show the interaction between the carbon pools. Question marks indicate the need of further investigations of the relevant processes occuring at the sediment water interface; OM = organic matter.

Organic matter mineralization

Upon reaching the seafloor, organic matter is subject to physical and chemical reactions collectively referred to as diagenesis (Berner, 1980). Most diagenetic reactions are driven by redox reactions, which involve the oxidation of organic matter. As a result, suboxic and anoxic conditions are common in marine sediments.

In marine environments organic matter is the most important electron donator, providing the energy needed to drive most of the biologically mediated redox reactions. Particulate organic matter (POM) is composed of a wide variety of materials including excreta, aggregates and living as well as dead tissues. The highest remineralization rates typically occur in the upper water column, resulting in an organic carbon flux decreasing from the surface to the sediment by the factor up to 10,000 (Lee et al., 1998). The second highest rates occur at the sediment water interface, where normally the highest abundance of organisms is located. Following the deposited organic material into the sediment, a sequence of microbially mediated redox reactions can be observed (Froelich et al., 1979). Oxygen is the first electron acceptor in organic matter mineralization yielding the highest free energy. Below this redox zone, bacteria oxidize organic matter in a sequence of reactions using nitrate, manganese, iron, sulfate and carbon dioxide as electron acceptors, respectively, yielding decreasing free energy following this sequence. The relative importance of these diagenetic pathways for organic matter mineralization vary in different settings. Over the whole seafloor, oxygen mediated mineralization is the most important diagenetic pathway, with sulfate reduction the next in importance (e.g. Canflied, 1993). In shelf and estuarine sediments oxygen respiration and sulfate reduction both account for approx. 50 % in organic carbon decay (Jørgensen, 1982). However, in deep sea sediments aerobic respiration accounts for 90 % of the organic carbon oxidation (Bender and Heggie, 1984). The importance of manganese and iron reduction as well as denitrification is still unclear. Their contribution to organic carbon degradation may depend more on regional conditions (Reimers et al., 1992; Thamdrup and Canfield, 1996; Canfield et al., 1993b; Aller, 1990; Devol, 1991).

Marine sediments are also a sink for carbon, because some of the organic carbon reaching the seafloor escapes remineralization and is buried. On the other hand, sediments are a secondary source of CO_2, not only released through respiration but also due to calcite dissolution. Quantifying these processes is one of the major goals in studying the marine carbon cycle as part of the global carbon cycle. Manuscripts I, II and IV of this thesis describe possible methods which may help to answer the question, "which diagenetic pathways are of

importance in shelf and deep sea sediments and how are marine sediments involved in the carbon cycle ?"

Calcite dissolution

Biogenic calcite is one of the major carbon species in the oceanic carbon cycle. Calcite production in the photic zone of surface waters and the dissolution occurring during the transport through the water column are major regulators of the pCO_2 level of the atmosphere. Since marine sediments are the final site where calcite is deposited, identifying and quantifying the factors influencing sedimentary $CaCO_3$ dissolution is crucial to understand the marine $CaCO_3$ cycle, its role in the marine carbon cycle, and controls on atmospheric pCO_2 levels. In particular it is essential to differentiate between: (a) effects of changes in surface water $CaCO_3$ productivity, (b) changes in the preservation/dissolution ratio that are driven by variations in the composition of the particle rain to the seafloor ($C_{org}/CaCO_3$ ratio), and (c) changes in ocean circulation that influence the dissolution/preservation reaction, such as the corrosiveness of the bottom water to $CaCO_3$ (bottom water saturation state) and bottom water dissolved oxygen distribution (Arrhenius, 1988; Boyle, 1988; Curry and Lohmann, 1985; Farrel and Prell, 1989; Lyle et al., 1988; Pedersen et. al., 1988).

The saturation state of the seawater (Ω) with respect to calcite is defined by

$$\Omega = [Ca^{2+}]\,[CO_3^{2-}] / K_{calcite,sp}\ ,$$

and is strongly influenced by pressure as the solubility of biogenic calcite ($K_{calcite,sp}$) increases and the carbonate ion concentration decreases with depth. Seawater is supersaturated ($\Omega > 1$) until depths exceeding 4000 m in the Atlantic Ocean and 1000 m in the Pacific Ocean. Because the carbonate system exhibits this depth dependence, *in situ* studies of the calcite dissolution processes are necessary. The strong effect pressure has on the carbonate system was nicely shown by Archer et al. (1989a), where they measured pH profiles twice in a box corer. First at a depth of 5000 m and than at a water depth of 1500 m. The reduction in pressure changes the solubility product of calcite, leading to a precipitation of calcite, which shifts the pore water pH toward the acidic (Murray et al, 1980; Emerson et al., 1982). Comparing *in situ* pore water pH profiles with laboratory values (Fig. 2) at a station in the equatorial eastern Atlantic at a water depth of 4500 m also exhibited this effect (Wenzhöfer unpublished data).

On a microscopic scale, the dissolution rate of $CaCO_3$ in sediments is determined by the concentration of CO_3^{2-} in the pore water and the concentration of $CaCO_3$ in the solid

phase. Pore water CO_3^{2-} concentration is intimately related to the distributions of the other inorganic carbon species CO_2 and HCO_3^- by the pH equilibrium buffer reactions for carbonic acid. Thus addition of CO_2, produced during organic matter mineralization, decreases the CO_3^{2-} pool and hence lowers the saturation state of the pore water with respect to $CaCO_3$. The production of HCO_3^- by suboxic NO_3^- and MnO_2 reduction will increase the saturation state, as does alkalinity production by sulfate reduction.

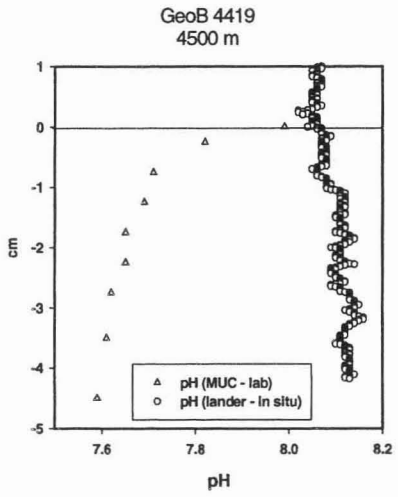

Fig. 2: *In situ* pH microprofile (circles) compared with a laboratory measurement (triangle) at a water depth of 4500 m in the western equatorial Atlantic (GeoB 4419). Sediment recovery caused pore water to shift toward the acidic, resulting from the precipitation of calcite at decreased pressure. (Laboratory pH data supplied by Dr. C. Hensen, Geology Department, University of Bremen).

Due to the difficulties in measuring biogenic calcite dissolution in the oceans, the impact of organic matter remineralization on carbonate dissolution in deep sea sediments was first addressed by modeling the processes (Emerson and Bender, 1981). Recently developed autonomous lander systems now provide the possibility for *in situ* studies. *In situ* microprofile measurements (O_2, pH and pCO_2) as well as most chamber incubation measurements indicated that metabolically CO_2 does drive calcite dissolution (Archer et al., 1989a; Berelson et al., 1994; Hales, 1995; Cai et al., 1995; Hales and Emerson, 1997a; Jahnke et al., 1997). But there are still same uncertainties in the quantitative influence of metabolic driven calcite dissolution, as Jahnke et al. (1994) found that metabolic CO_2 was not always the significant driving force of $CaCO_3$ dissolution in marine sediments. Therefore Jahnke et al. (1997) concluded that the extent of metabolic $CaCO_3$ dissolution may vary regionally.

Most of the *in situ* results as well as the laboratory data were fitted to the empirical rate law:

$$R = k (1- \Omega)^n ,$$

where R is the rate of dissolution, k is the dissolution rate constant and n is the reaction order (Morse, 1978; Keir, 1980). Laboratory dissolution studies showed that the reaction order varied between 2.7 and 4.5 (Walter and Morse, 1985; Keir, 1980), while recently Hales and Emerson (1997b) supported a first-order dissolution kinetics of calcite in seawater. Another factor which influences the dissolution of biogenic calcite in seawater is surface area kinetics. Only a small percentage of the surface area is reactive, resulting in an inhibition of dissolution (Walter and Morse, 1985). Dissolved species such as magnesium, phosphate and organic carbon are also known to inhibit dissolution (Morse and Mackensie, 1990). In manuscript II we show the first *in situ* calcite dissolution rates directly measured with Ca^{2+} microelectrodes, that together with pH and pCO_2 sensors provided the opportunity to define the saturation state of the pore water directly.

Microsensors

Microsensors have been used for several years in studying microbial ecology. They provide measurements of chemical and physical parameters with high spatial resolution (< 50 µm), which makes them a powerful tool for environments where high metabolic rates of dense microbial communities and molecular diffusion cause steep chemical gradients and narrow zones of microbial activity.

In recent years the development of new microsensors has accelerated, leading to a wide variety of available microsensors. The microsensors used for studying interfacial processes in sediments, biofilms, microbial mats, aggregates and other benthic systems can be divided in two groups: **(1) electro-chemical microsensors** and **(2) opto-chemical microsensors.**

The **electro-chemical microsensors** can further be subdivided into two types:

(a) *Potentiometric microelectrodes*, which are based on charge separation of ions across a membrane, generating an electrical potential difference according to the Nernst equation.

(b) *Amperometric microelectrodes*, measuring the current caused by electrochemical reactions of the analyte at the tip of the microelectrode.

Previously another sensing principle was adapted to aquatic biology, based on changes in an optical indicator - **microoptodes**. These sensor are based on the reversible change in the optical properties of an indicator which is immobilized at the fibre tip (Wolfbeis, 1991; Klimant et al., 1995; Holst et al., in press).

A third type of microsensor are **micro-biosensors**. The principle of these microsensors is based on the specific activity of bacteria growing in the tip of the sensor. The bacteria transform the chemical species to be measured and a second species (metabolite or reaction partner) is detected with a microsensor for these latter chemical species, which is placed close to the biosensor tip in the growing bacteria culture.

In Table 1 microsensors used in environmental studies are listed. In the following section only recently developed sensors used in my studies are described. More detailed reviews of microsensors and their application can be found elsewhere (Kühl and Revsbech, 1999; Revsbech and Jørgensen, 1986; Klimant et al., 1997b; Holst et al., in press; and references therein).

H_2S microelectrode

Jerschoweski et al. (1996) and Kühl et al. (1998) introduced a new H_2S microelectrode which is based on the basic design of the Clark-type sensors. Dissolved H_2S diffuses into the microsensor tip, which is filled with an alkaline electrolyte. Behind the membrane, H_2S is deprotonated to HS^-, which reduces ferricyanide to ferrocyanide. At the polarized platinum measuring anode, ferrocyanide is reoxidized which results in a surplus of electrons (Fig. 3).

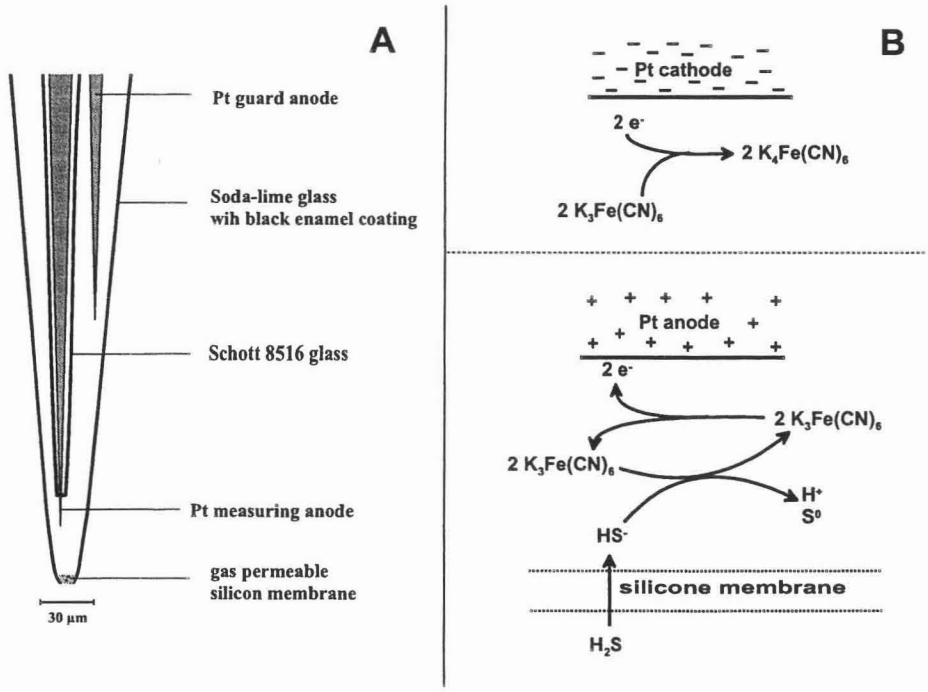

Fig. 3: Schematic drawing of the H_2S microelectrode (from Kühl et al., 1998). (A) Sensor tip design; (B) Chemical reaction at the counter electrode (upper part) and at the measuring electrode (lower part).

Table 1: Microsensors used in biogeochemical studies (modified from Kühl and Revsbech, 1999)

Microsensor type	**Reference**	**Microsensor type**	**Reference**
electrochemical		***electrochemical***	
O_2	Baumgärtl and Lübbers (1973)	Ca^{2+}	Amman et al (1987)
	Revsbech (1989a)		
H_2	Baumgärtl and Lübbers (1973)	S_2^-	Revsbech and Jørgensen (1986)
	Ebert and Brume (1997)		
N_2O	Revsbech et al. (1988)		
H_2S	Jeroscheski et al. (1996)	*Voltametric Sensors*	
	Kühl et al. (1998)		
pCO_2	De Beer et al. (1997a)	O_2, S, Fe^{2+}, Mn^{2+}	Brendel and Luther III (1995)
	Cai and Reimers (1993)		
	Zhao and Cai (1997)		
pH	Thomas (1978); Amman (1986)		
	VanHoudt et al. (1992)		
	DeBeer et al. (1997a)		
NO_3^-	DeBeer and Sweerts (1989)		
NO_2^-	DeBeer et al. (1997b)		
NH_4^+	DeBeer and Van den Heuvel (1988)		

Table 1 (continued)

Microsensor type	Reference	Microsensor type	Reference
microoptodes		**micro-biosensors**	
Temperature	Holst et al. (1997)	Glucose	Cronenberg et al. (1991)
			Van den Heuvel et al. (1992)
oxygen	Klimant et al. (1995)	CH_4	Damgaard and Revsbech (1997)
			Damgaard et al. (1998)
pH	Kohls et al. (1997a)	NO_3^- and NO_2^-	Larsen et al. (1997)
pCO_2	Kohls et al. (1997b)	DOC	Neudörfer and Meyer-Reil (1997)
fiber-optic-microprobes			
surface detection	Klimant et al (1997a)		
diffusivity and flow	DeBeer (1997)		
field radiance	Kühl and Jørgensen (1994)		
irradiance	Lassen and Jørgensen (1994)		

While the microelectrode detects H_2S, the local pH must be known to calculate the total sulfide concentration. These microsensors exhibit a fast response (t_{90} < 0.5 sec) and a linear response to H_2S over a range of 1 to > 1000 µM H_2S, and have a low stirring sensitivity. In contrast to the Ag/Ag_2S microsensor the H_2S microelectrode is insensitive to oxygen.

pCO_2 microoptode/microelectrode

There are two types of pCO_2 microsensors available: microelectrodes (Cai and Reimers, 1993; DeBeer et al., 1997a) and microoptodes (Hales et al., 1997; Kohls et al., 1997b) Both types of CO_2 sensors shown in Fig. 4 and 5 are based on the same chemical principle; CO_2 diffuses into the sensor tip and equilibrates with the electrolyte solution, causing a pH change in the electrolyte/dye solution. The pH change is measured with a pH electrode (CO_2-microelectrode) or as a color change to the pH sensitive dye solution (CO_2-microoptode). To increase the sensitivity and reduce the response time DeBeer et al. (1997a) and Kohls et al. (1997b) added carbonic anhydrase to the electrolyte. These CO_2 sensors have a response time of 30 seconds to 3 minutes (90% of the signal), depending on the CO_2 gradient. The detection limit of the CO_2 microsensors is ~5 µM, based on laboratory studies. These sensors experience interference from H_2S.

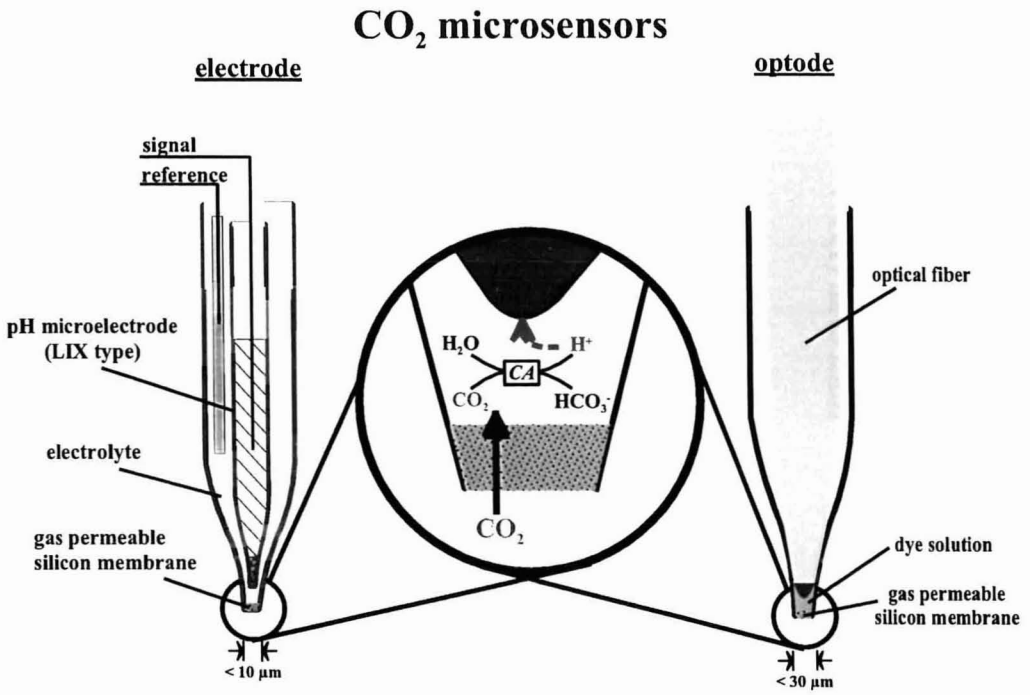

Fig. 4: Schematic drawing of the sensor design; (A) electro-chemical and (B) opto-chemical. The magnification illustrates the chemical reaction of both sensors.

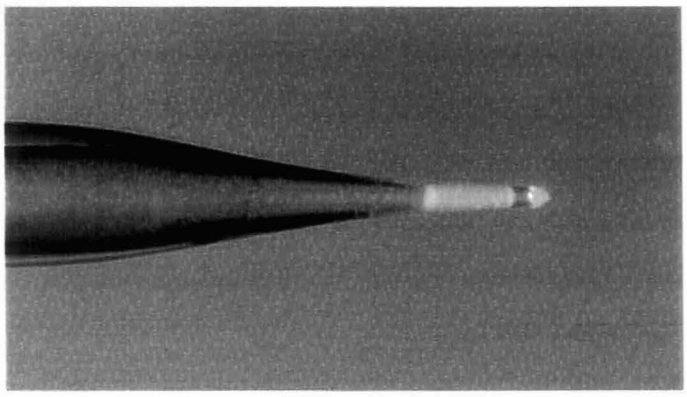

Fig 5: Photo of a pCO_2 microoptode. Sensor tip is illuminated (Photo provided by O. Kohls and G. Holst).

O_2 optodes

The measuring principle is based on the oxygen dependent dynamic luminescence quenching of a indicator dye immobilized on a fiber tip (Fig. 6). Therefore, the oxygen optode exhibits the highest signal at low oxygen concentrations. Two kinds of oxygen dyes can be used: Ruthenium and Porpyrine. These dyes have excitation maxima in the blue and blue/green part of the light spectrum, respectively, and they exhibit orange and red luminescence, respectively. As a light source, a light emitting diode (LED) is used and a photomuliplier detects either the luminescence intensity or the luminescence life-time (Holst et al., in press).

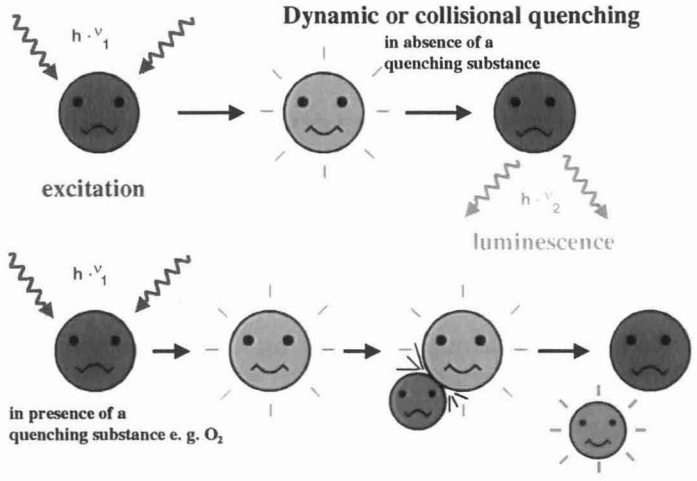

Fig. 6: Illustration of the dynamic quenching of luminescence (Graphic provided by G. Holst)

For lander use only the luminescence intensity based method has been applied (Glud et al., 1999; Wenzhöfer et al., Chapter 2 this thesis). The oxygen concentration can be calculated from an empirical relation based on the Stern-Volmer equation (Stern and Volmer, 1919; Klimant et al., 1995): $I/I_0 = \tau/\tau_0 = (f/1+K_{sv} *c) + (1-f)$, where I_0 is the luminescence intensity in the absence of oxygen, K_{sv} the Stern-Volmer or quenching coefficient, f the fraction of the indicator that is quenchable and c the oxygen concentration. The same equation is also valid for life-time measurements, only the luminescence intensity is replaced by the respective life-time parameter τ and τ_0.

The design of an oxygen optode for deep penetration measurements is shown in Chapter 2. The design of oxygen microoptodes is similar to the deep penetrating optodes, only the dye is immobilized on a tapered fiber, resulting in tip diameter of approx. 30 µm (Fig. 7).

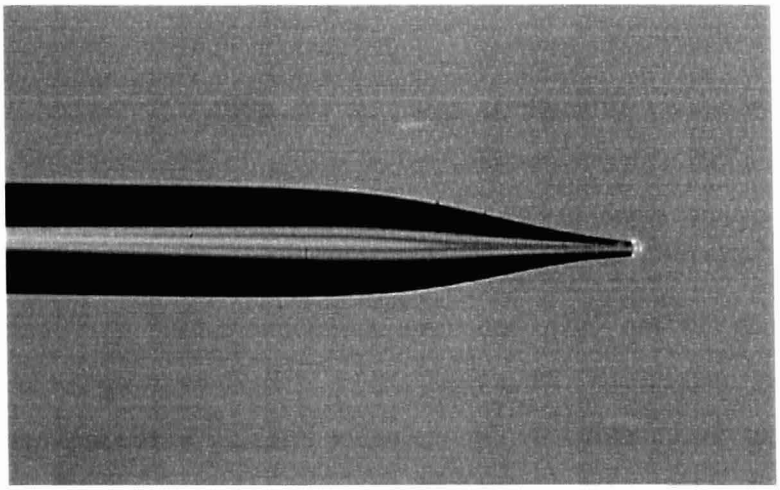

Fig. 7: Photo of a microoptode (provided by O. Kohls and G. Holst)

The opto-chemical technique has also been developed for two-dimensional mapping of oxygen distribution (Glud et al. 1996). This method can resolve the spatial heterogeneity that often occurs across benthic interfaces, e.g. at the sediment water interface. The measurement is based on the same principle as mircooptodes, but the dye is immobilized on transparent support foils. Using a digital camera and an imaging technique two dimensional oxygen dynamics can be measured (Fig. 8).

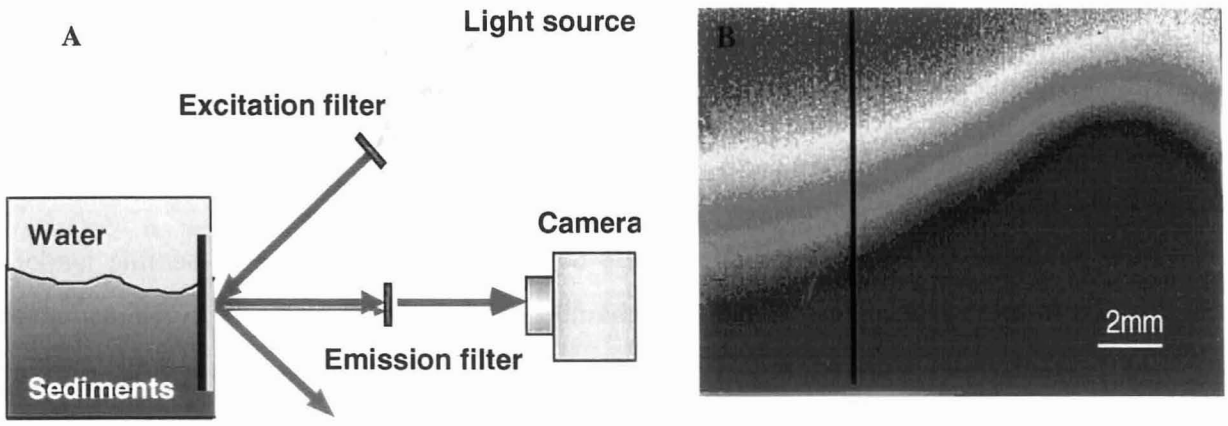

Fig. 8: (A) Schematic drawing of the experimental setup. (B) An oxygen image from a marine sediment; red equals 30 % air saturation and lilac 0 % air saturation (from Glud et al., 1996).

Lander

A fundamental understanding of biogeochemical processes in sediments requires a quantitative and qualitative assessment of rates of benthic processes. *In situ* high-resolution measurements of pore water concentration profiles of solutes have provided an effective means to quantify the diffusive flux across the sediment water interface. This information can be used to estimate the rates of metabolic and chemical reactions in sediments and provide important insights into the balance of processes that control sediment biogeochemistry. While laboratory measurements require recovery and disturbance of the sediment, profiling *in situ* leaves the sediments in place and thereby the natural gradients of metabolites and substrates intact. Because of these attributes, *in situ* profiling has become very important for studying benthic mineralization and microsensors have been used to assess O_2-concentration gradients and pH-profiles across the sediment water interface.

Since the first deep sea microprofiles were measured by Reimers et al. (1986) using oxygen electrodes, the *in situ* field has grown rapidly. Several landers using O_2 electrodes to measure oxygen dynamics of marine sediments have been developed (Reimers, 1987; Hales et al., 1994; Hales and Emerson, 1996). Archer et al. (1989a) adapted pH microelectrodes to lander systems and Gundersen et al. (1992) used a Ag/Ag_2S-sulfide-electrode for measuring profiles through a *Beggiatoa* mat in the hydrothermal area of Guayamas Basin, Gulf of California. In previous investigations on the marine carbon cycle, the use of pH and pCO_2 sensors on profiling landers resulted in the first *in situ* estimates of rates of organic matter

decay and mineral dissolution (Cai et al., 1995; Hales and Emerson, 1997a). Recently, several new microsensors have been developed for studying biogeochemical processes (for an overview see Table 1) and some of these have been adapted for lander use (Manuscript I, II, III).

At the same time profiling landers were developed, a second type of benthic lander was applied to marine deep sea science; the chamber lander (Smith et at., 1976; Berelson et al., 1987; Jahnke and Christiansen, 1989). The chamber lander encloses an area of the seafloor and measures fluxes of solutes from the overlying water into the sediment and from the sediment into the overlying water. The changes in concentrations are either measured by electrodes (oxygen) or by taking water samples during the incubation period. An overview of profiling and chamber landers used in marine science is given by Tengberg et al. (1995).

Recently, Greeff at al. (1998) developed a third type of benthic lander for radio tracer studies. This lander is used to quantify the amount of organic matter mineralized by sulfate reduction near the sediment surface. Labeled sulfate ($^{35}SO_4^{2-}$) is injected into sediment cores which have been driven into the sediment. After lander recovery the incubated cores are sectioned and the turnover rate of the radiolabelled SO_4^{2-} is measured to determine a sulfate reduction rate (SRR).

The next generation of deep sea instruments is the autonomous unmanned vehicle called Rover from Smith et al. (1997). The vehicle is built to conduct long time-series studies of benthic oxygen fluxes in the deep sea. The Rover is deployed as a free vehicle, and is able to crawl across the seafloor. At each sampling site chamber incubations as well as microprofiles can be performed.

In this thesis, the application and use of four recently developed techniques and sensors on our profiling lander system is shown. The autonomous profiling lander used in the studies was a modified version of the lander "Profilur" used by Gundersen and Jørgensen (1990) and Glud et al. (1994). I modified the lander for use as a modular-system. The modular-system allows measurements with different techniques either simultaneously or separately, such as new sensors (Manuscript I: oxygen optodes; Manuscript II: CO_2-microoptode, Ca^{2+}-microelectrode) or gel-peeper technique for *in situ* high resolution pore water studies (Holby, Fones and Wenzhöfer not published). The application and use of the newly developed H_2S-microelectrode on a miniaturized lander system is shown in Manuscript III.

Main goals

The oceans, with their high content of reactive carbon play a major role in the global carbon cycle. Within the ocean carbon cycle, the sediments are the place where carbon can be permanently buried and therefore taken out of the cycle for many years. However, to understand the global interactions of the single components, the processes of these components have to be studied and known. In this thesis the study of biogeochemical processes at the sediment water interface were the main object.

Many studies of the oxygen and carbon dynamics in coastal areas have been performed, however very little is known about these dynamics in the deep sea sediments. There are two major facts which makes the studies of oxygen uptake rates in deep sea sediments complicated. First, recovery of sediment cores alters the pore water oxygen concentration and therefore result in an overestimation of oxygen mediated organic matter mineralization (Glud et al., 1994). This fact implicates the need for *in situ* devices, for example autonomous lander systems (Reimers, 1987; Smith et al., 1976; Tengberg et al., 1995). Second, in deep sea sediments oxygen penetration depths often reach several decimetres or metres which is not measurable with oxygen microelectrodes. To study the mineralization in those deep sea sediments we developed a new deep penetration oxygen sensor for measuring deep oxygen dynamics *in situ*.

Another major process which regulates the amount of buried carbon is the dissolution/precipitation of calcite in marine sediments. Model estimations showed that metabolically mediated CO_2 production is a major process driving calcite dissolution. The carbonate system is also highly influenced by pressure and therefore the use of *in situ* systems is necessary. Recent studies with profiling and chamber landers indirectly measured the rate of calcite dissolution using O_2, pH and pCO_2 microelectrode measurements or flux chamber measurements of dissolved inorganic carbon, alkalinity and Ca^{2+}. We used O_2 and pH microelectrodes together with new developed pCO_2 - microoptodes and Ca^{2+} - microelectrodes to study the sediment carbonate system directly.

There are a number of studies that have investigated the importance of the different diagenetic pathways in marine sediments, however only a few *in situ* data are available. Deploying three benthic lander systems at the same sites gave us the opportunity to measure the importance of the single carbon degradation pathways *in situ*. The results distinguish between the importance of different pathways within the sediment and to determine the relative amount of each process to the total carbon mineralization.

Beyond the deep ocean which has a major impact in the global biogeochemical cycles there exist several small special systems which also have to be taken into account in resolving the processes controlling the global cycles. One such environment are hydrothermal vent systems. With the use of manned submersibles, a number of investigations have been performed to study the deep hydrothermal vent systems but less is known about shallow hydrothermal vents. Using *in situ* microsensors we studied the circulation of a shallow hydrothermal vent system and the impact of enhanced CO_2 released by the seep fluid on the surrounding environment.

Overview of Research

As part of my Ph.D. studies I was involved in several cruises, measuring *in situ* profiles across the sediment water interface to study biogeochemical processes. Since not all of these studies are in my thesis a short overview of the individual studies is given below.

I

Wenzhöfer F, Kohls O and Holby O

Deep penetrating oxygen profiles measured *in situ* by oxygen optodes

The first *in situ* deep penetration oxygen profiles from oligotrophic sediments are presented. Deep penetrating O_2 optodes (working range: 55 cm) in combination with microsensors (microelectrodes or microoptodes) provide an excellent tool for the study of the oxygen dynamics in deep sea sediments. The oxygen penetration depth, in conjunction with O_2 microprofiles provides a way to evaluate the rate of carbon mineralization within the sediment. Also the reoxidation of reduced species can be investigated. Due to the strong effect sediment recovery has on pore water chemistry (oxygen penetration depth decreases up to 50 %) quantification of benthic carbon mineralization has to be determined from *in situ* measurements.

II

Wenzhöfer F, Adler M, Kohls O, Hensen C, Strotmann B, Boehme S, Schulz HD

Calcite dissolution driven by benthic mineralization in the deep sea : *In situ* measurements of Ca^{2+}, pH, pCO_2, O_2

We present the first ever *in situ* Ca^{2+} microprofiles. These profiles were used to quantify the flux across the sediment water interface from the Ca^{2+} gradient. This is an important improvement from early studies that estimated calcite dissolution indirectly from O_2, pH and pCO_2 profiles or from fluxes of dissolved inorganic carbon, alkalinity and Ca^{2+} measured with a chamber lander. Our combination of pH, pCO_2, Ca^{2+} and O_2 microprofiles means we can define the pore water carbonate system directly. First measurements in the

eastern South Atlantic exhibited fluxes of 0.6 mmol m^{-2} d^{-1} for sediments with a low calcite content.

Modeling our profiles result in a calcite dissolution rate constant of 7000 mol kgw^{-1} a^{-1} which equals a rate of 663 % d^{-1}. This value is higher than most of the reported *in situ* estimated dissolution rates (0.01 - 125 % d^{-1}), but it is in the range of laboratory determined numbers (1000 - 3000 % d^{-1}).

III

Wenzhöfer F, Holby O, Glud RN, Nielsen H and Gundersen JK

***In situ* microsensor studies of a hydrothermal vent at Milos (Greece)**

Hydrothermal vent systems create characteristic concentric circles of yellow (sulfur), white (silicate with drops of sulfur) and brown (manganese) precipitates around a seep outlet. Microprofiles of O_2, pH, H_2S and temperature measured *in situ* and in the laboratory from the different vent areas resolved a microcirculative pattern. This circulation induced a downward transport of oxygenated water, creating small convective cells which efficiently reoxidise upwardly diffusing H_2S.

Laboratory incubations and microsensor profiling indicated that photosynthesis was not carbon limited and consequently the excess DIC released by the vent system presumably had no effect on the benthic primary production. However, benthic net primary production is compared with macrophyte and pelagic primary production, which is of major importance at this oligotrophic setting.

IV

Greeff O, **Wenzhöfer F**, Riess W, Weber A, Holby O and Glud RN

Carbon oxidation in sediments of Gotland Basin, Baltic Sea, measured *in situ* by use of benthic landers

Benthic mineralization processes were measured *in situ* with three different lander systems for the first time. A transect from shallow oxygenated bottom water conditions to deeper oxygen depleted conditions indicated a shift in the importance of the different mineralization processes. Only at the shallowest station was organic matter decay with

oxygen of importance. At the remaining oxygenated stations, oxygen uptake was almost exclusively used to reoxidise sulfide. It was shown that sulfate reduction was the major carbon mineralization process.

V

Weber A, Riess W, **Wenzhöfer F** and Jørgensen BB

Sulfate reduction in Black Sea sediments, *in situ* and laboratory radiotracer measurements from the shelf to 2000 m

In situ sulfate reduction rates (SRR) were measured on a transect from the oxygenated shelf to the deep anoxic basin of the Black Sea, to determine the importance of sulfate reduction at these sites. Measurements of the different mineralization pathways were performed using three benthic landers (radiotracer, chamber and profiling lander). On the shelf the predominant mineralization process is oxygen respiration. The importance of sulfate reduction, increases gradually from the well oxygenated sites to the transition zone (5 - 50 %). SRR were in the range of 0.2 to 2 mmol m^{-2} d^{-1}. The measurements indicate, that the mineralization of organic matter is limited by bottom water oxygen concentration and quality of settling organic material.

VI

Riess W, Luth U and **Wenzhöfer F**

Importance of mussel covered shelf sediments for remineralization processes in the Black Sea: *In situ* measurements with a free falling benthic chamber lander

Large areas of the Romanian shelf in the Black Sea are covered with benthic macrofauna. The impact of this community on organic matter remineralization and oxygen uptake was studied using three benthic lander systems on a transect from the oxygenated shelf to the anoxic deep basin of the Black Sea. The study indicated that the macrofaunal biomass decreased with water depth, while the meiofauna biomass was low except at the station at the oxic-anoxic transition. The contribution of the macrofaunal community to the total remineralization of organic matter was in the range of 45 to 70 % compared to mineralization with oxygen, manganese, iron and sulfate. The benthic community covering the sediment surface acts as an efficient barrier keeping carbon from reaching the underlying sediment.

VII

Riess W, **Wenzhöfer F** and Dittert L

***In situ* measurements of respiration and metabolism of the deep sea shrimp *Heterocarpus grimaldii* (Pandalidae) – a case study**

The impact of migrating macrofauna on the carbon flux to the deep sea sediment surface was investigated using two benthic lander systems. The respiration of four deep sea shrimps (*Heterocarpus grimaldii*) captured with a benthic chamber lander was 0.05 µmol O_2 mg wet wt^{-1} d^{-1}. The study indicated that organic matter was transported by the macrofauna from the water column to the sediment surface, enhancing the amount of settling organic matter. The enhanced organic carbon content of the surface sediment influences the biogeochemical processes responsible for organic matter decay.

Chapter 2

Deep penetrating oxygen profiles measured *in situ* by oxygen optodes

Frank Wenzhöfer, Ola Holby [1], Oliver Kohls

Max Planck Institute for Marine Microbiology, Celsiusstr. 1, D-28359 Bremen, Germany

[1] present address: Högskolan Dalarna, Rödavägen 3, 781 88 Borlänge, Sweden

Abstract

For the first time *in situ* deep penetration oxygen profiles were measured in abyssal sediments in the western South Atlantic. Construction and adaptation of deep penetrating O_2 optodes to a benthic profiling lander are described. Opto-chemical oxygen sensors were used to measure oxygen concentrations to a depth of 55 cm in marine sediments. With a vertical resolution of 0.5 cm the oxygen dynamics in oligotrophic sediments can be described adequately, while the oxygen concentration across the sediment water interface needs a resolution of 100 µm.

Oxygen penetration depth (OPD), diffusive oxygen uptake (DOU) and oxygen consumption rates were determined at 4 stations north of the Amazon fan and one at the Mid-Atlantic Ridge. Diffusive oxygen uptake rates ranged from 0.1 to 0.9 mmol m^{-2} d^{-1}. Carbon consumption rates calculated from the diffusive oxygen uptake rates were in the range of 0.3 and 3.0 g C m^{-2} a^{-1}. Comparison between *in situ* and laboratory DOU and OPD measurements confirmed previous findings that core recovery have strong effects on the oxygen dynamics in deep sea sediments. Laboratory measurements yielded a decrease of 50 to 75 % in OPD and consequently an increase in DOU by 1.5- and 18-times. Deep penetration oxygen optodes provide a new tool to accurately determine oxygen dynamics (and thereby calculate carbon mineralization rates) in oligotrophic sediments.

Introduction

The oceans cover approx. 71 % of the earth, of which approx. 55 % have water depths grater than 3500 m. In those deep-sea sediments oxygen is the dominant electron acceptor for organic carbon mineralization and aerobic respiration accounts for more than 90 % of the carbon oxidation in oligotrophic deep-sea sediments (Murray and Grundmanis, 1980; Bender and Heggie, 1984; Jahnke and Jackson, 1992). The penetration of oxygen in sediments is controlled by a number of processes including advection, bioturbation, degradation of organic material and the reoxidation of reduced substances (e.g. NH^{4+}, Fe^{2+}, Mn^{2+}, HS^{-}). In oligotrophic deep sea sediments, oxygen consumption is predominantly controlled by the amount of organic material reaching the seafloor. Remineralization in shallow marine sediments accounts for approx. 10 % of the organic matter exported from the photic surface waters, while in deep sea sediments the share can rise up to 45 % (e.g. De Baar and Suess, 1993; Jahnke, 1996). In oligotrophic waters, where the organic matter is efficiently decomposed during descent in the water column, less than 0.1 % of the primary production is permanently buried in the sediment (Berger, 1989). The oxygen penetration in such sediments often reaches several decimetres or even meters (Murray and Grundmanis, 1980; Rutgers van der Loeff, 1990).

Oxygen glass electrodes have been an excellent tool for studies of the oxygen dynamics in marine sediments (Reimers et al., 1986; Revsbech and Jørgensen, 1986; Revsbech, 1989a; Glud et al., 1994). However, the profiling length of glass electrodes is limited, and for *in situ* measurements, the maximum working depth is 10 to 15 cm.

A common indirect method to define the base of the oxic zone in marine sediments is to determine the Mn^{2+} profile in pore waters. The zone were Mn^{2+} is depleted is considered to be equal to the oxygen penetration depth (Froelich et al., 1979; Sayles and Livingston, 1987; Cai and Sayles, 1996). There are still some uncertainties in the exact penetration depth of oxygen in such sediments, and until this study, deep O_2 penetration profiles have not been measured *in situ*.

Recently Klimant et al. (1995) adapted the optode technique for measuring oxygen concentration in aquatic biological systems. The optode technique is based on dynamic quenching of a luminophor by O_2 which is immobilised on a fiber cable (Klimant et al., 1995; Klimant et al., 1997b). Glud et al. (1999) showed that microoptodes are an alternative to electrodes for use on benthic lander systems. Oxygen optodes are easier to manufacture, and

they do not consume oxygen and therefore are insensitive to stirring. For benthic lander use, they also have better long-term stability.

To determine *in situ* O_2 penetration occurring at depths greater than those accessible by glass electrodes, a new deep penetration O_2 optode for benthic profiling lander use was developed. We describe here the construction of deep penetrating oxygen optodes, their first *in situ* application in the South Atlantic and discuss the results in relation to depth resolution and benthic mineralization.

Materials and Methods

Study area

This study was performed during a cruise in March/April 1997 aboard the R/V Meteor in the South Atlantic. *In situ* lander deployments were made at 4 stations north of the Amazon fan at water depths between 3511 m and 4487 m (Table 1 and Fig. 1). A fifth deployment was performed at the mid Atlantic ridge at a water depth of 3185 m. The bottom water characteristics and the organic carbon content of the surface sediment are summarised in Table 1.

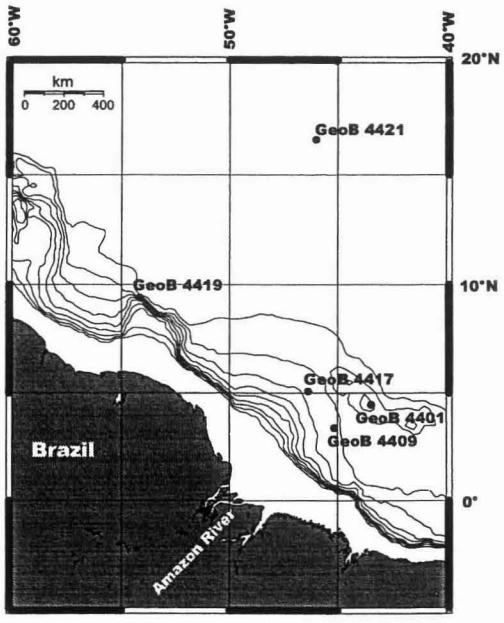

Fig. 1: Map of the western South Atlantic showing the station locations.

Table 1: Geographical positions and water depths of the investigated stations. Bottom water (BW) oxygen concentration and temperature (T) and surface sediment organic carbon content (Corg) for all 5 stations.

station	position		depth [m]	T [°C]	BW oxygen [µM]	C_{org} [1] [%]
4401	**04 45.706 N**	**43 45.861 W**	**3353**	**2.8**	**263**	**0.39**
4409	**03 38.459 N**	**45 14.466 W**	**3849**	**2.6**	**273**	**0.42**
4417	**05 08.246 N**	**46 34.533 W**	**3511**	**2.8**	**278**	**0.64**
4419	**09 40.209 N**	**54 15.454 W**	**4487**	**2.5**	**265**	**0.78**
4421	**16 59.379 N**	**46 00.918 W**	**3185**	**3**	**257**	**0.31**

[1] data supplied by Dr. C. Hensen Geology Dept., University of Bremen

In situ measurements

An autonomous profiling lander (Fig 2A) was used to measure the oxygen dynamics and oxygen penetration depth in deep sea sediments (Reimers et al., 1986; Gundersen and Jørgensen, 1990). During this cruise a modified version of the profiling lander described by Glud et al. (1994) was used. Our profiling lander was equipped with two measuring systems (Fig. 2). Electro-chemical measurements were performed with a modified electronic system used by Glud et al. (1994). The electro-chemical electronic unit controls the glass electrode measurements, the bottom water sampling and lander release mechanism. The opto-chemical electronics is separated from the electro-chemical electronics in a separate pressure housing, and is comparable to the system described by Glud et al. (1999). The separation allows independent use of the two systems.

Lander-Optode-System

To measure deep sediment oxygen profiles a new elevator system (Fig. 2B) for driving the sensors into the sediment was designed. This system consists of a platform which carries 4 oxygen optodes, driven by a step controlled motor. The optoelectronics are a modified version of the electronic system described by Glud et al. (1999). The oxygen optode sensors are constructed by placing the fiber cable in a stainless steel tube (length: 95 cm and diameter: 6 mm), with a 1 mm diameter needle used as sensor tip (Fig. 2C). During this cruise the complete profiling length was set to 55 cm with a step resolution of 0.5 cm.

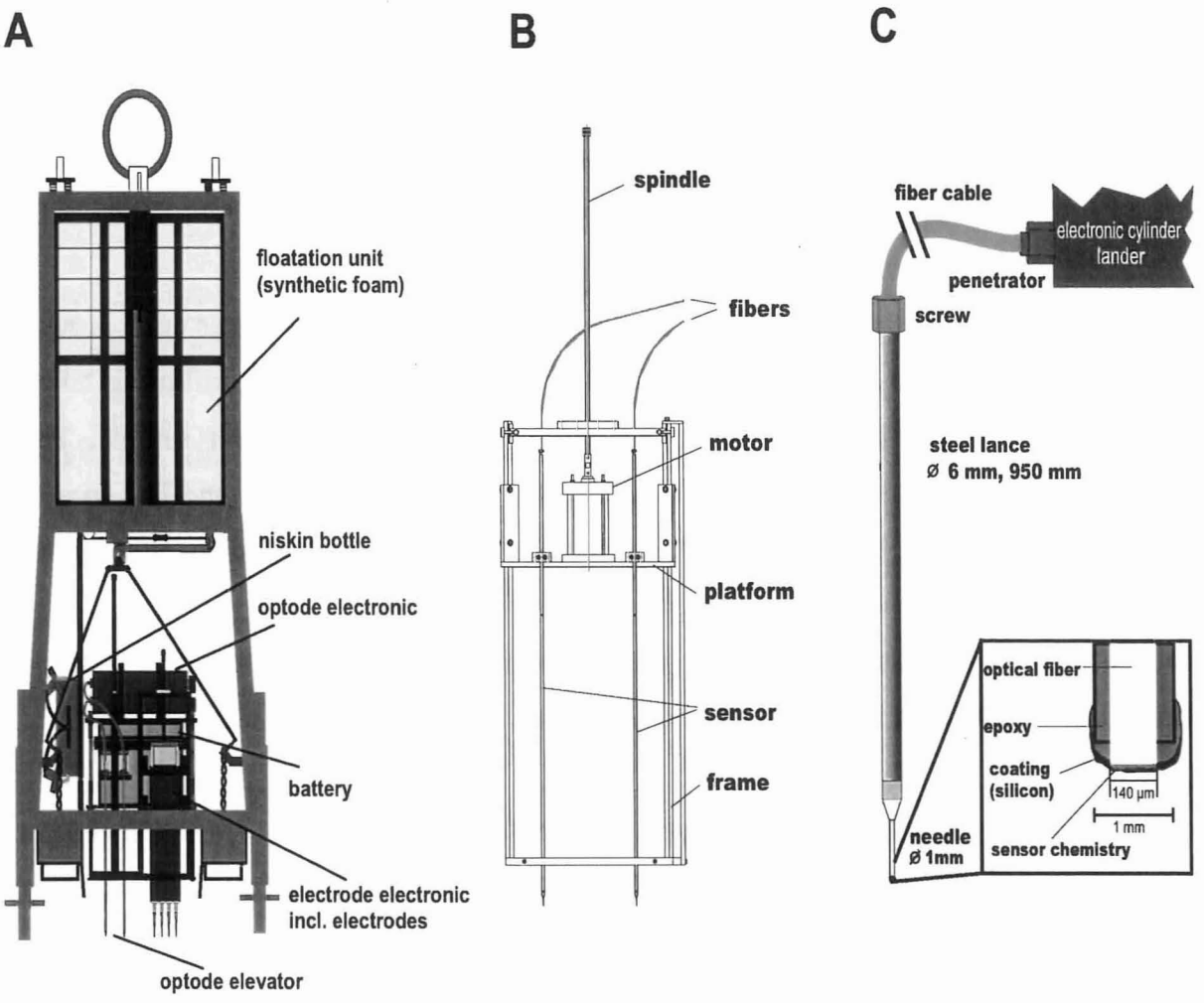

Fig. 2: Schematic drawing of: (A) the profiling lander system, (B) optode elevator system with oxygen optodes and (C) deep optode sensor and a magnification of the sensor tip with the sensor chemistry.

The oxygen optodes are constructed from multimode silica-silica step index fibers with 100 µm core diameter and 140 µm cladding diameter (RADIALL Fiber-Optik, Rödermark). The design of the sensor tip is shown in Fig. 2C. The fiber is glued in the injection needle so that only a short part (approx. 1 mm) of the fiber extends out of the needle. The oxygen sensitive dye, a ruthenium-diphenylphenanthroline perchlorate complex in polystyrene (5 mM), is immobilised on the fiber tip. To avoid artefacts from reflection of sediment particles, the sensor tip is coated with black silicone. Because of the coating and the sensor size (140 µm) the response time increases (longer diffusion distances) and therefore the complete measuring time was set to 3 min at each step interval. Two optode fibers were

connected to one detector (Photomultipliere, PMT) by an optical switch, leading to alternate readings of the sensors. After a delay of 40 sec, the sensor signal was recorded 10 times from one sensor and then 10 times from the second sensor. This routine was repeated 3 times, so that a data set of 3 sets of 10 signals for each sensor were recorded. The first two signal records of each set of 10 were deleted (due to a time delay of the optical switch; Glud et al., 1999) and the remaining readings were averaged for each depth.

The calibration of the optode signal versus the oxygen concentration was done *in situ*, using a 2 point calibration. The constant reading in the bottom water before profiling is taken as bottom water concentration, determined by Winkler titration of a water sample. The constant reading in the anoxic part of the sediment is taken as zero oxygen. The *in situ* calibration was checked by an onboard calibration at *in situ* water temperature after compensation for pressure and PMT temperature (Glud et al., 1999).

To calculate the oxygen concentration from the recorded signal, an empirical relation based on the Stern-Volmer equation is used (Stern and Volmer, 1919; Klimant et al., 1995):

$$I_0/I_C = [(0.85/(K_{SV}\ C) + 1) + 0.15]^{-1}$$

Where I_0 and I_C are the luminescent intensities in the absence and presence of O_2 at an oxygen concentration C, respectively. The quenching constant, K_{SV} quantifies the quenching efficiency.

Lander-Electrode-System

In situ microelectrode measurements were also made in the upper 10 cm of the sediment using a profiling unit described by Glud et al. (1994) and Gundersen and Jørgensen (1991). The system was equipped with 4 oxygen electrodes, which were lowered in vertical steps of 100 µm into the sediment. At all stations where electrode measurements were performed, 2-3 successful profiles were obtained. The oxygen microelectrodes were of Clark type with an internal reference (Revsbech, 1989). The tip diameter of the electrodes was 5 – 20 µm, with a stirring sensitivity < 1% and a 90 % response time < 2 sec. The sensors were calibrated using the *in situ* bottom water oxygen concentration and the zero value recorded onboard at *in situ* temperature. All sensors (opto-chemical and electro-chemical) were checked for signal drift by comparing the reading in the bottom water before and after the profiling. Photographs of the sensors during profiling into the sediment were taken every 20 min. with a camera system (PHOTOSEA MODEL 1000A) mounted on the lander (Fig. 3).

Fig. 3: Photograph of the sediment surface at GeoB 4419. Oxygen optodes can be seen in the front, while the microelectrodes penetrating across the sediment surface can be observed in the back.

Laboratory measurements

Oxygen profiles were also measured shipboard on sediment cores recovered by a multiple corer (Barnett et al., 1984). The sediment surface appeared undisturbed, and the overlying water was clear, but during recovering the temperature in the overlying water increased up to 17°C. Directly after recovery the cores were incubated at *in situ* temperature and oxygen concentration. The overlying water was gently stirred to create a DBL similar to *in situ* conditions (Rasmussen and Jørgensen, 1992). Oxygen microprofiles were measured with microelectrodes mounted on a motor-driven micromanipulator controlled by a computer (Revsbech and Jørgensen, 1986). The oxygen microelectrodes were of the same type as the microelectrodes used for *in situ* measurements.

Calculations

The thickness of the diffusive boundary layer (DBL) was determined directly from the measured microprofiles. The transition between the homogeneous oxygen concentration in the turbulent bottom water and the linear gradient in the DBL was used as the upper DBL boundary (Jørgensen and Revsbech, 1985). The lower DBL boundary was determined from

the change in slope of the oxygen concentration gradient across the sediment water interface due to the impeded diffusion in the sediment relative to that in the water (Sweerts et al., 1989). To calculate the diffusive oxygen uptake (DOU) of the sediment, Fick´s first law was used: DOU = D_0 dC/dz, where D_0 is the molecular diffusion coefficient in water at *in situ* salinity and temperature (corrected from Li and Gregory, 1974 and Broecker and Peng, 1974) and dC/dz is the linear oxygen concentration gradient in the DBL. At station GeoB 4421 only optode measurements with a step resolution of 0.5 cm were performed. Therefore the DBL could not be determined and the oxygen flux was calculated from the O_2 gradient just below the sediment surface using Fick´s first law as well as the empirical relations for the sediment diffusion coefficient: DOU = Ø D_S dC/dz and Ds = D_0 Ø $^{m-1}$, where Ø is the porosity, D_S the sediment diffusion coefficient and m = 3 (Berner, 1980; Ullmann and Aller, 1982). Oxygen consumption rates were modelled using constant porosity in the oxic zone and a zero order kinetics for the oxygen consumption (Nielsen et al., 1990). The oxygen penetration depths from station GeoB 4401 and 4409 were modelled using the two layered oxic zone model from (Epping and Helder, 1997). The model uses two discrete consumption rates in each sublayer to fit to the measured oxygen profiles. The amount of degraded organic carbon was calculated from the diffusive oxygen uptake assuming steady state and a C:O ratio of 0.77 (Froelich et al., 1979; Berner, 1980).

Results

Oxygen dynamics at GeoB 4419 were measured simultaneously with optodes and electrodes (Fig. 3). Both methods exhibited a similar decrease in oxygen concentration, while the anoxic sediment horizon was only reached by optodes (Fig. 4A). The penetration depth of oxygen measured with the deep penetrating optodes was 11 cm.

An enlarged sequence of the oxygen profile illustrates the linear oxygen decrease in the DBL, which is used to calculate the diffusive oxygen uptake, and a change in slope of the O_2 gradient at the sediment water interface is apparent (Fig. 4B). Due to the low resolution (0.5 cm) for optode measurement, only one signal record of each optode just below the sediment surface was recorded (Fig. 4B). The estimated thickness of the DBL at GeoB 4419 was 600 µm. The average DBL of the other stations varied between 600 and 950 µm (Tab. 2).

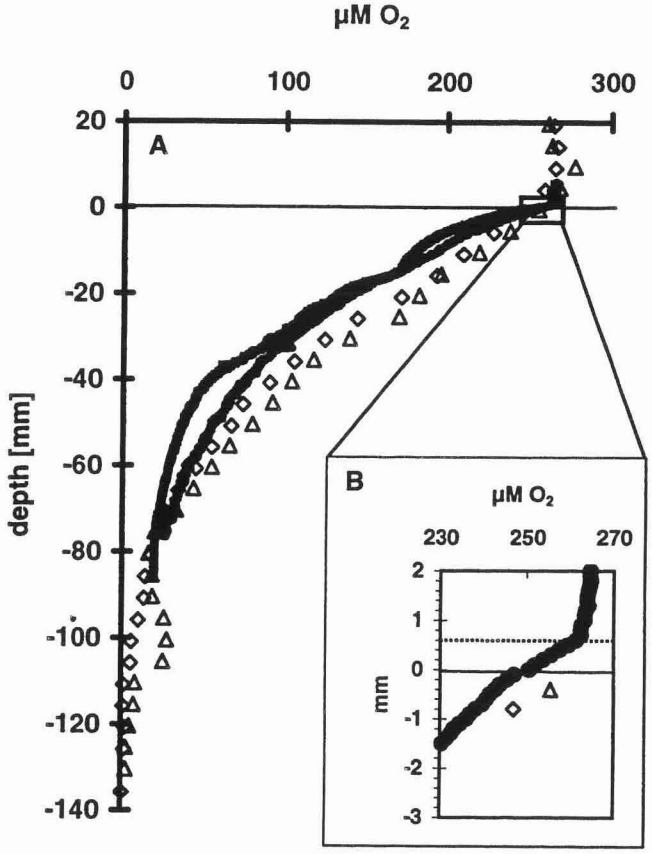

Fig. 4: Comparison of high resolution oxygen electrode (closed symbols) and low resolution oxygen optode (open symbols) profiles measured at GeoB 4419 in 4487 m water depth. Magnification shows the DBL at the sediment water interface.

Oxygen profiles from the 5 stations in the Equatorial South Atlantic are shown in Fig. 6. Oxygen penetration depth ranged from 11 to 26 cm at GeoB 4417, 4419 and 4421 (Tab. 2). At station GeoB 4401 and 4409 where only microelectrode measurements were obtained, the sensors did not penetrate into the anoxic zone and consequently the oxygen penetration depth could only be modelled (8 and 9 cm (± 1 cm) respectively; Tab. 2). Diffusive oxygen uptake rates (DOU), calculated from the linear gradient in the DBL of the oxygen profiles ranged from 0.1 and 0.9 mmol m^{-2} d^{-1} (Tab. 2).

Oxygen consumption rates from station GeoB 4417 and 4419 indicated high activities at the sediment surface (Fig. 7). At GeoB 4419 the oxygen profile exhibited a consumption rate of 4.4 nmol cm^{-3} d^{-1} over the first 7 cm, resulting in a decrease of organic carbon from 0.8 to 0.5 % over the upper centimetre of the sediment (Fig. 5). While at GeoB 4417 the oxygen consumption rate was constant with depth resulting in a decrease in organic carbon of approx. 0.2 %(ww) (Fig. 5 and 7).

Table 2: Oxygen penetration depths (OPD), diffusive boundary layer thickness (DBL), diffusive oxygen uptake (DOU) and organic carbon consumption rates (CCR) measured *in situ* and shipboard. Values in parentheses indicate the numbers of profiles used for each determination.

station	in situ				laboratory		
	OPD [cm]	DBL [µm]	DOU [mmol m^{-2} d^{-1}]	CCR [g C m^{-2} a^{-1}]	OPD [cm]	DBL [µm]	DOU [mmol m^{-2} d^{-1}]
4401	8 (1) [1]	800	0.9 (1)	3.0	-	-	-
4409	9 (2) [1]	950 ±36	0.6 ± 0.06(2)	2.0	-	-	-
4417	12 (1)	700	0.4 (1)	1.3	5.7 ±0.3 (3)	n.d.	0.56 ±0.06 (3) [2]
4419	11 (3)	600 ±33	0.5 ± 0.02(3)	1.7	2.9 ±0.3 (6)	500 ±65	9.0 ±0.2 (6)
4421	26 (2)	n.d.	0.1 ± 0.01(2) [2]	0.3	-	n.d.	-

[1] OPD modelled from microelectrode profiles (Epping and Helder, 1997)

[2] DOU calculated from optode profile

n.d. not determinable due to measuring resolution of 0.5 cm

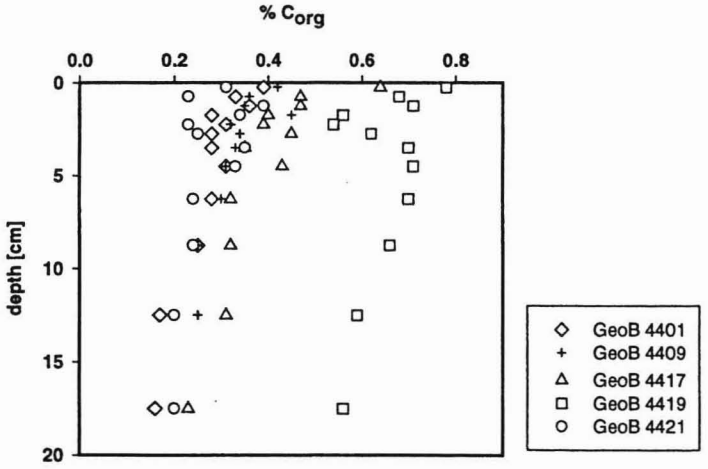

Fig. 5: Organic carbon content at the five stations.

At 2 stations (GeoB 4417 and 4419) laboratory oxygen profiles were measured on cores using O_2 microelectrodes to compare to *in situ* determinations of DOU and OPD. At both stations 4417 and 4419, the oxygen penetration measured in the laboratory was much shallower than the *in situ* depths (Tab. 2). At station 4417 the OPD decreased from 12 cm (*in*

situ) to 6 cm (lab) resulting in a calculated DOU that was 1.5-times higher than the *in situ* value. At station 4419 the OPD decreased from 11 cm to 3 cm thereby predicting a DOU that was 18-times higher than the *in situ* O_2 uptake rate.

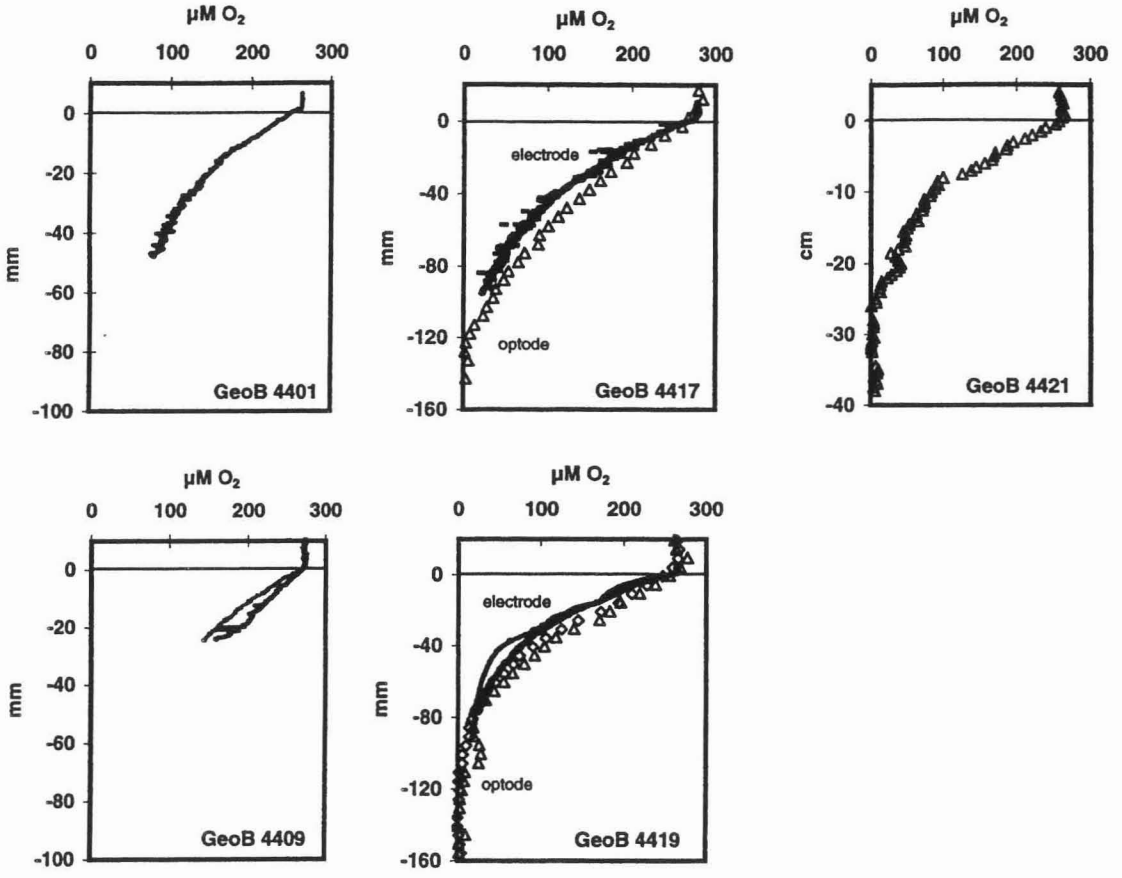

Fig. 6: *In situ* oxygen profiles. GeoB 4401 and 4409 electrode measurements; GeoB 4417 and 4419 electrode (closed symbols) and optode (open symbols) profiles; GeoB 4412 optode measurement.

Discussion

High and low resolution profiles

In oligotrophic deep sea sediments only a small percentage of organic material produced in the surface water reaches the seafloor. This leads to very low oxygen respiration rates and consequently, the oxygen concentration gradient changes only slightly with depth and oxygen can penetrate deep into the sediment. These conditions allow us to describe the O_2 dynamics quite well with a vertical resolution of 0.5 cm (our optode resolution). However,

most deep sea sediments have a DBL between 0.2 and 1.5 mm, depending on the flow velocity in the water above the sediment surface and the roughness of the solid surface (Archer et al., 1989b; Glud et al., 1994). With our step resolution of 0.5 cm the DBL is impossible to detect. To calculate oxygen uptake rates from the linear concentration gradient in the DBL, a finer vertical resolution is necessary. Even rates calculated from a profile resolution of 1 mm predicted lower rates than calculated from 0.25 mm resolution profiles (Cai et al., 1995). On the other hand high resolution profiles leads to a long overall measurement time if used to determine OPD in oligotrophic sediments with oxygen penetration of several decimetres. Our results indicate that a step resolution of 100 µm for the first 2 cm (for determination of the DBL) and a further vertical resolution of 0.5 cm (for oxygen penetration depth) are optimal for measuring the oxygen dynamics in marine sediments of an oligotrophic area. The combination of microelectrodes and deep penetration optodes allows us to compare oxygen uptake rates determined from gradients in the diffusive boundary layer with rates modelled from the oxygen penetration depths. Deep oxygen profiles can also be used to estimate the oxygen consumption rates and compare the rates with the degradation of organic matter in the sediment.

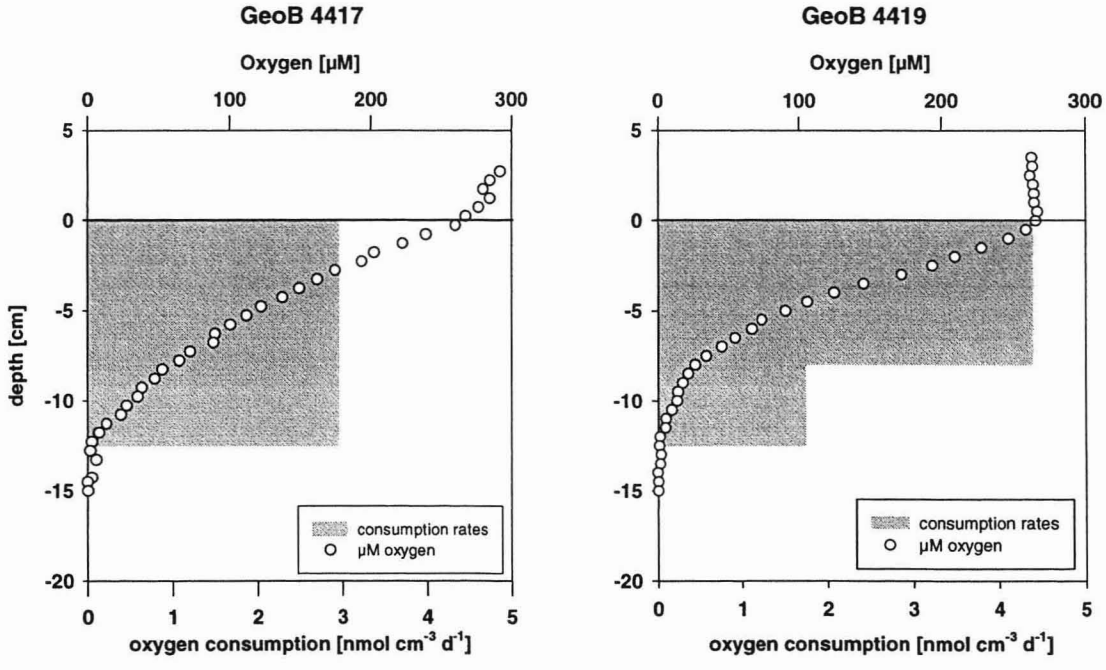

Fig. 7: Oxygen consumption rates at station GeoB 4417 (3511 m) and 4419 (4487 m) modelled from an *in situ* oxygen optode profile.

Comparisons of *in situ* and laboratory measured OPD and DOU rates exhibit strong differences, especially in sediments from abyssal depths. The pore water chemistry of the recovered cores is altered or compacted due to decompression and warming effects (Yayanos and Dietz, 1982; Smith and Hinga, 1983; Turley et al., 1988; Glud et al., 1994; Glud et al., in press). This may lead to unrealistic zonations of the chemical species measured in the laboratory. Therefore indirect determinations of the oxygen penetration depth (e.g. Mn^{2+} depletion depth from porewaters; Froelich et al., 1979; Cai and Sayles, 1996) measurements may underestimate the oxygenated sediment zone and consequently overestimate the mineralization of organic matter by oxygen in those oligotrophic sediments.

Comparison of oxygen uptakes rates

A comparison of our measured fluxes with a global benthic oxygen flux map (Jahnke and Jackson, 1992; Jahnke, 1996) showed that the model estimated fluxes of 0.06 - 0.25 mmol m^{-2} d^{-1} slightly underestimate our measurements. Oxygen fluxes calculated from *in situ* microprofiles were 2- to 4-times higher than those estimated from the global maps. However, at the mid Atlantic ridge (GeoB 4412) the *in situ* rates were similar to the calculated oxygen fluxes for this area (Jahnke and Jackson, 1992; Jahnke, 1996). Mineralization rates measured at similar water depths in the Equatorial Pacific exhibit values between 0.40 and 0.46 mmol m^{-2} d^{-1}, respectively (Berelson et al., 1997), which is in the range of our measured rates of 0.4 to 0.9 mmol m^{-2} d^{-1} (Tab. 2).

In shelf sediments, oxygen consumption rates show two peaks, at the sediment surface and at the oxic-anoxic interface. The latter results from reoxidation of reduced compounds (Jørgensen, 1982). The low uptake rates, the absence of secondary peaks and deep penetration of oxygen suggest that reoxidation and other mineralization processes are of minor importance at these oligothrophic stations (Fig. 6). Our results support the argument that in deep sea sediments oxygen is the dominant electron acceptor for mineralization of organic material (Jahnke and Jackson, 1992).

Assuming steady state oxygen dynamics and a C : O ratio of 0.77 (Berner, 1980), the carbon consumption rates range between 0.3 and 3 g C m^{-2} a^{-1} at our stations (Tab. 1). The supply of organic matter from surface waters through the water column to the sediment surface can be calculated from transport equations (Betzer et al., 1984; Berger et al., 1987) using the primary production estimates from Berger (1989). With an annual productivity for oligotrophic areas between 40 – 60 g C m^{-2} a^{-1}, only 1 – 2 % of the organic matter reaches the

sediment-water interface. Carbon consumption rates modelled from our DOU data indicate 2 to 3 times higher values. This result is in agreement with other *in situ* studies, where the carbon consumption rates calculated from benthic oxygen uptake rates were up to 3-times higher than estimations from surface primary production (Smith et al., 1989; Jahnke et al., 1990; Walsh, 1991).

A more seasonally characterised primary production, as reported for this area, may lead to a higher export rate (Muller-Karger et al. 1988). Furthermore, there is evidence for relatively fast sinking rates of the particles and therefore more organic carbon could reach the sediment water interface (Berger et al., 1989; Berger and Wefer, 1990). The impact of episodic changes in the input of organic matter on oxygen consumption rates and penetration depths was stressed by Gehlen et al. (1997) in deep-sea sediments of the western Mediterranean. They found an increase of oxygen uptake rates ranging from 1.26 to 1.82 µmol m^{-2} d^{-1} at different organic carbon contents. The corresponding change in carbon mineralization rate, however, was small and the required increase of reactive organic carbon was 1 % of the surface organic carbon content (0.6 % wt/wt) (Gehlen et al., 1997). Further processes that enhance the organic matter flux to the seafloor are lateral transport of sediment particles (Walsh et al., 1981) and migration of benthic organisms (Jahnke et al., 1990).

Conclusions

We present the first *in situ* deep penetration O_2 profiles from oligotrophic sediments. Oxygen dynamics in these oligotrophic sediments were determined using a combination of microsensors (for measuring steep oxygen gradients in the DBL) and deep penetrating optodes (for measuring the oxygen penetration depth). Due to the strong effect that sediment recovery has on pore water chemistry, previous determinations of oxygen penetration depth from shipboard or pore water Mn^{2+} profiles may overestimate the amount of organic matter mineralizated with oxygen. Benthic respiration is supported by the rain of organic matter from surface waters, but estimated fluxes at same oligotrophic settings from surface production and benthic mineralization exhibit different values. Our results indicate the need for continued *in situ* profiling in oligothrophic sediments to estimate the importance to carbon remineralization world wide.

Acknowledgements - We gratefully acknowledge the captain and crew from the RV Meteor for their skillful assistance during the cruise. We thank Stephan Meyer for construction of the optode measuring system and his skillful assistance in deploying the lander. Gabrielle Eickert, Anja Eggers and Vera Hübner are thanked for construction of the glass electrodes and Volker Meyer for building the opto-electronics. Dr T. Wagner is thanked for measuring the carbonate samples. We would like to thank Dr Ronnie Glud and Dr Susan Boehme for their valuable comments and for carefully reading the manuscript. This work was funded by the German Science Foundation (contribution no. 123 of Special Research Project SFB 261, The South Atlantic in the Late Quaternaty at the University of Bremen).

Chapter 3

Calcite dissolution driven by benthic mineralization in the deep sea: *In situ* measurements of Ca^{2+}, pH, pCO_2, O_2

Wenzhöfer F[1], Adler M[2], Kohls O[1], Hensen C[2], Strotmann B[1], Boehme S[1], Schulz HD[2]

1 Max Planck Institute for Marine Microbiology, Celsiusstr. 1, D-28359 Bremen, Germany

2 Dept. for Geoscience, University of Bremen, P/O Box 330 440, D-28334 Bremen, Germany

Abstract

In situ measured microprofiles of O_2, pH, pCO_2 and for the first time Ca^{2+} were performed to quantify the $CaCO_3$ dissolution and organic matter mineralization in marine sediments in the eastern South Atlantic. Further, a numerical model was used to simulate the organic matter decay with oxygen and to estimate the calcite dissolution rate. Metabolic CO_2 drives calcite dissolution in these sediments overlain by supersaturated water. Fluxes across the sediment water interface calculated from the *in situ* Ca^{2+} microprofiles were 0.6 mmol m^{-2} d^{-1} for two stations at a water depth of 1300 m. The CO_2 that is produced in the sediment dissolves up to 85 % of the calcite rain to the seafloor. Modeling our O_2, pH and Ca^{2+} profiles from one station predicted a calcite dissolution rate constant for this calcite-poor site of 7000 mol kgw a^{-1}, which equals 663 % d^{-1}. This rate constant is the highest ever reported *in situ* value, but still in the range of laboratory rates.

Diffusive oxygen uptake (DOU) and oxygen penetration depth (OPD) were measured at four stations along a 1300 m isobath of the eastern African margin and one in front of the river Niger at a water depth of 2200 m. DOU rates were in the range of 0.3 to 3 mmol m^{-2} d^{-1} and showed a decrease with increasing water depth, corresponding to an increase in OPD.

Introduction

Burial of carbon as $CaCO_3$ and organic matter in marine sediments is a major process in the oceanic carbon cycle and consequently it is the major driving force in the global carbon cycle (Broecker and Peng, 1982; Wollast et al., 1993). Calcium carbonate precipitation or dissolution alters the carbonate system of seawater causing a change in the CO_2 content at chemical equilibrium in surface waters and hence atmospheric pCO_2 (Broecker and Peng, 1987). Archer and Maier-Reimer (1994) pointed out that changes in preservation/dissolution of $CaCO_3$ in the deep sea are required to explain the shifts in atmospheric pCO_2 of glacial-interglacial transitions.

As carbonate sinks through the water column, calcite dissolution is mainly driven by the saturation state of the water which is dependent on the pressure and pH. However once the carbonates reach the seafloor secondary processes can alter these materials. A major benthic process influencing carbonate preservation/dissolution in deep sea sediments is the oxidation of organic matter. The first model to estimate the influence of organic matter on carbonate dissolution in deep sea sediments was presented by Emerson and Bender (1981). In their model, the importance of determining the depth distribution of organic matter oxidation was emphasized, because metabolically mediated CO_2 causes $CaCO_3$ dissolution within sediments, even when the overlying water is supersaturated with calcite.

The extent and efficiency with which metabolic CO_2 leads to $CaCO_3$ dissolution depends on a number of factors which themselves are likely to vary in different environments including the saturation state of the overlying water, the depth profile of organic carbon mineralization rate, the $C_{org}/CaCO_3$ ratio of the sedimenting particulate matter, and the dissolution kinetics of $CaCO_3$. The study of $CaCO_3$ dissolution in deep sea sediments has been advanced in previous years by the deployment of *in situ* benthic flux chambers (Berelson et al., 1990; Jahnke et al., 1994, 1997) and *in situ* microprofilers (Archer et al., 1989a, Hales et al., 1994, 1996). However, in most *in situ* microprofiling studies, O_2 and pH microprofiles were used to constrain the dissolution rate of calcite. The $CaCO_3$ saturation state of the pore water can not be defined with pH values, and so recent investigations used pCO_2 sensors in combination with pH and O_2 to estimate *in situ* $CaCO_3$ dissolution (Cai et al., 1995; Hales et al., 1997). $CaCO_3$ dissolution rates based on these microprofiles measurements predict that < 50 % of the sedimenting $CaCO_3$ dissolve (Hales et al., 1994, 1996; Hales and Emerson, 1997a; Emerson and Archer, 1990; Archer, 1991; Martin and Sayles, 1996), while *in situ* benthic flux chamber measurements do not always support high rates of metabolically driven $CaCO_3$ dissolution (Jahnke et al., 1994). A combination of benthic chamber and

microelectrode measurements from California continental margin sediments exhibited that benthic fluxes of alkalinity and inferred $CaCO_3$ dissolution rates can only be fully reconciled, if the influence of metabolically produced CO_2 is included (Jahnke et al., 1997). Based on this recent study Jahnke et al. (1997) concluded that the extent of metabolic $CaCO_3$ dissolution may vary regionally.

In previous studies, rates of $CaCO_3$ dissolution have been determined either indirectly using O_2, pH and pCO_2 sensors to define carbonate systematics, or by measuring fluxes of Ca^{2+} in samples collected with benthic chambers. In this study we have directly measured Ca^{2+} profiles *in situ* with a Ca^{2+} microsensor. The preliminary results from this microsensor were used in combination with the classic microelectrodes (O_2 and pH) and a recently developed CO_2 microoptode to describe the saturation state of the pore water and the calcite dissolution rate. Furthermore the model CoTReM was used to evaluate the measured profiles, using one-dimensional early diagenetic and thermodynamical equilibria reactions. The simulation quantifies the interdependency of the four different chemical profiles (O_2, pH, pCO_2, Ca^{2+}) and determines the calcite reaction rate.

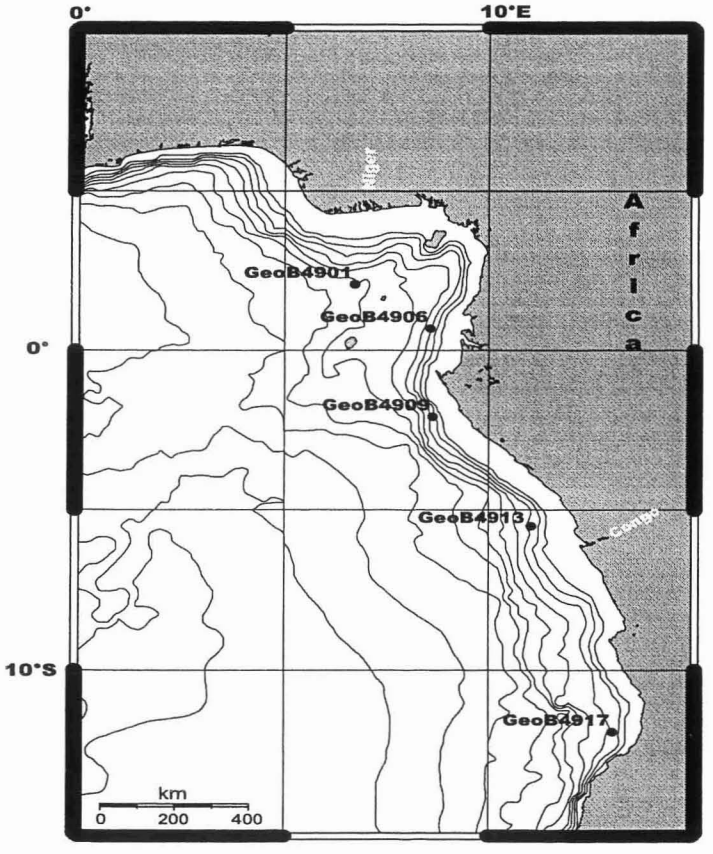

Fig. 1: Locations of the 5 stations along the African coast

Material and Methods

Site description

Lander deployments were performed on the continental slope off west Africa, on a R/V Meteor cruise in February and March of 1998. Four stations were located on the 1300 m isobath along the continental slope. Additionally, a fifth station was located at a water depth of 2200 m in front of the river Niger (Fig. 1). Geographical locations and bottom water characteristics are summarized in Table 1. The individual and accumulated percent of organic carbon and calcite versus depth in the sediment is illustrated in Fig. 2. Surficial sediments at all stations have an organic carbon content of approx. 3.5 %, except station 4901 (2200m water depth) with 1.5 %. Additionally, the calcium carbonate content in surface sediments at all stations, except 4901, is low, ranging from 1 -11 %. With increasing depth, $CaCO_3$ content increases at all stations (Fig. 2). The porosity at all stations decreases from 0.9 at the surface to 0.8 at 30 cm (data not shown).

Table 1: Geographical position of the stations and bottom water charcteristics.

station	position		depth [m]	T [°C]	pH	O_2 [µM]	Ω
4901	02°40.77 N	06°43.82 E	2185	3.5	7.97	233	1.31
4906	00°41.17 S	08°22.94 E	1251	4.6	7.9	184	1.24
4909	02°04.35 S	08°37.54 E	1317	4.6	7.92	184	1.55
4913	05°29.91 S	11°04.46 E	1303	4.5	7.89	194	1.45
4917	11°54.40 S	13°04.36 E	1300	4.2	7.89	190	1.27

In situ measurements

At each station, *in situ* measurements were performed using an autonomous profiling lander (Reimers et al., 1986; Gundersen and Jørgensen, 1990). The profiling lander was used to measure microprofiles of O_2, pH, pCO_2 and Ca^{2+} across the sediment water interface. During this study our profiling lander consisted of two measuring systems (electro-chemical and opto-chemical), a Niskin bottle for bottom water characterization and a time lapse camera.

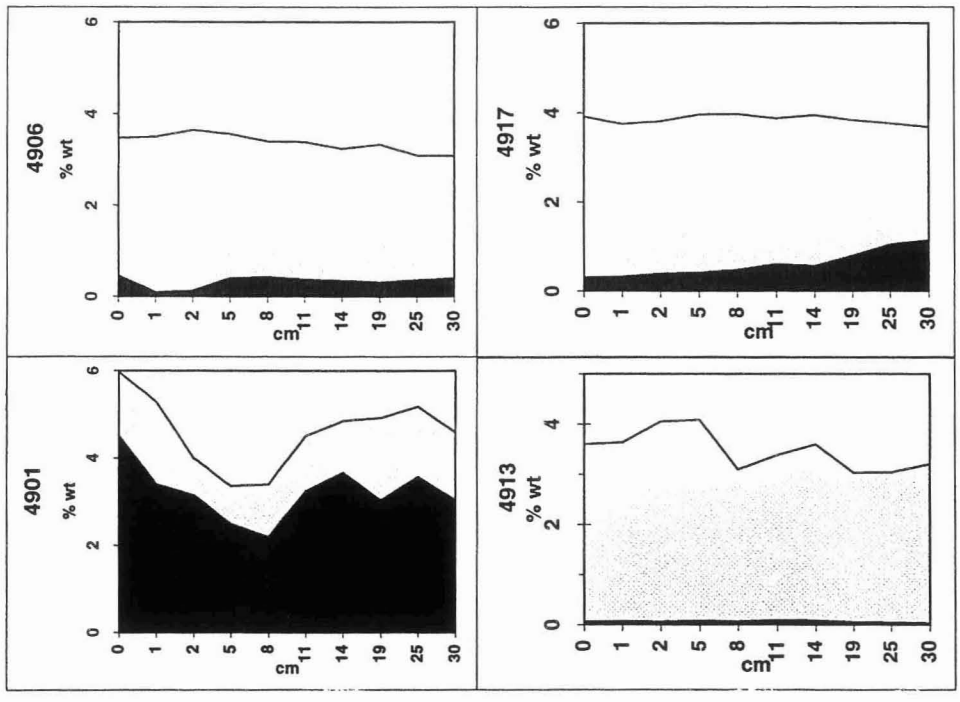

Fig. 2: Sediment content of calcite (dark) and organic carbon (light)

In situ microelectrode measurements

Microelectrode measurements were made *in situ* using an updated version of the system used by Glud et al. (1994). On each deployment the microelectrode system consisted of 4 O_2 microelectrodes, 3 pH microelectrodes, 1 Ca^{2+} microelectrode and one reference electrode. The sensors are driven down into the sediment with a step resolution of 100 µm. At each measuring horizon the electrode signals were stored after 30 sec to guarantee equilibrium between the surrounding water and the electrode. The electrodes were checked for drift by comparing the signal in the bottom water before and after sediment profiling.

O_2 microelectrode

The oxygen microelectrodes were of Clark type with an internal reference (Revsbech, 1989a). All electrodes had an outer diameter between 10 – 30 µm, a stirring sensitivity < 1 % and a 90 % response time of < 2 sec. A two point calibration of the sensors was made *in situ* using the constant signal in the bottom water and in the anoxic zone of the sediment.

pH microelectrodes

The pH microelectrodes were constructed as described by Revsbech et al. (1983). The outside tip diameter of the pH sensitive glass was 20 – 30 µm. A two point calibration was

performed to determine the slope of each pH electrode. The pH sensors were immersed in sea water at *in situ* temperature and the pH was changed by adding small amounts of acid (H_2SO_4). A commercial pH electrode was used to determine the pH at each calibration point.

Ca^{2+}microelectrodes

Liquid ion-exchanging membrane (LIX) microsensors for Ca^{2+} with solidified tips were prepared as described by Ammann et al. (1987) (Fig. 3A). Green soda lime glass tubes (8516, Schott) were pulled to a tip of approximately 10 – 20 µm using a heat coil and then silanized. LIX I consisted of a solution of 5 % (wt/wt) Calcium Ionophore II (ETH 129) and 1 % (wt/wt) potassium tetrakis(4-chlorophenyl)borate in 94 % (wt/wt) 2-nitrophenyl octyl ether and was used as ion-exchange membrane. LIX II was a mixture of LIX I and 10 % (wt/wt) poly(vinylchloride) diluted with 3 volumes of tetrahydrofuran. All chemicals used were obtained from Fluka. The electrodes were back-filled with 10 mM CaCl solution and a solidified membrane was created in the tip, by pulling first LIX I and then LIX II into the sensor tip. Calibration was done in a dilution series of Ca^{2+} in a calibration solution with the ionic strength of sea water (adding $MgCl_2$, KCl and NaCl).

In situ microoptode measurements

The electronics for the optode measuring system were stored in a pressure stable housing and modified from Glud et al. (1999) and Wenzhöfer et al. (submitted). As a light source, a light emitting diode (LED) was used and light with a wavelength of 450 nm was guided through the fiber to the pH sensitive dye solution in the sensor tip. Emission light of 520 nm was guided back to a photomultiplier used as the detector. On each deployment the optode-system was equipped with 2 CO_2 microoptodes.

CO_2-microoptode

CO_2 microoptodes were constructed as described by Kohls et al. (1997b) (Fig. 3 B). The optode housings were made of a glass capillary pulled to an outer tip diameter of 20 µm and sealed with a CO_2 permeable silicon membrane (E 43 silicon). The internal dye solution contains 0.5 M Hydroxypyrenetrisulfonacid (HPTS, Fluka) in which 1 mg ml^{-1} carbonic anhydrase was added and adjusted to a pH of 8 (deBeer et al., 1997a). A multimode silica/silica step index optical fiber (100/140 µm core/cladding diameter) was tapered down to tip diameter of approximately 15 µm and inserted into the housing so that the dye solution was only in front of the fiber (Fig. 3 B). The back of the optode was filled with paraffin oil.

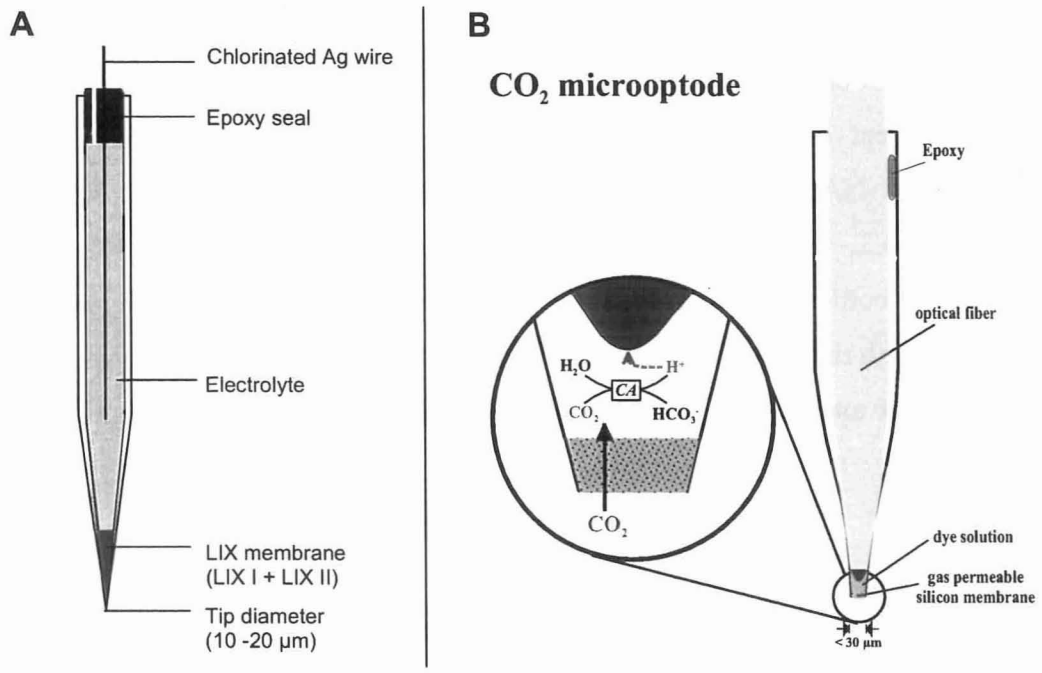

Fig. 3: Schematic drawing of the Ca^{2+}-LIX-microelectrode (A) and the CO_2-microoptode (B). The magnification shows the chemical reaction occurring in the sensor tip.

The CO_2 microoptode was calibrated by determining the slope of the signal using a series of 5 sea water samples at *in situ* temperature with different pH values. Subsequently, the optode readings from each *in situ* profile were referenced to its readings in the overlying water, and the calibration slope and calculated pCO_2 in the bottom water were used to determine pCO_2 concentrations at each profiling depth. The pCO_2 concentration of the 5 calibration samples and the bottom water were calculated from measured pH values (Commercial pH electrode; RADIOMETER), DIC concentrations, and equilibrium relationships and constants from Weiss (1974) and Roy et al. (1993).

The CO_2 microoptodes were driven on a profiling device separated from the microelectrode system. The microoptodes were moved in increments of 200 µm for the first 7 cm and for the following 8 cm a resolution of 500 µm was used. The sensors were kept at each depth horizon for 3 min; after a 30 sec delay the microoptode signals were recorded 10 times every 20 sec until the 3 min were completed. The first two signal records of each set of ten were deleted due to a time delay of the optical switch which connects two microoptodes to one detector (Glud et al., 1999).

Bulk sediment measurements

The total carbon content was measured in dried and ground sediment subsamples taken from sediment cores. The analysis was conducted with a FISONS Instruments elemental analyzer (NA 1500 N) using sulfanilamide as analytical standard. To determine inorganic carbon, 0.3 - 0.5 g of dried sediment was acidified with 15 ml 0.5 N hydrochloric acid in gastight bottles. The evolved CO_2 in the headspace was measured by gas chromatography with thermal conductivity detection. Organic carbon content was determined as the difference of total carbon and inorganic carbon content (Cutter and Radford-Knoery, 1991).

Calculations

The *in situ* oxygen microprofiles were used to determine the thickness of the diffusive boundary layer (DBL) (Sweerts et al., 1989). The diffusive oxygen uptake (DOU) was calculated from the microprofiles in the diffusive boundary layer above the sediment surface using Fick´s first law:

$$DOU = D_0 \, dC/dz \qquad (1)$$

where D_0 = molecular diffusion coefficient in water (from Li and Gregory, 1974 and Broecker and Peng, 1974; corrected for temperature and salinity) and dC/dz = linear gradient of oxygen within the DBL. Diffusive fluxes of Ca^{2+} were obtained using the sediment profiles and Eqn. (1) as well as the empirical relations for diffusion coefficients in the sediment:

$$J = \phi \, Ds,i \, dC/dz \qquad (2)$$

and

$$D_{s,i} = D_0 \, \phi^{m-1} \qquad (3)$$

where ϕ = porosity, Ds,i = diffusion coefficient in the sediment of species i corrected for temperature and pressure (Li and Gregory, 1974; Broecker and Peng, 1974) and m = 3 (Ullmann and Aller, 1982; Berner, 1980).

Model (CoTReM) description

The complete description of the computer model (CoTReM) (Hensen et al., 1997) is not within the scope of the present study, however, a brief overview of the capabilities of the software is given below. A more detailed description of the developments to the model is available in Adler et. al. (in prep.).

CoTReM calculates one-dimensional transport and reaction of species in porous media. The general diagenetic equation, a partial differential equation (PDE) as proposed by Berner

(1980) is used as the modeling approach. Equation (4) is written for the homogeneous one-dimensional case. This is independent of porosity and applies to a homogeneous model area (or cell).

Species conc. Diffusion and Dispersion

$$\partial_t C_i = -\partial_x (v \cdot C_i) + \partial_x (D_i \cdot \partial_x C_i) + \alpha_x (C_{0,i} - C_i) + R_i (C_1, \mathrm{K}, C_{n_i}) \quad i = 1, \mathrm{K}, n_i \quad \frac{\mathrm{mol}}{1 \cdot \mathrm{a}} \qquad (4)$$

Sediment advection Bioirrigation Reactions

with: C_i: concentration of the ith-species
D_i: sum of diffusion (of the ith-species) and dispersion coefficient
v: sedimentation rate (plus flow velocity, if applicable)
t: time
x: sediment depth
R_i: reaction rate of the ith-species (source term)
$C_{0,i}$: bottom water concentration of ith-species
α_x: exchange coefficient of depth x

The discretisation in one-dimensional space divides the model area into a series of cells. The thickness of the cells vary with depth. The transport and chemical processes are calculated independently and follow the operator-splitting-method (Fig. 4).

Transport

In this simulation, bioirrigation, dispersion and sedimentation are not included, therefore the diffusion PDE can be defined by:

$$\partial_t C_i = D \cdot \partial_x^2 C_i \qquad i = 1, \mathrm{K}, n_i \quad \mathrm{mol}/(1 \cdot \mathrm{a}). \qquad (5)$$

D is constant in a cell (variable with depth due to changes in porosity) for each species and is solved in a system of linear PDEs simultaneously for all cells.

Chemical Reactions

The operators R_i change the concentration of chemical species within a cell without being dependent on other cells:

$$\partial_t C_i = R_i (C_1, \mathrm{K}, C_{n_i}) \qquad i = 1, \mathrm{K}, n_i \quad \mathrm{mol}/(1 \cdot \mathrm{a}) \qquad (6)$$

The chemical reactions are split in irreversible redox reactions and thermodynamic equilibria calculations.

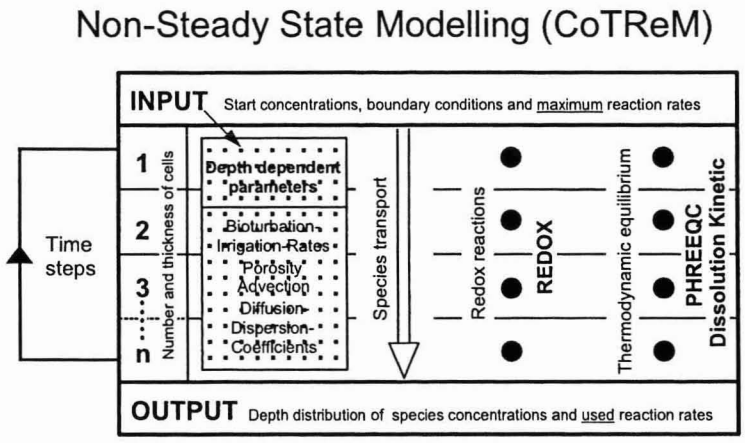

Fig. 4: General structure of the model CoTReM.

The results of redox reactions $\bar{o}_t\, C_{i\ (\text{species, depth})}$ are controlled by depth-dependent maximum rates for each implemented redox reaction in CoTReM. These are reduced to actual rates $R_{(\text{reaction, depth})}$, if any of the participating species at any depth are not available in sufficient quantities. The change of the concentration distributions are calculated with the stoichiometric coefficients of the reaction $SC_{(\text{species, reaction})}$ and the numerical time step *dt*:

$$dt \cdot \bar{o}_t\, C_{i\ (\text{species, depth})} = R_{(\text{reaction, depth})} \cdot dt \cdot SC_{(\text{species, reaction})} \qquad (7)$$

Finally, the thermodynamic equilibrium reactions are calculated in each cell separately with the algorithms of PHREEQC (Parkhurst, 1995), which are incorporated in CoTReM.

Up to this point, the processes (transport and reoxidation) are calculated using species concentrations. However, thermodynamic equilibrium distributions of species or dissolution/precipitation processes depend on species activities rather than concentrations. PHREEQC applies activities to each ion or complex in the porewater solution. Then, the ion activity product *IAP* is used in relation to dissociation constants K_{Species} and solubility products $K_{\text{sp, Mineral}}$ (only calcite used within this study) to equilibrate the mineral phases to all ions and complexes in the modeled porewater solution. For calcite dissolution, a kinetic reaction similar to the one suggested by Keir (1980) is used. The dissolvable part of the calcite concentration *dC* [mol/kgw] within a time step is calculated according to:

$$dC = DR \cdot dt \qquad (8)$$

$$DR = k \cdot (10^{1} - \Omega_{\text{Mineral}})^{n} \qquad (9)$$

$$\Omega_{Mineral} = IAP / K_{sp,\,Mineral} \quad (10)$$

$$SI = \log_{10} \Omega_{Mineral} \quad (11)$$

With:

dC	[mol / kgw]	:	Calcite concentration
dt	[a]	:	Time step
DR	[mol / (kgw · a)]	:	Dissolution rate
k	[mol / (kgw · a)]	:	Dissolution rate constant
n	[-]	:	Reaction order
$\Omega_{Mineral}$	[-]	:	Saturation state of the mineral
IAP	[-]	:	Ion activity product
$K_{sp,\,Mineral}$	[-]	:	Solubility product of the mineral, dependent of temperature and pressure
SI	[-]	:	Saturation index of the mineral

The time step is ended with these PHREEQC calculations for all cells.

Results

In situ O_2 microprofiles

Oxygen penetration at the 1300 m stations (4906, 4909, 4913 and 4917) varied between 14 and 25 mm, while at 2200 m (4401) oxygen penetrated down to 90 mm (Table 2; Fig. 5 a - e). The measured oxygen microprofiles at the 1300 m stations showed a significant difference between the single microelectrode readings on the same deployment, indicating a lateral variability in oxygen consumption within an area of 125 cm^2. This heterogeneity was not observed at station 4901 (2200m), where the O_2 microelectrode profiles were similar. Photographs taken during each deployment confirmed this observation showing a flat and homogeneous sediment surface at station 4901, while at the shallower stations the sediment surface was covered with microtopography and biogenic structures. The high oxygen consumption was also reflected by the diffusive oxygen uptakes (DOU) ranging between 2 and 3 mmol m^{-2} d^{-1} at 3 of the 1300 m stations compared to 0.3 mmol d^{-2} d^{-1} at station 4901 (Table 2). An exception was station 4909 which exhibited a somewhat lower DOU associated with a deeper penetration of oxygen compared to the other 3 stations (1300 m).

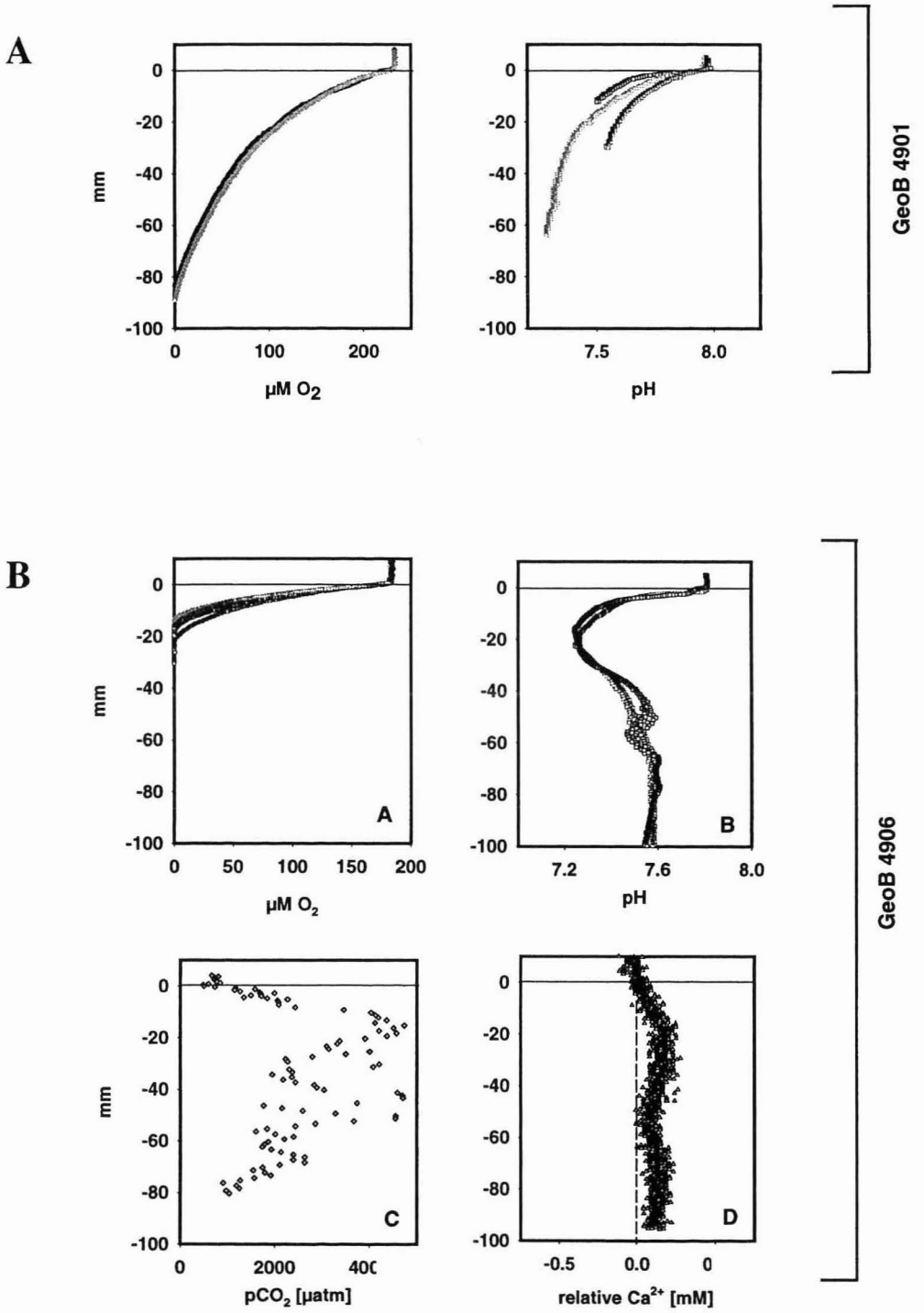

Fig. 5 a/b: *In situ* microprofiles from station 4901 (a) and 4906 (b)

In situ pH and pCO_2 microprofiles

In situ pH decreased with depth in the oxygenated sediment horizon at all of the stations. The pH minimum was associated with the oxic-anoxic horizon (Fig. 5 a/b/c/e). Below this zone an increase in pH was observed at station 4906 and 4917, while the pH at

4909 was more or less constant with depth. At 4901 the pH gradually decreased with depth, while no minimum was observed because the pH microelectrodes never reached the anoxic sediment horizon (Fig 5a).

In situ pCO_2 increased gradually below the sediment water interface reaching a maximum at the oxic-anoxic interface in the sediment. In general the pCO_2 profiles mirror the pH profiles (Fig. 5 b/c/d). At 4909 and 4913 the pCO_2 gradually increased with depth reaching maximum values of approx. 2500 and 1000 µatm, respectively, at a depth of 90 mm. Unfortunately no pH profile was measured at station 4913, due to problems with the reference electrode.

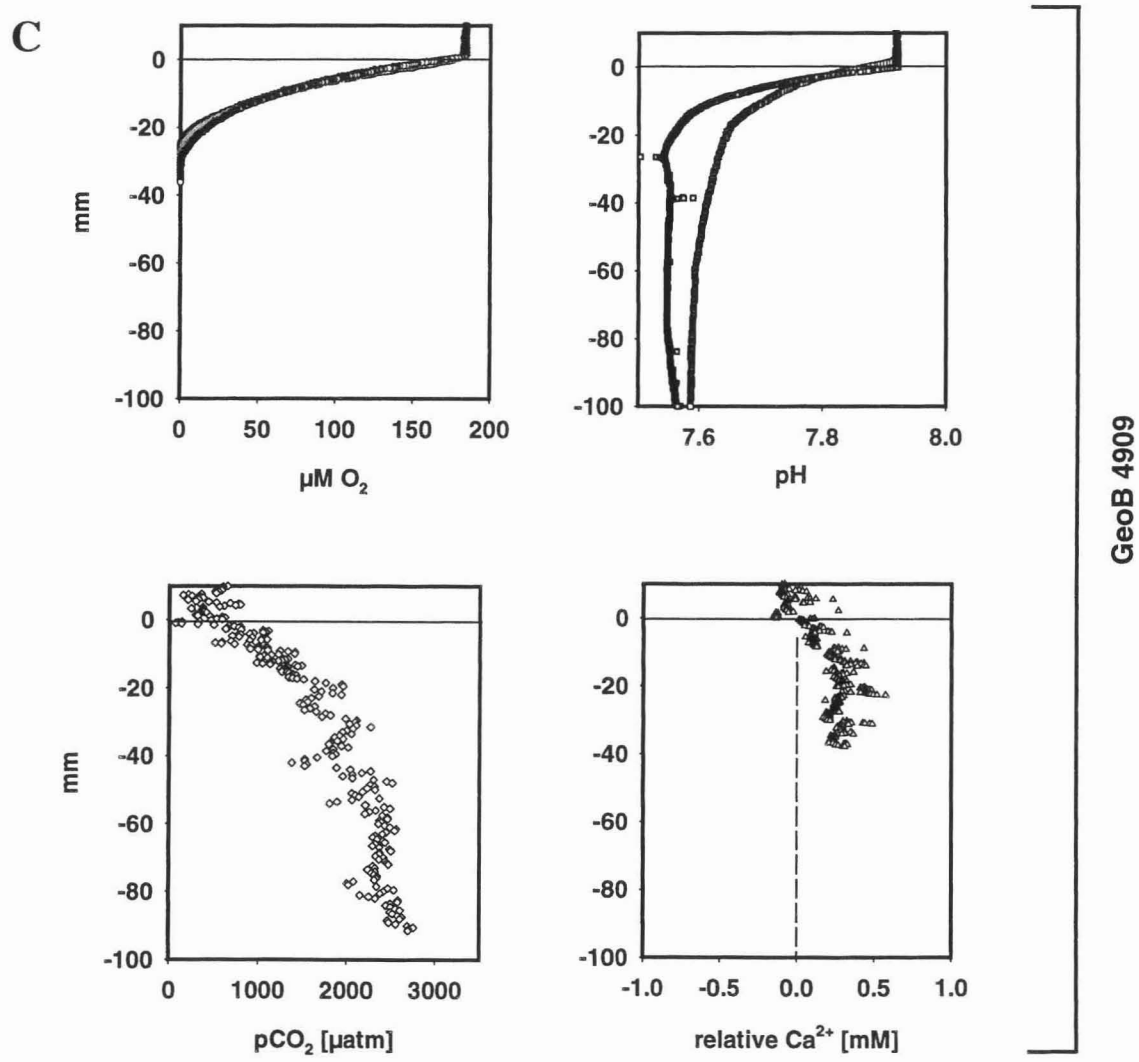

Fig. 5 c: *In situ* microprofiles of O_2, pH, pCO_2 and Ca^{2+} from stations 4909

In situ Ca^{2+} microprofiles

In situ Ca^{2+} microprofiles were measured at two stations (4906 and 4909) for the first time. The two stations exhibited an increase in Ca^{2+} below the sediment surface (Fig. 5 b/c). The depths of this increase correspond to the decrease of pH and O_2 and an increase in pCO_2 reaching a maximum Ca^{2+} concentration at approx. 20 mm at both stations. At 4906 the Ca^{2+} microprofile also showed a decrease at approx. 30 mm (Fig. 5 b). A flux of 0.55 and 0.58 mmol m^{-2} d^{-1} at 4906 and 4909, respectively, was calculated from the Ca^{2+} gradient across the sediment water interface. The sensor signal exhibited some scattering due to the sensitivity of the LIX membrane to contact with sediment grains. However, the sensors were kept at each depth interval for half a minute, giving the sensor chemistry enough time to adapt to the physical environment.

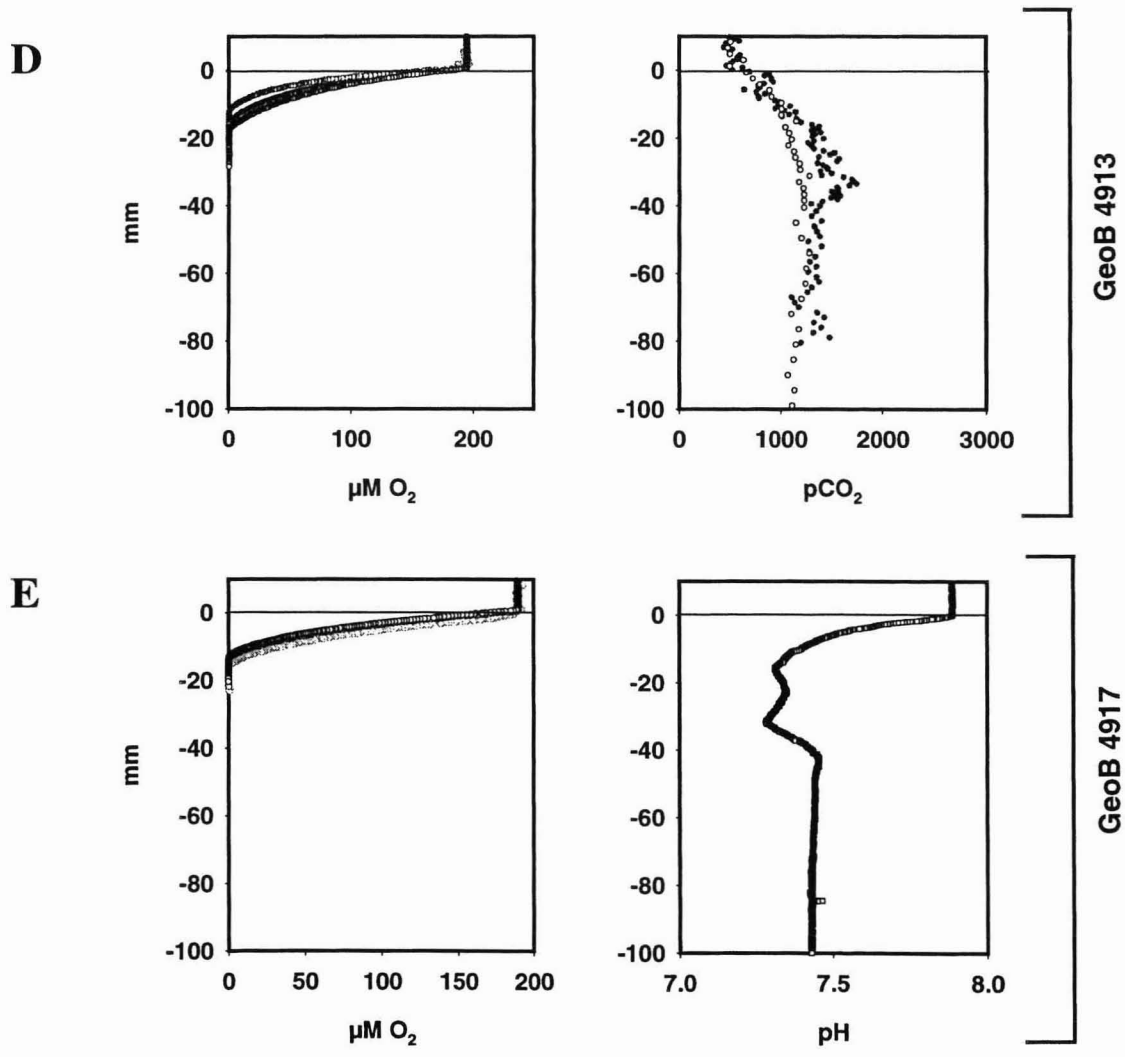

Fig. 5 d/e: *In situ* microprofiles from station 4913 (d) and 4917 (e).

Table 2: Oxygen penetration depth (OPD), diffusive oxygen uptake (DOU) and Ca^{2+} flux calculated from measured microprofiles.

station	OPD [mm]	DOU [mmol m^{-2} d^{-1}]	Ca^{++}-flux [mmol m^{-2} d^{-1}]
4901	90	0.3	-
4906	15.5 (13-20)	2	0.55
4909	25 (23-28)	1	0.58
4913	15 (11-17)	2.9	-
4917	14 (12-15)	3	

Model results from station 4909

Station 4909 was chosen for modeling because the O_2, pH, pCO_2 and Ca^{2+} profiles appeared internally consistent and therefore less impacted by horizotal variability. Station 4906, the other station where Ca^{2+} profiles were measured, exhibits subpeaks in the CO_2, pH and Ca^{2+} profiles. These data will be modeld in Adler et al. (in prep.) but are beyond the scope of this paper.The oxygen profile was fitted using zero-order reaction rates and O_2 consumption rates as shown in Fig 6A for organic matter degradation. For the composition of the organic matter the stoichometry of the Redfield Ratio was used:

$$(CH_2O)_{106}(NH_3)_{16}(H_3PO_4)_1 + 138\ O_2 \Longrightarrow 106\ HCO_3^- + 16\ NO_3^- + 1\ PO_4^{3-} + 16\ H_2O + 125\ H^+ \quad (9)$$

Molecular diffusion coefficients used within the simulation were corrected for porosity after Ullmann and Aller (1982). This approach resulted in the modeled steady state profile for oxygen (Fig. 6A). The effects of the CO_2 and H^+ release on the $CaCO_3$-CO_2-system were investigated by calcite equilibrium calculations. All species concentrations (Na^+, Cl^-, Mg^{2+}, Ca^{2+}, K^+, HCO_3^-, SO_4^{2-}, NO_3^-, H^+ and OH^-), apart from O_2, measured in the bottom water were set as background concentrations for the whole model area. Na^+, Cl^-, Mg^{2+}, K^+ and SO_4^{2-} were also used to calculate the ionic strength of the pore water and therefore to appropriately define the activities for the relevant species of the $CaCO_3$-CO_2-system.

The solubility product $K_{sp,\ Calcite}$ was corrected for temperature and pressure resulting in a value of -8.036 to keep the pore water concentrations in an equilibrium state after the first PHREEQC calculation. Carbon dioxide concentrations produced from organic matter decay with oxygen were not sufficient to describe the measured pH profile. Therefore a distinct source of inorganic carbon diffusing into the model from deeper layers caused by anoxic mineralization processes was introduced. In our simulation, a fixed concentration of 3.8 mmol

l^{-1} ΣCO_2 was set as lower boundary condition, approximating the HCO_3^- and pH of the lower part of the model area.

Attempts to model the pH profile without calcite dissolution kinetics resulted in unrealistic profiles (data not shown; Adler et al., in prep.). The pH profile was then fitted with the parameters of the dissolution kinetics ($DR = k (1-\Omega)^n$). The best fit of the pH profile was achieved with the kinetic parameters of $n = 4.5$ and $k = 7000$ (Fig. 6 B/C). However, changing the k value up to 8400 (+20%) did not have a significant impact on the curve fit.

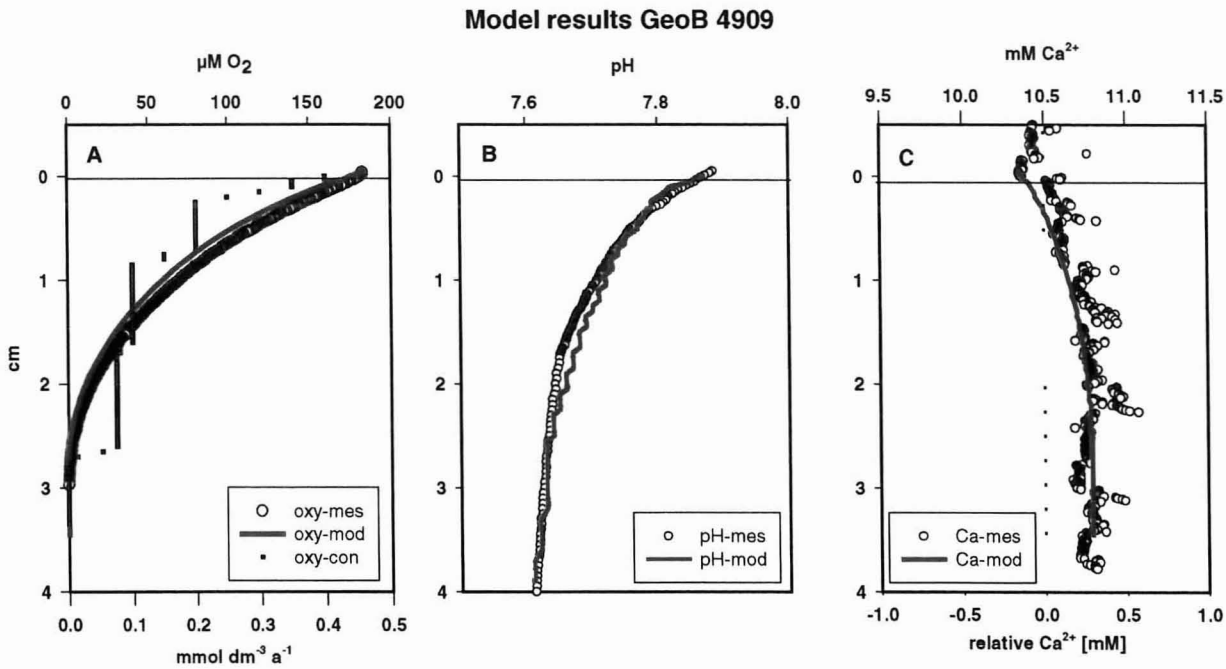

Fig. 6 : Comparison of the modeled (red line) and *in situ* measured (symbols) profiles of O_2, (A) pH (B) and Ca^{2+} (C) at station 4909. The lines are the model outputs using the illustrated consumption rates (A; blue squares) for oxygen and the reaction order n = 4.5 and the dissolution rate constant k = 7000 mol kgw^{-1} a^{-1} for pH and Ca^{2+}.

Discussion

A direct measurement of the dissolution rates is essential to accurately quantify the $CaCO_3$ cycling in modern oceans. We have estimated the calcite dissolution rate using the first *in situ* measured Ca^{2+} microprofiles together with pH and pCO_2 to define the saturation state of the pore water. In combination with O_2 microelectrodes we also quantified the amount of organic matter mineralized in these sediments. To evaluate the interdependence of our

measured profiles, a numerical model was used, which also determined the calcite dissolution rate constant.

Calcite dissolution estimated from Ca^{2+} microprofile

Pore water microprofiles of Ca^{2+}, pH, pCO_2 and O_2 indicate that even under supersaturated bottom water conditions, sedimenting $CaCO_3$ is dissolved within the sediment. Carbon dioxide released during mineralization of organic material creates a microenvironment which is undersaturated with respect to calcite resulting in a dissolution of $CaCO_3$. Our results confirm recent investigations on metabolically driven calcite dissolution (Archer et al., 1989a; Cai et al., 1995; Jahnke et al., 1997). Hales and Emerson (1997a) and Martin and Sayles (1996) estimated calcium fluxes in the range of 0.14 to 0.2 mmol m^{-2} d^{-1} for stations which were supersaturated with respect to calcite in a water depths of 3300 m in an oligotrophic area of the equatorial West Atlantic. In Hales and Emerson (1997a), the calcite dissolution was modeled from obtained O_2 and pH microprofiles, while Martin and Sayles (1996) calculated the diffusive Ca^{2+} flux from pore water calcium profiles measured on samples collected with an *in situ* pore water sampler. Our estimated Ca^{2+} fluxes based on *in situ* measured microprofiles indicate 3-times higher fluxes (0.55 and 0.58 mmol m^{-2} d^{-1} for station 4906 and 4909, respectively). Our measurements were performed at shallower water depth and the oxygen consumption rates at our sites were 3-times higher. Chamber incubations from the equatorial Pacific (calcite rich sediments) and from continental margin of California (calcite poor sediments) exhibited similar Ca^{2+} fluxes, ranging between 0.5 and 1.0 mmol m^{-2} d^{-1} (Jahnke et al., 1997; Berelson et al., 1994).

Using particle flux measurements from Wefer and Fischer (1993) and Fischer and Wefer (1996) we quantified the amount of dissolved $CaCO_3$ from sedimenting calcite rain to the sediments. Sediment trap measurements from a station close to our settings exhibited an average annual flux for Corg of 0.5 mmol m^{-2} d^{-1} and for $CaCO_3$ of 0.66 mmol m^{-2} d^{-1}, leading to a C_{org} / C_{CaCO3} ratio of 1.3. Comparing these water column fluxes to our measured Ca^{2+} flux results in a dissolution of approx. 85 % of the calcite rain. This calculation indicates that most of the $CaCO_3$ produced in the surface waters is dissolved and very little is buried in the sediment. Bulk sediment $CaCO_3$ confirm this observation, since the sediment surface contains only 1.25 % (wt) . Recently modeled dissolution rates of metabolically mediated $CaCO_3$ dissolution are consistent with our results and predict that $\geq$ 50 % of the calcite deposited dissolve (Hales et al., 1994; Emerson and Archer, 1990; Archer, 1991).

Modeled $CaCO_3$ dissolution rate constant at station 4909

Our measured Ca^{2+} flux is predicted by the model when the reaction order n = 4.5 and the dissolution rate constant k = 7000 mol kgw^{-1} a^{-1} was used. Our modeled k of 7000 mol kgw a^{-1} equals a rate constant of 663 % d^{-1}. This value is within the range of values reported from laboratory studies (1000 - 3000 % d^{-1}; Keir, 1980). Jahnke et al. (1997) also estimated a high k (1000 % d^{-1}) for a calcite poor station at the California continental margin. Recently reported rate constants from other field studies were in the range of 0.05 to 125 % d^{-1} (Archer, 1991; Berelson et al., 1990; Cai et al., 1995; Hales and Emerson, 1996), however these studies were performed in sediments with low oxygen consumption rates.

Most of these studies estimating the calcite dissolution rate assumed a reaction order of n = 4.5 (Archer et al., 1989a, Berelson et al., 1990; Cai et al., 1995, Jahnke et al, 1994, 1997). Recently Hales and Emerson (1997a) showed that measured *in situ* pH profiles of a calcite-rich sediment were more consistent with first-order dissolution than with 4.5-order kinetics. Using the sensitivity to uncertainties in $\Omega_{Calcite}$, due to the nature of the term (1 - $\Omega_{Calcite}$), they calculated a lower calcite solubility. However, the first-order kinectics did not resolve the discrepancy of 2 - 3 orders of magnitudes differences between the *in situ* and laboratory rates. There is still a debate about the reaction order, differing between 3 - 5 for biogenic carbonates inferred from laboratory studies (Morse, 1978; Keir, 1980; Walter and Morse, 1985). We chose n = 4.5 in order to compare our model simulations with previous studies (e.g. Archer et al., 1989a; Archer, 1991; Jahnke et al., 1994, Jahnke et al., 1997; Hales and Emerson, 1997; Martin and Sayles, 1996). However, model runs with n values < 4.5 should also be made to estimate the difference in resulting dissolution rate constants.

O_2 consumption

Our oxygen microprofiles indicate that oxygen is consumed rapidly in the top sediment horizon, while the OPD increases with increasing water depths. Our estimated DOU rates of 0.3 to 3 mmol m^{-2} d^{-1} agree with measurements from Glud et al. (1994) performed in 1992 in the upwelling area of the eastern South Atlantic. Their measured DOU were in the range of 0.5 to 5 mmol m^{-2} d^{-1} for stations at water depths of 500 to 5000 m. To calculate the amount of organic carbon degraded by oxygen two factors have to be considered: Steady state reactions are assumed using a Redfield ratio for C : O and secondly, some oxygen can be consumed by reoxidation of reduced species diffusing upward from the anoxic sediment zone. In marine sediments, sulfate reduction is typically the second dominant remineralization process and sulfate reduction rates (SRR) range from 0.1 to 0.3 mmol m^{-2} d^{-1} for our stations (Strotmann et al., in prep). Taking reoxidation of H_2S into account, the amount of organic

matter mineralized by oxygen varies between 0.6 and 2 mmol carbon m^{-2} d^{-1}. These calculated fluxes of organic matter mineralization are 1 to 4-times higher than annual fluxes determined from sediment traps close to our stations (Wefer and Fischer, 1993; Fischer and Wefer, 1996). The higher carbon mineralization rates estimated from our *in situ* oxygen profiles most likely result from lateral and down slope transport of organic material (Jahnke et al., 1990). Further, local variations in surface water primary production and sedimentation due to the upwelling areas in the study region and enhanced carbon discharge from the river Congo can also cause higher organic matter input to the sediments.

pH and pCO_2 microprofiles

Pore water pH decreased sharply below the sediment water interface in response to the oxic degradation of organic matter and the reoxidation of reduced species diffusing upward to the oxygenated horizon. Reactions affecting the pH in the pore water have been described and modeled by Boudreau (1987), Boudreau and Canfield (1993) and Van Cappellen and Wang (1996) and our profiles follow the general trends described in these models. Below the oxic layer pH increases again (station 4906 and 4917), but the increase of our measured pH values was not as high as the modeled profiles predict (Van Cappellen and Wang, 1996). At station 4909 the pH is constant with depths below the oxic sediment zone. This may be due to lower rates of organic matter mineralization by NO_3^-, Mn and Fe resulting in a minor shift of pH towards more alkaline conditions.

There is one major uncertainty in calculating the state of saturation from the measured microprofiles. Using the microprofiles horizontally displaced by on average 25 cm makes it necessary that the geochemical zones within the sediment are horizontally as well as vertically homogenous. Laboratory pH and pCO_2 microelectrode measurements showed that DIC gradients calculated from the obtained microprofile are in good agreement with pore water extracted DIC values (Komada et al., 1998). However, differences in pH of 0.05 lead to an uncertainty in dissolved inorganic carbon (DIC) of approx. 12 %. Heterogeneity in deep sea sediments with less fauna may not be that important, nevertheless microprofiles measured in an area of 125 cm^2 often exhibit varying penetration depths of oxygen (Fig. 5 a-e; Tab. 2). Also individual pH microelectrodes profiling at the same site show variability. For example one sensor indicated a distinct subpeak (Fig. 5 b) not seen in a second profile from the same site. These differences are important to consider when calculating for carbonate equilibrium distribution in the pore water and consecquently in estimating Ca^{2+} dynamics in sediments.

Ideally, 2 - 3 profiles of each chemical species should be measured to evaluate horizontal variability.

Conclusions

Earlier investigations on calcite dissolution based their estimates of calcite fluxes on modeling pore water profiles of O_2, pH and pCO_2. Our data sets provide the opportunity to calculate the amount of dissolved calcium directly from the measured Ca^{2+} microprofiles. At station 4906 and 4909 high fluxes (0.55 and 0.58 mmol m^{-2} d^{-1}) across the sediment water interface were measured. This Ca^{2+} flux results in an efficient dissolution (approx. 85 %) of the $CaCO_3$ rain to the seafloor. Modeled calcite dissolution rate constant (one station) predicted a high *in situ* rate, comparable to one other calcite poor site (Jahnke et al., 1997). More *in situ* profiles of Ca^{2+}, pH and pCO_2 at different sites are necessary to resolve the discrepancy on the saturation states of the pore water and consequently on the calcite dissolution rate.

Acknowledgements- We gratefully acknowledge the captain and crew of the R/V Meteor for their assistance during the cruise. We thank Stephan Meyer for assistance during the lander deployments and together with Axel Krack for preparing the equipment. Thanks are due to Gaby Eickert, Vera Hübner and Anja Eggers for constructing excellent microsensors and measuring the Ca^{2+} samples. This work was funded by the German Science Foundation (contribution No. 123 of Special Research Project SFB 261, The South Atlantic in the Late Quaternary at the University of Bremen).

Chapter 4

In situ microsensor studies of a hydrothermal vent at Milos (Greece)

Frank Wenzhöfer[1], Ola Holby[1,+], Ronnie N. Glud[2], Helle K. Nielsen[3], Jens K. Gundersen[3]

1 Max Planck Institute for Marine Microbiology, Celsiusstr. 1, D-28359 Bremen, Germany
2 Marine Biological Laboratory, University of Copenhagen, Strandpromenaden 5, 3000 Helsingør, Denmark
3 Dept. of Biology, University of Aarhus, Ny Munkegade, Building 550, 8000 Aarhus, Denmark

+ present address: Högskolan Dalarna, Rödavägen 3, 781 88 Borlänge, Sweden

Abstract

The microenvironment and microcirculation of a shallow water hydrothermal vent system was studied together with the benthic primary production at Milos (Greece). *In situ* microprofiles of O_2, pH, H_2S and temperature were obtained using a miniaturised version of a profiling instrument. The sediment temperature increased toward the centre of the vent system, reaching a surface maximum of 100°C in the central yellow coloured sulfidic area. The oxygen penetration depth decreased from the unaffected sediment surrounding the vent system towards the vent centre, however, at the inner vent area the O_2 penetration increased again. Similar results were obtained during laboratory measurements. H_2S concentrations increased rapidly beneath the oxygenated zone in the different vent areas and reached values of approx. 900 mM at sediment depths of 7 - 17 mm in the central vent areas. The microprofiles resolved a microcirculative pattern where local pressure differences in the

outflow of seep fluid induced a downward transport of oxygenated water, creating small convective cells which efficiently reoxidised H_2S in the seep fluid.

Patches of benthic diatoms covered the sediment surface in the areas surrounding the vent system. The net photosynthesis of this community increased from 25 mmol O_2 m^{-2} d^{-1} to 41.8 mmol O_2 m^{-2} d^{-1} from early morning to mid day. The amount of daily net fixated carbon, calculated from the *in situ* oxygen microprofiles accounted for 0.67 mmol C m^{-2} d^{-1}. Laboratory incubations indicated that photosynthesis was not carbon limited and consequently the excess dissolved inorganic carbon contained in the vent fluids presumably had no effect on primary production.

Introduction

Hydrothermal vents are known from many regions of the world (Stein 1984; Hoaki et al., 1995; Kamenev et al, 1993; Tarasov et al., 1990). Depending on the vent type, the seep fluid chemistry can, to various degrees, differ from the surrounding water, and typically the sea floor in the vicinity of vents, host a special geochemistry. This geochemical environment may have significant effects on the biology of the area, and specialised microbial consortia and faunal adaptations have been described from various vent sites (Thiermann et al., 1997; Dando et al., 1995a; and references therein). Hydrothermal activities around the islands of the hellenic volcanic arc in the Aegean Sea have recently been described (Varnavas, 1989; Cronan and Varnavas, 1993; Varnavas and Cronan, 1991; Dando et al., 1995a). These vents tend to be low-temperature discharges precipitating mainly iron and manganese oxides (Cronan et al., 1995). Palaeochori Bay at the island of Milos (Greece) is one of the most active geothermal submarine areas of the Aegean Sea. Previous studies have demonstrated that the seep fluid is influenced by hydrothermal processes, and is enriched by Na^+, Ca^{2+}, K^+, SiO_2, Mn^{2+} and NH_3 (Fitzsimons et al., 1997). Additionally the fluid contains gases of: CO_2 (54.9 – 91.9 %), CH_4 (> 9.7 %), H_2S (> 8.1 %) and H_2 (> 3 %) (Dando et al., 1995b).

Characteristic concentric circles of yellow, white and brown precipitates occur around the vent centres. The yellow colour of the inner vent area results from sulphur condensing on sand grains. The white precipitate is a mixture of amorphous silica, Si nodules and hollow tubes containing elemental sulphur on the outer surfaces (Fitzsimons et al., 1997; Dando et al., 1995b). The brownish zone of the vent system consists of Mn-oxides which predominately precipitate at increasing distances from the vent outlet. The precipitates are assumed to be

associated with microbial mat communities (Fitzsimons et al., 1997; Dando et al., 1995a). The colourless sulphur bacterium *Archromatium volutans* was isolated from the white precipitates (Dando et al., 1995a).

The purpose this study was to investigate and describe the microcirculation of the seep fluid and the overlying water around these vent sites. We also investigated the microenvironments of the associated microbial communities and evaluated to what extent the massive release of CO_2 affected the benthic primary productivity of the area.

Methods

Study area

Palaeochori Bay is a sandy bay covering approx. 34 km^2, located at the Southeast coast of Milos, Greece (Fig. 1). Seep outlets were found over the whole bay at water depths ranging from 3 to 110 m, creating coloured patches on the sediment surface. The position and size of the patches was dynamic and influenced by local hydrodynamics; it was observed that storm events completely destroyed otherwise well developed vent structures at shallow water depths.

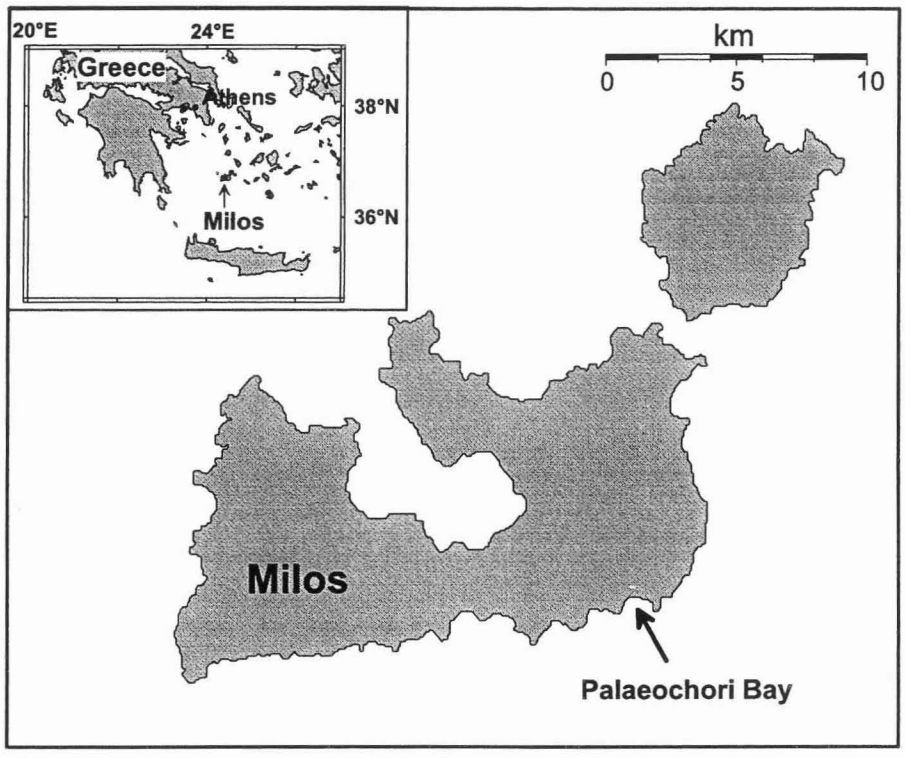

Fig. 1: Map of Aegean Sea and the island Milos, including a magnification of the study area of Palaeochori Bay.

The vent system we investigated covered an area of approx. 36 m^2 and was located at the west side of the bay at a water depth of 3.5 m. The sediment around the vent outlet was yellow (0.5 m in diameter), surrounded by a white area (approx. 1.5 m in diameter) which again was surrounded by an outer brownish area (approx. 5.5 m in diameter) (Fig 2).

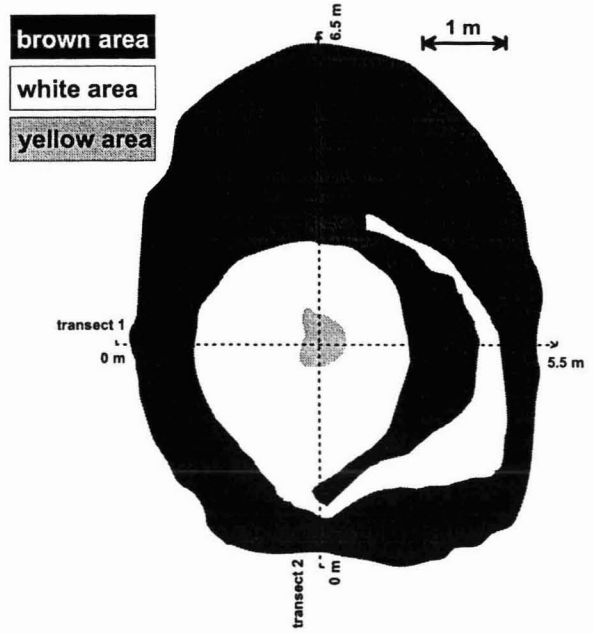

Fig. 2: Schematic drawing of the vent zones; dashed arrows indicate the temperature transects measured by divers.

In situ measurements

In June, 1997, *in situ* chemical microgradients were measured using a modified and miniaturised version of the microprofiling instrument, PROFILUR (Gundersen and Jørgensen, 1990). The modified lander was easily deployable from a zodiac with diver assistance. In order to minimise any sediment disturbance and to assist the divers in positioning the profiling instrument, buoyancy was added. After positioning the tripod carefully on the sediment the buoyancy was released. After a 30 min. delay the microsensors were electronically moved into the sediment in increments of 50 µm. At each depth horizon the sensors were allowed to equilibrate for 13 sec. before the signals were recorded. Four O_2 microelectrodes, two pH microelectrodes, two H_2S microelectrodes and one temperature microelectrode were mounted on the electronic casing during each deployment.

O_2: The oxygen microelectrodes were of Clark type with a guard cathode and internal reference (Revsbech, 1989a). The outer diameter of the sensor tip was 10 - 20 µm, the stirring sensitivity was less than 1%, and the 90% response time < 1 sec. A two point calibration was applied, using the signal in the overlying water and in the anoxic part of the sediment. The O_2 concentration in bottom water samples was determined by Winkler titration (Grasshoff, 1983). The measured sensor signal was corrected for temperature effects after Gundersen et al. (1998). During oxygen measurements at the unaffected area, irradiance was recorded at the sediment surface by a miniaturised light logger (StowAway, Onset).

pH: The pH-microelectrodes were constructed as described by Revsbech and Jørgensen (1986). The outside diameter of the electrodes was 20 - 30 µm and the length of the pH-sensing glass was 75 - 150 µm. Before each deployment the electrodes were calibrated by immersing the sensors in seawater at the *in situ* temperature, and subsequently changing the pH by adding small amounts of H_2SO_4. The microelectrode signals were then compared to the readings of a commercial pH-electrode (Radiometer) calibrated in NBS-buffer. The pH values were corrected for temperature using the measured temperature microprofiles (Westcott, 1978).

Temperature: The temperature microsensors consisted of a soldered miniature Cupper-Konstantan thermocouple (25 µm; California Fine-wire Company) inserted into a glass capillary. A two point calibration against a commercial thermometer was performed in seawater. Temperature transects across the vent system at sediment depths of 2, 6 and 10 cm were performed by SCUBA divers using hand held thermometers (Fig. 2).

H_2S: Amperometric H_2S microsensors were constructed as described by Jeroschewski et al. (1996) and Kühl et al. (1998). The outer diameter of the electrodes was 20 - 50 µm with a response time < 1 sec and a sensitivity of approx. 2 µM. The H_2S microelectrodes were calibrated with degassed 0.2 M phosphate buffer solution (pH 7.5; 100 mL). During calibration the headspace was continuously flushed with N_2 , and the H_2S concentration was increased stepwise adding known aliquots of a 100 mM Na_2S solution. The H_2S concentrations were subsequently measured in subsamples (fixed in 0.5 mL 1.5M NaOH and 2 mL 0.12 zinc acetate) with a spectrophotometer after Gilboa-Garber (1971) at 670 nm. The

measured electrode signals were later corrected for temperature effects (Jeroschewski et al., 1996; C. Steuckart, pers. com.).

Laboratory measurements

Sediment cores were collected by divers for measurements of oxygen profiles in the laboratory. The cores were incubated in a water bath at *in situ* temperature and the overlying water was gently stirred to create a diffusive boundary layer (DBL) comparable to the *in situ* conditions (Rasmussen and Jørgensen, 1992). Microprofiles were measurements with O_2 microelectrodes mounted on a motor-driven micromanipulator interfaced to a computer (Revsbech and Jørgensen, 1986). The microelectrode characteristics were comparable to the microelectrodes applied *in situ*. Oxygen dynamics within the precipitated surface material of the white vent area was measured by gently transferring this material to agar-membranes. Microprofiles were measured from the overlying water through the white precipitate into the agar.

Calculations

The diffusive oxygen exchange across the sediment water interface was calculated from Fick´s first law: DOU = D_0 dC/dz, where D_0 = the molecular diffusion coefficient in water corrected for temperature and salinity (from Li and Gregory, 1974 and Broecker and Peng, 1974) and dc/dz = the linear gradient of oxygen within the DBL. Diffusive fluxes within the sediment were calculated using Fick´s first law as well with the empirical relations for diffusion coefficients in sediments: $D_s = D_0 \phi^{m-1}$, where ϕ = porosity, D_s = diffusion coefficient in the sediment corrected for temperature and pressure (Li and Gregory, 1974; Broecker and Peng, 1974) and m = 2 for sandy sediments (Ullmann and Aller, 1982; Berner, 1980). Net fluxes of O_2 from the photic zone at the unaffected sites was defined as the sum of the up- and downward flux away from the photosynthetic active community (Glud et al., 1992).

Results

Temperature transect

The surface sediment temperature increased towards the centre of the vent system reaching a maximum of approx. 100°C. On the average, the temperature increased by approx.

0.6°C cm^{-1} in the white area and the steepest increase was observed at the border between the white and yellow area (Fig. 3). The vertical temperature gradient (in the upper 10 mm) was steep in all areas of the vent system and was on the order of 2, 15 and 40 °C cm^{-1} in the brown, white and yellow vent area, respectively (Fig. 4f-h). The steepest gradient was at the sediment water interface in the yellow area (Fig. 4h). Temperature was constant with depth in the unaffected area (Fig. 4e).

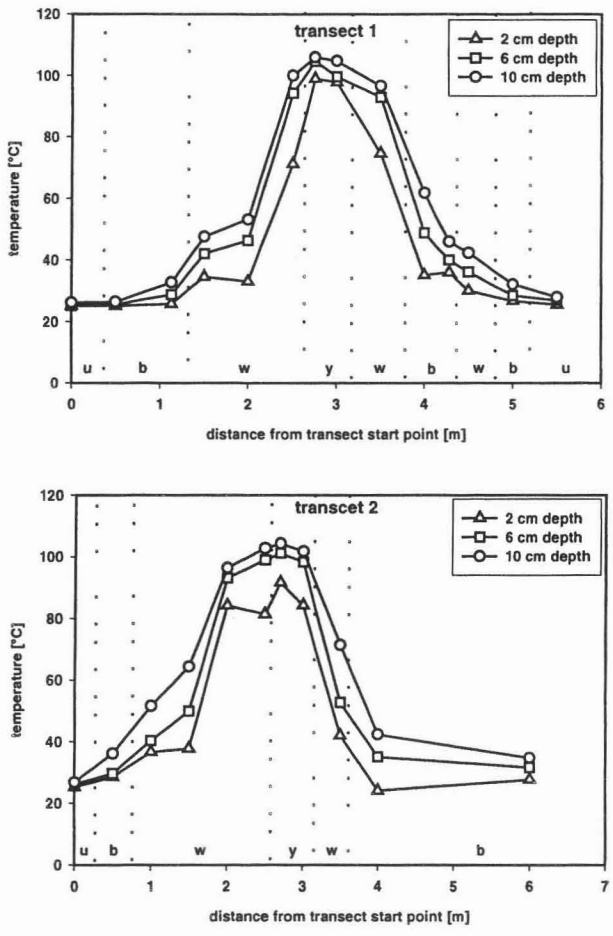

Fig. 3: Sediment temperature transects (1 and 2) across the vent system at 2, 6 and 10 cm dept. Temperature was measured along the transects as indicated in Fig. 2 (u = unaffected area, b = brownish area, w = white area, y = yellow area).

In situ microprofiles

The oxygen penetration depth gradually decreased from the unaffected area towards the white area (Fig 4a-d, Tab. 1). Thereafter the oxygen penetration increased to a maximum of 6 mm in the yellow vent centre (Fig 4d, Tab. 1). In the central part, the O_2 signal became irregular with highly fluctuating values, most likely due to convection of pore fluids.

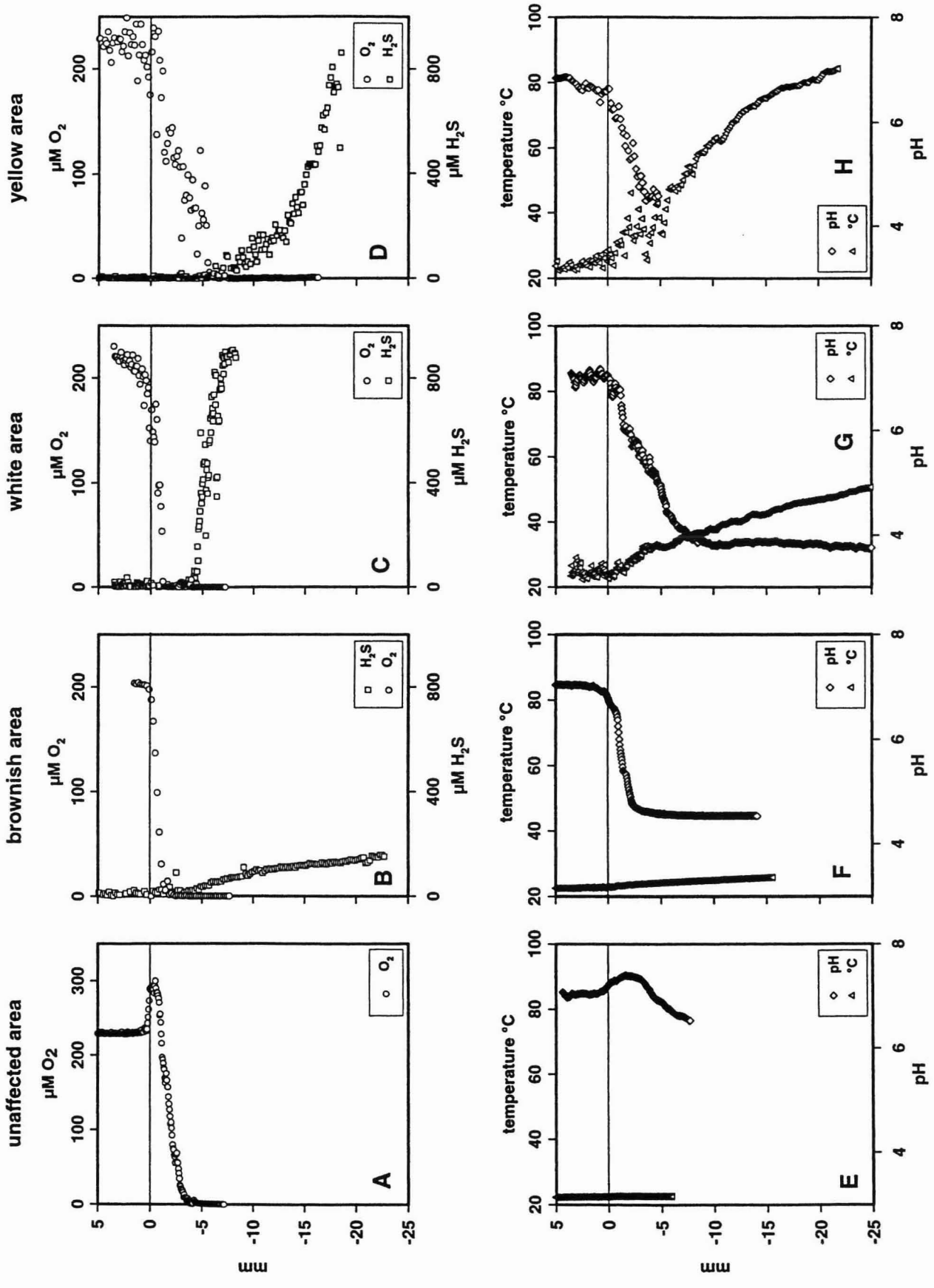

Fig. 4: *In situ* microprofiles of O_2, H_2S, pH and temperature measured at an unaffected (A/E) and the different vent areas (brown: B/F, white: C/G and yellow: D/H).

Table 1: Oxygen penetration depth (OPD) and diffusive oxygen uptake (DOU) measured *in situ* and in laboratory from the different vent areas. OPD and DOU determined in sediment cores separeted from the white fluff (white –fluff) and in the white fluff. Numbers of profiles used for the calculation shown in parentheses.

	In situ	laboratory	
	OPD [mm]	**OPD [mm]**	**DOU [mmol m^{-2} d^{-1}]**
unaffected	**4.2 ± 0.3 (3)**	**3.4 ± 0.2 (4) [1]**	**11.7 ± 1.4 (4) [1]**
brown	**2.0 ± 0.4 (3)**	**1.7 ± 0.2 (3)**	**19.8 ± 0.7 (3)**
white	**1.3 ± 0.1 (3)**	**0.4 ± 0.1 (3)**	**55.1 ± 2.8 (3)**
yellow	**6.0 ± 1.4 (3)**	**0.9 ± 0.1 (3)**	**28.1 ± 6.3 (3)**
white (- fluff)	-	**0.3 ± 0.1 (3)**	**48.0 ± 9.3 (3)**
fluff	-	**0 (2)**	**0 (2)**

[1] no diatoms present on the sediment surface of the core

Continuous O_2 microprofiles during a daily cycle at the unaffected sediment site covered with diatoms demonstrated a gradual increase in O_2 concentration at the sediment surface (Fig. 5a/b). At the investigated site (covering approx. 125 cm^2), a maximum of 350 µM was reached at approximately noon (Fig. 5a). The sediment community had an light compensation point of ~ 114 µE, where the O_2 produced by photothrophs balanced the O_2 consumption rate. In darkness the O_2 consumption rate at the surface sediment (upper ~ 0.8 mm) was ~ 25 mmol m^{-2} d^{-1}. From the net photosynthetic rates and the light measurements, a PI relationship (photosynthesis vs light intensity) was constructed and was fitted to an exponential equation; oxygen flux = $38 * (1-e^{-0.007*(x-96)})$ (Fig. 5c). The net photosynthesis reached a saturation at approx. 300 µE where the net release rate of O_2 was approx. 40 mmol m^{-2} d^{-1}. By combining the light and the net rates and assuming that 1 CO_2 is net fixated per 1 O_2 released the daily net C fixation of the photosynthetic community was 0.67 mmol C m^{-2}. It must be underlined that the diatoms had very patchy distribution and that our measurements do not necessarily represent the average conditions at the shallow areas of Palaeochori Bay.

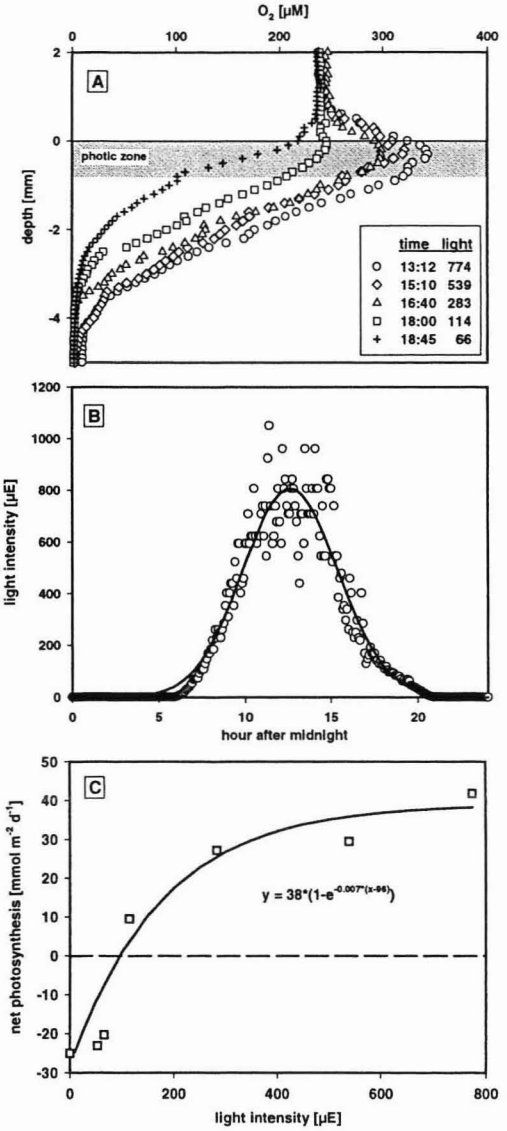

Fig. 5: (A) *In situ* oxygen microprofiles at various light intensities (units are µE), (B) daily cycle of light intensity at the sediment surface and (C) net photosynthesis plotted against light intensity (PI-curve) at the unaffected sediment site.

While no H_2S was measurable in the unaffected sediments, the vertical microprofile in the brown area exhibited a gradual increase in H_2S with depth (11 µM mm^{-1}; Fig. 4b). However, in the white and yellow area the H_2S concentration very rapidly increased below the oxic zone and reached a H_2S concentration of approx. 900 mM at 7 mm and 18 mm in the white and yellow area, respectively (Fig. 4c/d). Maximum gradients in the white and yellow vent area were 300 and 100 µM mm^{-1}, respectively. Beneath these depth horizons the sensor signal at both areas went off scale but was still working for the complete profiling distance of 3 cm, because the sensor signal showed the same value in the overlying water after the

profiling. This sensor behaviour indicates that the H_2S concentration was at least higher than 800 µM (the maximum measurable value for these sensors). Comparable sulfide concentrations ranging from 400 to 1300 µM at 2 and 5 cm sediment depth has been measured by Thiermann et al. (1997) in white areas of a hydrothermal vent system close to our study site. The brown and yellow area exhibited an overlap of downward transported oxygen and upwards transported H_2S, but this overlap was not found in the white area.

In the unaffected area, the pH microprofile increased with depth indicating a CO_2 fixation at the sediment surface associated with a significant pH increase (Fig. 4e). In the brown, white and yellow area, microprofiles exhibited decreasing pH values (Fig. 4f-h). The minimum in pH of 4.5 in the brown vent area was found at the same depth as the oxic-anoxic interface (Fig. 4f). In the white area, the pH minimum occurred where the H_2S concentration began to increase (Fig. 4g). While in the yellow vent area pH decreased gradually down to a value of 4.5 at a sediment depth of 5 mm (Fig. 4h).

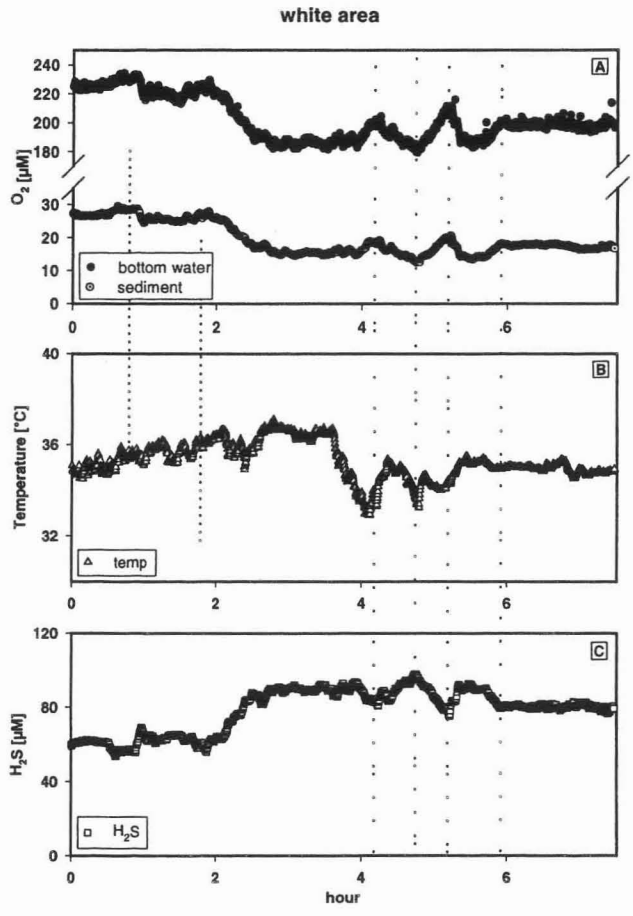

Fig. 6: Time series measurements in the white vent area (sensors were horizontally displaced between 2.5 and 7.5 cm): (A) oxygen 1 mm below and 0.75 mm above sediment surface, (B) temperature 4.4 mm below the sediment surface and (C) H_2S 5.0 mm below the sediment surface.

Time Series

Time series measurements of O_2 at 1 mm below and 0.75 mm above the white precipitates (sensors horizontally displaced by 7.5 cm) showed relatively constant signals over a 7.5 hour period (resolution of 15 sec; Fig. 6a). However, occasional events where O_2-enriched or O_2-depleted water passed the sensors tips was apparent and the signals of the two sensors were coupled (Fig. 6 and 7a). The temperature and H_2S concentration (recorded 4.4 and 5.0 mm below the sediment, respectively) showed a similar trend and was negatively correlated to the O_2 concentration (Fig. 6b/c and 7b). Time series measurements in the yellow area were very sporadic due to electronic failure, however, the recorded fluctuations were characterised by higher frequency and larger amplitudes as compared to the white area (data not shown). The fluctuations in the brownish vent area were small, and non-existent outside the vent area (data not shown).

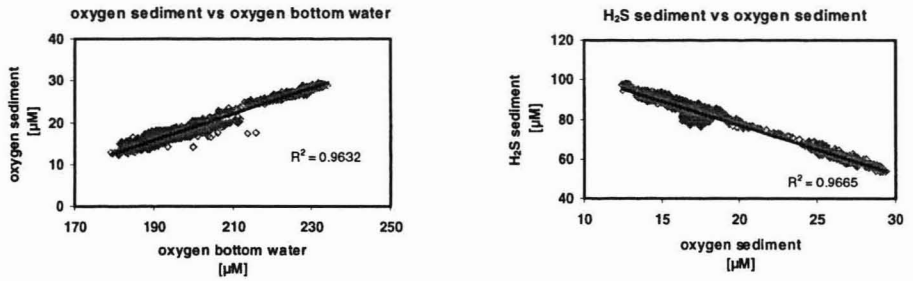

Fig. 7: Correlations of oxygen concentration below the sediment surface (-1 mm) vs bottom water oxygen concentration (0.75 mm) and (A) oxygen concentration below the sediment surface (-1 mm) vs H_2S concentration below the sediment surface (-5.0 mm) at the white vent area.

Laboratory

Oxygen microprofiles in the laboratory cores showed the same trend as the *in situ* profiles; with penetration depths gradually decreasing toward the white area and increasing again in the yellow area (Fig. 8a-d; Tab. 1). The elimination of the thermal induced convection in the cores collected from the white area lead to more stable gradients. The diffusive oxygen fluxes calculated from the laboratory microprofiles reflected the O_2 penetration pattern *in situ* with maximum O_2 consumption in the white vent area (Tab. 1). The fluxes indicated that the white area was most reduced and the yellow surface was more oxidised presumably due to the *in situ* microcirculation of oxygenated water. Measurements in the sediment cores from the white area with and without fluff present, indicated only marginal

oxygen consumption at the SiO_2-precipitates (Fig. 8c/e; Tab. 1). This observation was confirmed by measurements in isolated crystals (Fig. 8f; Tab. 1). Microscopic examinations showed very little microbial activity and mat-like structures could not be confirmed.

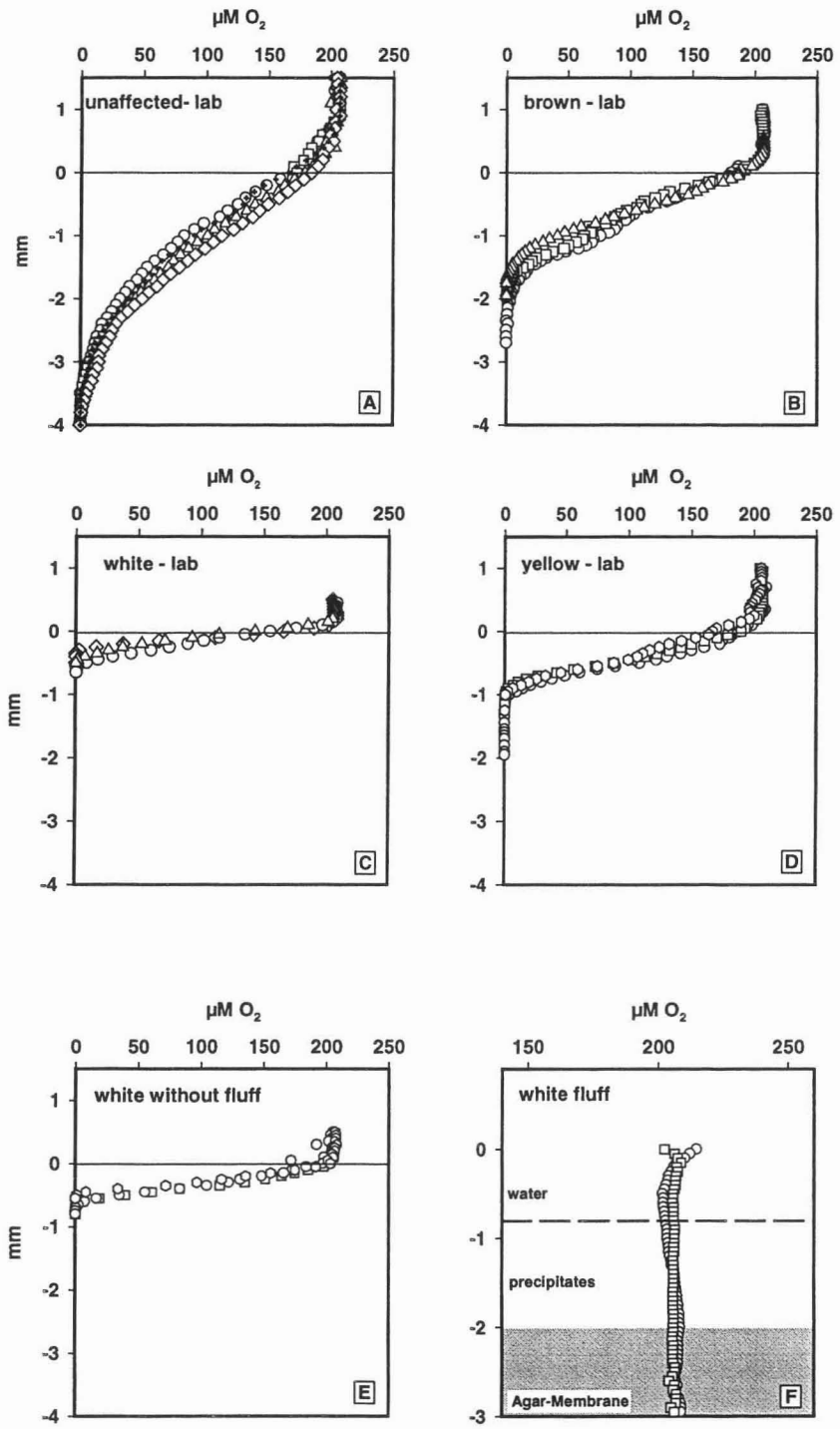

Fig. 8: Laboratory O_2 microprofiles from the unaffected (A), brownish (B), white (C) and yellow (D) vent area. Laboratory O_2 microprofiles measured in a sediment carefully separated from the white fluff (E) and through the removed white precipitate prepared on a Agar-membrane (F).

Photosynthesis of the benthic diatoms was investigated in sediment cores from the unaffected area incubated at *in situ* temperature and constant light intensity (355 µE) with increasing DIC concentrations. Net photosynthetic rates were not affected by changing DIC concentrations from 1800 to 2600 µM (*in situ* value approx. 2400 µM) (Tab. 2).

Table 2: Laboratory measurements of the oxygen penetration depth (OPD) and the up and down flux of oxygen from the photic zone at a light intensity of 355 µE incubated at different dissolved inorganic carbon (DIC) concentrations. Numbers of profiles used for the calculation shown in parentheses.

DIC [µM]	OPD [mm]	flux up from photic zone [mmol m^{-2} d^{-1}]	flux down from photic zone [mmol m^{-2} d^{-1}]
1800	**5.5 ± 0.7 (5)**	**19.4 ± 1.6 (5)**	**20.7 ± 2.9 (5)**
2200	**5.7 ± 0.1 (7)**	**18.4 ± 2.2 (7)**	**14.2 ± 1.7 (7)**
2600	**5.4 ± 0.4 (6)**	**19.8 ± 4.0 (6)**	**19.0 ± 2.5 (6)**

Discussion

Vent pattern and zonation

The hydrothermal activity in Palaeochori Bay produces advective flow through the overlying sediments. By comparing the microprofiles of O_2, H_2S, pH and temperature, a microcirculative pattern was resolved where seep fluid escapes in the central yellow vent area. The outgoing jet in the yellow area creates local pressure differences in the sediment sucking down O_2 , resulting in small convective cells. The effect, however, of sucking down O_2 extends into the white area, where it is gradually dampened. Microprofiles of O_2 and H_2S indicated that the microcirculation presumably leads to an efficient H_2S reoxidation in the centre of the vent system and very little dissolved H_2S escapes to the overlying water (Fig. 9). The oxidation of hydrogen sulfide, $2\ H_2S + O_2 \rightarrow S^\circ + H_2O$, most likely forms elemental sulphur or polythionates, which condense at sediment grains. Analyses of the yellow deposits yielded sulphur concentrations of 1.1g dm^{-3} (Fitzsimons et al., 1997). Seep fluid investigations showed that the escaping water was enriched in SiO_2 (Fitzsimons et al. 1997). Decreasing temperature with increasing distance from the vent outlet reduces the solubility of $Si(OH)_4$

(log k at 84°C –4.0 decreasing to log k of –3.36 at 25°C), presumably leading to the precipitation of amorphous SiO_2 resulting in the white area of the vent system (Fig. 9). Particles of elemental sulphur may attach to the "strings" of amorphous silica giving rise to the gradually colour change from yellow to white (Fitzsimons et al., 1997; Von Damn et al., 1985).

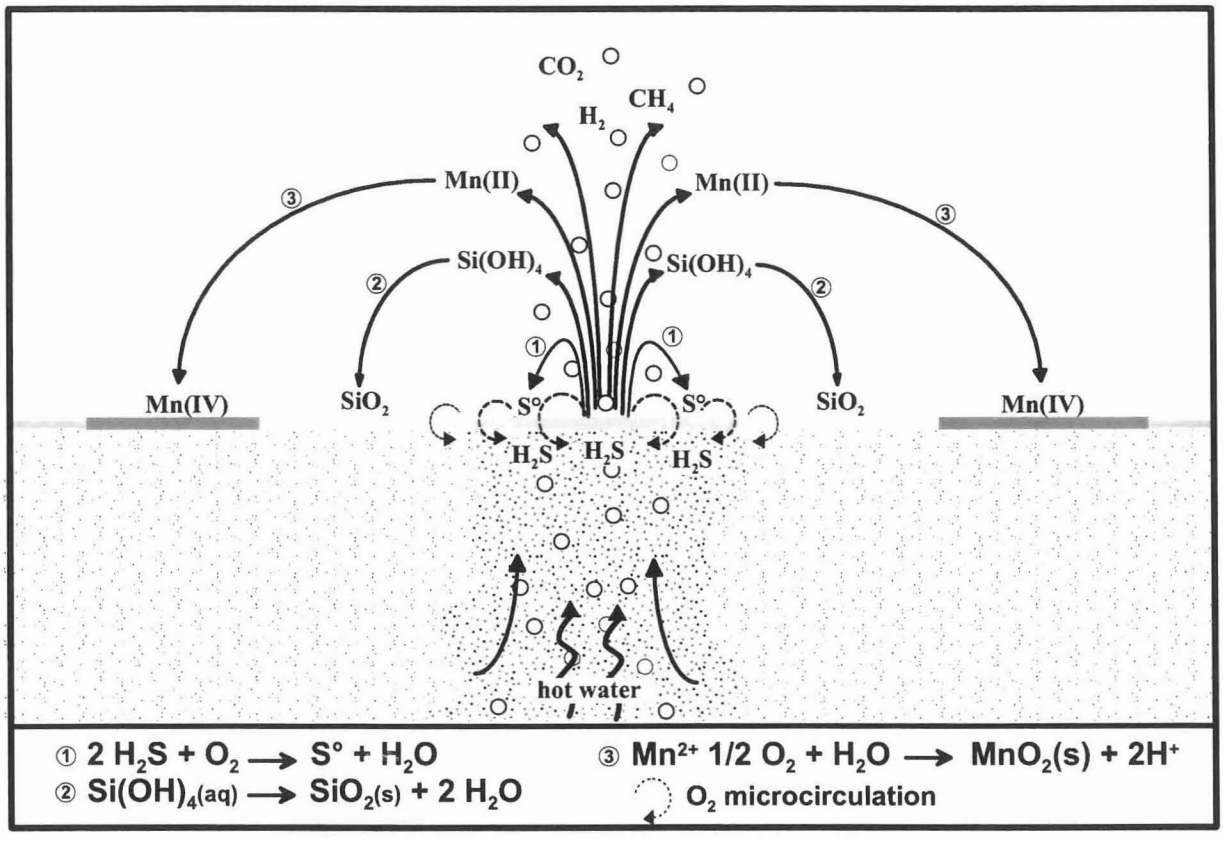

Fig. 9: Illustrastion of the chemical and hydrothermal circulation including the chemical reactions around the vent system.

The escaping seep water was enriched with Mn(II) which is spontaneously oxidised to MnO_2 according to $Mn^{2+} + ½ O_2 + H_2O \rightarrow MnO_2(s) + 2H^+$. The precipitate spread over larger areas but primarily settled at a distance of approx. 1.5 m from the vent outlet (Fig. 9). Similar observations on Mn discharge and precipitation at seep outlets of the island Santorini (Greece) have previously been described (Smith and Cronan, 1983).

We were not able to confirm the existence of any bacterial/mat-like structure around the vent site. The vent site we investigated was stable for a period >1 month and during these

period no significant microbial colonisation was observed. These findings were confirmed by microscopic investigations of samples from the vent site. While shallow vent systems are more exposed to storms and associated resuspensions, sites at deeper water depths are probably more stable and bacterial/mat-like structures may potentially evolve there.

Photosynthesis and CO_2 fixation at an unaffected area

Areal net photosynthesis of the diatom-covered unaffected sediment accounted for an approximate daily C fixation of 8 mg m^{-2}. It must be stressed that this number is an estimate since the diatom coverage was patchy. However, the rate is low compared to other coastal environments (Joint, 1978; Cadee and Hegeman, 1974, 1977; Barranguet et al., 1998). This probably reflects the relatively oligotrophic setting of Palaeochori Bay. The net activity and gross rate of oxygen production (not shown) were not affected by increased availability of DIC, indicating that the photothrophic community was limited by light (up to approx. 300 µE) and nutrients rather than DIC. The pelagic net primary production measured in the shallow water hydrothermal systems was also very low with rates less than 12 mg C m^{-3} d^{-1} (Robinson, in press). The macrophytes of Palaeochori Bay accounted for a C fixation of approx. $^2/_3$ of our estimates for benthic microphytes, estimated from shoot production at seegrass patches (Nielsen et al. unpubl. data). These numbers underline the importance of benthic diatoms as primary producers of this oligothrophic setting.

Acknowledgements - We wish to thank Preben Sørensen and Lars B. Pedersen (University of Aarhus) for assistance during the field trip in Milos and building the microsensors. Gabriele Eickert (MPI, Bremen) is thanked for building the H_2S microsensors. We would also like to thank Prof. D. Dyrssen for numerous constructive discussions. Dr. S. Boehme is thanked for carefully reading the manuscript. This study was funded by the Commission of the European Community under MAST III program, project No. CT95 - 0021. FW was partly supported by the Deutsche Forschungsgemeinschaft (SFB 261, University of Bremen) and MPI, Bremen. RNG was partly supported by Danish Natural Science Research Council.

Chapter 5

Carbon oxidation in sediments of Gotland Basin, Baltic Sea, measured *in situ* with benthic landers

Oliver Greeff, Frank Wenzhöfer, Wolfgang Riess, Andreas Weber, Ola Holby[1], Ronnie Nøhr Glud[2]

Max Planck Institute for Marine Microbiology, Celsiusstraße 1, D-28359 Bremen, Germany

[1] Present address: Högskolan Dalarna, Röda Vägen 3, 78188 Borlänge, Sweden
[2] Present address: Marine Biological Laboratory, University of Copenhagen, Strandpromenaden 5, 3000 Helsingør, Denmark

Abstract

Benthic carbon mineralization was studied *in situ* at 4 stations of the Gotland Deep (Baltic Sea). The measurements were performed with three benthic landers measuring diffusive oxygen uptake (DOU), total oxygen uptake (TOU), and sulfate reduction rates (SRR). At the three oxic stations DOU varied between 7.6 and 8.7 mmol m^{-2} d^{-1}, while the O_2 penetration depth was relatively constant around 1 mm. TOU was found to vary between 4.3 and 10 mmol m^{-2} d^{-1}. SRR's were moderately high for coastal settings (0.7 - 9.0 mmol m^{-2} d^{-1}), and were the major degradation pathway of the benthic community. Laboratory determined sulfate reduction exhibited slightly higher rates as compared to *in situ* rates. Carbon mineralization rates estimated from TOU compared to SRR within a factor of 2.

Introduction

About 90% of the world's annual organic carbon input to marine sediments is believed to be deposited in areas of the ocean underlain by surficial sediments with oxygen penetration depths ≤ 2 cm (Berner, 1982; Hedges and Keil, 1995). Microbial mineralization under oxic or anoxic conditions recycles a significant fraction of carbon and nutrients in sedimenting organic matter, while the remainder is permanently buried in the sediment. This fraction is positively correlated to the sediment accumulation rate and consequently it is high in coastal and shelf sediments (e.g. Canfield, 1989; Henrichs, 1992). The quantitatively most important electron acceptors for benthic degradation have proven to be oxygen and sulfate (Bender and Heggie, 1984; Henrichs and Reeburgh, 1987), with Fe-oxides and Mn-oxides being of importance in some sediments (e.g., Canfield *et al.*, 1993a). The contribution of oxygen to overall degradation in coastal marine sediments (with oxygenated bottom water and high deposition rates) has been quantified to be in the order of 5 - 20% (Canfield *et al.*, 1993b), while sulfate reduction usually accounts for the major fraction. The benthic oxygen consumption is often used as a measure of the total mineralization rate (Smith and Hinga, 1983). Total oxygen uptake of a sediment includes two fractions: 1) direct heterotrophic respiration, and 2) oxygen consumed by reoxidation of reduced products from anaerobic degradation pathways. In euxinic and semi-euxinic environments, however, sulfate reduction rates (SRR) alone are considered a good measure of the total carbon degradation (Westrich, 1983; Canfield, 1989).

This study represents the first attempt to study benthic remineralization and the importance of sulfate reduction as a degradative pathway with three autonomous benthic landers capable of measuring different key parameters in carbon mineralization (diffusive and total oxygen uptake, and sulfate reduction). All 3 landers were deployed at 4 stations along a transect from the oxic slopes of Gotland Basin into its anoxic center.

Materials and Methods

Study area and sediment description

The Baltic Sea is the largest brackish water body in the world, covering an area of approx. 372,000 km^2. A permanent halocline at approx. 60 - 80 m depth prevents vertical mixing between the almost homohaline surface waters and deeper water masses of higher salinity; additionally, a seasonal thermocline develops during the summer months in the surface water body, producing an intense stratification (Kullenberg, 1981). During stagnation periods the deep water can be subdivided into two bodies: a subhalocline layer with a permanent oxygen deficiency but no

anoxia, and the bottom water below approx. 170 m that is frequently anoxic (Grasshoff and Voipio, 1981; Stigebrandt and Wulff, 1987). Gotland basin is a flat basin with gentle slopes and a maximum depth of 249 m that displays almost permanently anoxic conditions in its deepest parts. Annual sediment accumulation rates of 1.0 - 1.3 mm a^{-1} have been estimated in the central Gotland Basin, but on the slopes these values are lower and occasionally erosional events occur (Winterhalter *et al.*, 1981). The Holocene muds in the Central Baltic have very high organic matter content (10- 15% dry weight, Winterhalter *et al.*, 1981). The surface sediments of the investigated stations were soft, black, organic-rich muds with porosities around 0.9 (Tab. 1).

Table 1: Porosity and macroinfauna of the stations.

Station	porosity 0-2 cm	porosity 3-6 cm	**Macoma balthica** individuals m^{-2}	**Monoporeia affinis** individuals m^{-2}
1	0.93	0.85	30 – 40	200 - 250
2	0.90	0.91	0	0
3	0.99	0.93	0	0
4	0.96	0.98	0	0

Station locations and sampling methods

Four stations along a transect from the oxic into the anoxic part of Eastern Gotland Basin, Baltic Sea, were visited in August 1996 (Fig. 1). CTD profiling revealed a stratified water column with thermocline and pycno-/oxycline at each station (data not shown). Basic station information is summarised in Tab. 2. Sediment was sampled at each station with a multiple corer for laboratory incubation measurements (Barnett et al., 1984). The three benthic landers were deployed once at each station in order to measure oxygen-microprofiles (PROFILUR, Gundersen and Jørgensen, 1990), total oxygen uptake (ELINOR, Glud *et al.*, 1995) and sulfate reduction rates (LUISE, Greeff *et al.*, 1998) *in situ*. Each lander was deployed once at each station.

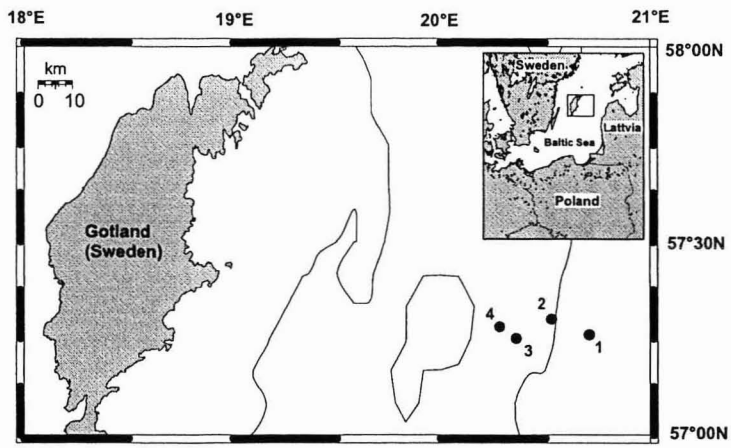

Fig. 1: Map of the study area and position of the stations along the transect into Gotland Basin. Water depth increases to the west. The map in the lower left corner shows the Baltic proper and, in the enlarged section, the position of the study area.

Table 2: Station characteristics. Oxygen data are from water samples taken by landers, other hydrographical data are from CTD casts and refer to bottom water.

Station	*Position*		Depth	Temperature	Bottom water O_2		Salinity	pH
			m	°C	µM	% air sat.	‰	
1	57°16 N	20°43 E	75	4.5	112	29.4	8.5	6.98
2	57°18 N	20°32 E	115	4.5	68	18.1	11	7.06
3	57°15 N	20°21 E	155	4.3	40	10.6	11	7.04
4	57°17 N	20°17 E	210	4.0	0	0	12	6.96

Oxygen microprofiles obtained by PROFILUR

PROFILUR is a pre-programmed free falling benthic lander system (Reimers, 1987; Gundersen and Jørgensen, 1990; Glud *et al.*, 1994) designed to measure *in situ* microprofiles of oxygen. During this cruise PROFILUR was equipped with six oxygen microelectrodes and the depth resolution was set to 100 µm. The oxygen microelectrodes were of Clark type with a guard cathode, internal reference, and an outer tip diameter of 10-30 µm (Revsbech, 1989a). Response

time was $t_{90} < 1$ sec, and stirring sensitivity was 1 - 2%. The lander was also equipped with a Niskin bottle to collect bottom water, which was used for electrode calibration by Winkler titration. All electrodes were checked for drift by comparing *in situ* readings in bottom water before and after the profiling. Typically 3 - 4 parallel microprofiles were obtained at each oxic station (2 - 3 electrodes did not function or broke during the deploxment). The oxygen penetration depth and the thickness of the diffusive boundary layer (DBL) were determined directly from the profiles as described by Jørgensen and Revsbech (1985). The position of the sediment surface was estimated from a change of the slope of the oxygen concentration gradient due to impeded diffusive conditions in the sediment as compared to the bottom water (Revsbech, 1989b; Sweerts *et al.*, 1989). Diffusive oxygen uptake was calculated using Fick's first law of diffusion: $J = (-) D_0 \, dC/dz$, where D_0 = sea water diffusion coefficient and dC/dz = the linear oxygen gradient in the DBL. The sea water diffusion coefficient (D_0) for oxygen given in Li and Gregory (1974) was corrected for the *in situ* temperature by the Stokes-Einstein equation. The dC/dz was calculated from the linear concentration change in the DBL of the obtained microprofiles.

A model to calculate activity zones of oxygen consumption in the sediment was applied to the averaged profiles (Berntsen and Ramsing, in prep.). The model finds a best fit for the shape of the profile and optimises the minimum number of activity zones that describe the profile best. The porosity values (vol/vol) used in the model and for calculating SRR were determined at a resolution of 1cm in a core subsampled from a multiple corer (24h drying of a known amount of sediment to constant weight at 70°C).

Measurements of TOU and nutrient fluxes by the benthic lander ELINOR

ELINOR is a free falling lander system equipped with a chamber that incubates 30 x 30 cm of sediment. After landing at teh seafloor the chamber penetrates 20 to 30 cm into the sediment and a lid closes (Glud *et al.*, 1994). Two Clark type oxygen mini-electrodes are mounted in the lid to monitor the decrease of oxygen in the enclosed bottom water during the incubation. Electrodes were calibrated from an onboard zero reading at *in situ* temperature and the constant reading in the bottom water. During the incubation the water was gently mixed by a central stirrer (8 rpm), which creates a DBL of approx. 500 µm (Glud *et al.*, 1995), depending on the roughness of the sediment surface. During the incubation, a shovel closes, isolating the incubated sediment from the sea floor. After recovery of the lander, the sediment is sieved and analysed for macrofauna.

Measurements of sulfate reduction by the benthic lander LUISE

The autonomous benthic lander LUISE incubates six sediment cores (max. 60 cm length) with radiolabeled sulfate ($^{35}SO_4^{2-}$) to determine sulfate reduction rates (SRR) *in situ*. The six cores are inserted into the sediment together after the instrument lands, and the sediment is injected with radiolabeled sulfate in each core at pre-programmed times (Greeff *et al.*, 1998). To overcome the artefacts of transient warming and decompression during ascent and recovery of the lander, the turnover of three cores injected shortly before the return of the lander are subtracted from the turnover of the remaining cores which have been incubated *in situ* for a given incubation time (see Greeff *et al.*, 1998). Upon recovery, the cores from LUISE were immediately sliced in 1 cm intervals and fixed in 20 ml 20% zinc acetate to stop metabolic activity (slicing procedure was approx. 20 min. per core at room temperature).

In order to evaluate potential differences between *in situ* and laboratory studies, the injection and incubation pattern of the lander was mimicked in the laboratory (incubation time and temperature). However, these cores were recovered by a multiple corer and were injected sideways through silicone-stoppered ports.

In the laboratory the samples collected *in situ* and onboard were distilled in an acid Cr(II) solution to volatilise and trap the reduced sulfur species (Fossing and Jørgensen, 1989). Sulfate reduction rates were calculated according to Jørgensen (1978). Sulfate was measured unsuppressed by ion chromatography (WATERS) from the samples fixed in zinc acetate. Incubation times were chosen between 13 and 18 h and SRR were calculated as an average of the 3 replicates.

Results

Oxygen dynamics

At the oxic stations DOU varied between 7.6 mmol m^{-2} d^{-1} and 8.7 mmol m^{-2} d^{-1}, and the O_2 penetrations were 1.2, 1.4 and 0.7 mm at station 1, 2, 3, respectively (Tab. 3, Fig. 2). Total oxygen uptake (TOU) as measured by *in situ* uptake rates in the benthic chamber was higher than DOU at Station 1 (20%, Tab. 3), the only station with benthic macrofauna. At Station 2 DOU and TOU were similar, while the TOU at station 3 was lower by 56%. At Station 4 (210 m) no oxygen was present in the bottom water (Tab. 2).

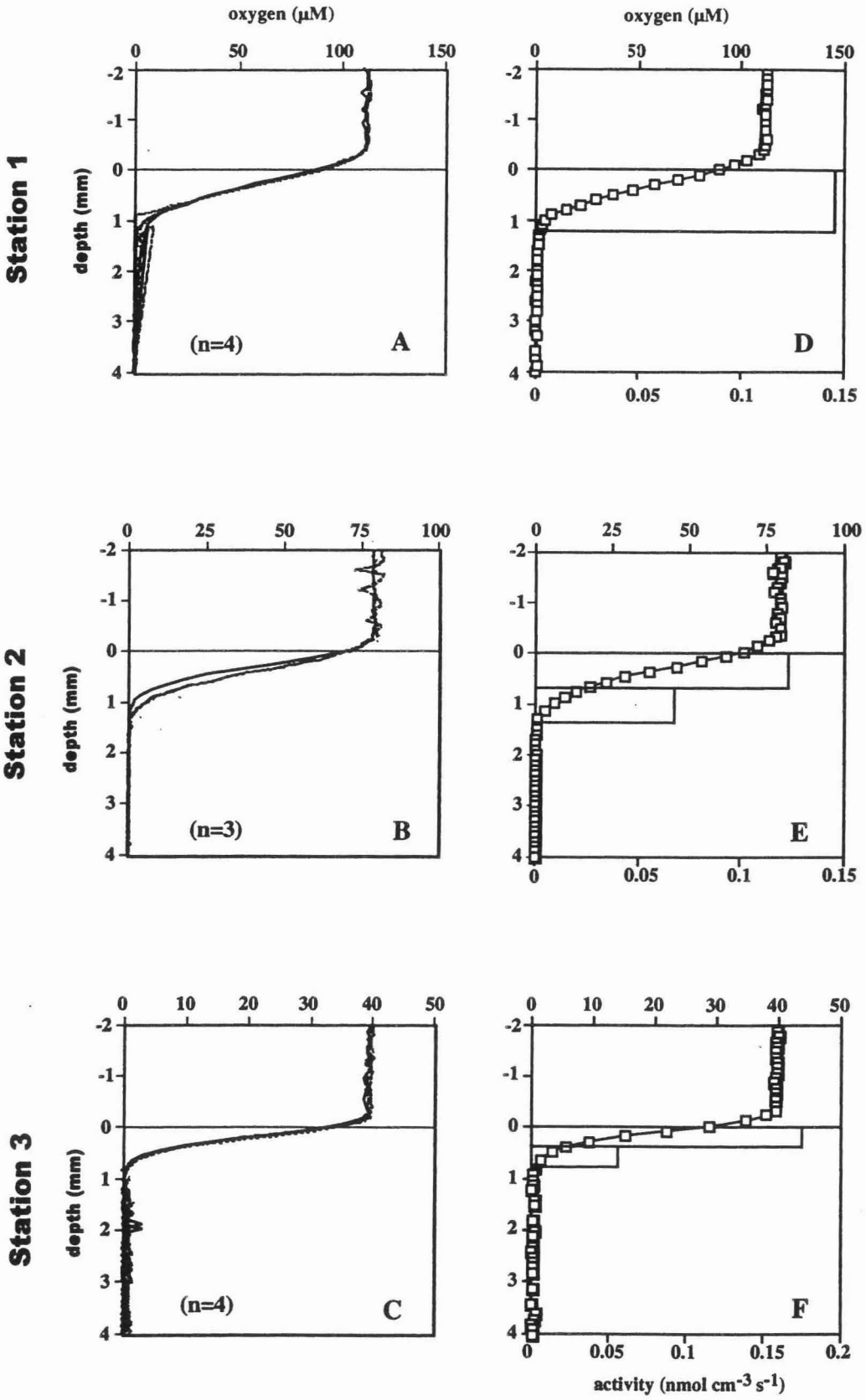

Fig. 2: Oxygen microprofiles of Stations 1 - 3 obtained by the lander Profilur. A-C shows all profiles used for the calculation of the average profile. D-F depicts average profile and modelled activity zones of oxygen consumption.

Table 3: The calculated oxygen fluxes from *in situ* microprofiles (DOU) and benthic chamber lander incubations (TOU). Standard deviation given in parentheses. +/- indicates fluxes out of and into the sediment, respectively.

Station	DOU [1] mmol m^{-2} d^{-1}	TOU [2] mmol m^{-2} d^{-1}
1	-8.3 (± 0.76)	-10.0
2	-8.7 (± 1.03)	-8.9
3	-7.6 (± 0.36)	-4.3
4	0	0

[1] DOU = diffusive oxygen uptake, calculated from the *in situ* microprofiles.
[2] TOU = total oxygen uptake measured *in situ*.

Sulfate reduction rates

The measured sulfate reduction rates (SRR) of Stations 1 to 4 are presented in Fig. 3. The *in situ* incubations from Stations 2-4 showed the maximum activity at the sediment surface and a rapid decline with depth. In several cores the SRR was negligible below a depth of approx. 15 cm. This pattern was not due to sulfate limitation in the deeper sediment strata, as concentration was > 2 mM (data not shown). The depth integrated SRR activity (0 - 15 cm) was highest in cores at station 1 (75 m water depth) - where there was a distinct secondary subsurface peak at approx. 8 cm sediment depth. The lowest SRR were measured at station 4 (210 m; Tab. 4). At station 2 and 3 the SRR profiles obtained in the laboratory and *in situ* were compareable, and exhibited no significant differences between the depth integrated rates (Fig. 3; Tab. 4). However, at Station 1 and 4, the two *in situ* and laboratory results differed. The distinct subsurface peak between 4 and 10 cm observed in all *in situ* cores at Station 1 could not be found in the laboratory profiles. As a result the depth integrated *in situ* rate from Station 1 was higher by a factor of 2 as compared to the laboratory rate (Tab. 4). Station 4, however, exhibited the opposite picture in all laboratory replicates; rates at a given horizon derived from laboratory incubations were higher by a factor of up to 9 than the corresponding *in situ* incubations, resulting in 6 times higher depth integrated rates (Tab. 4).

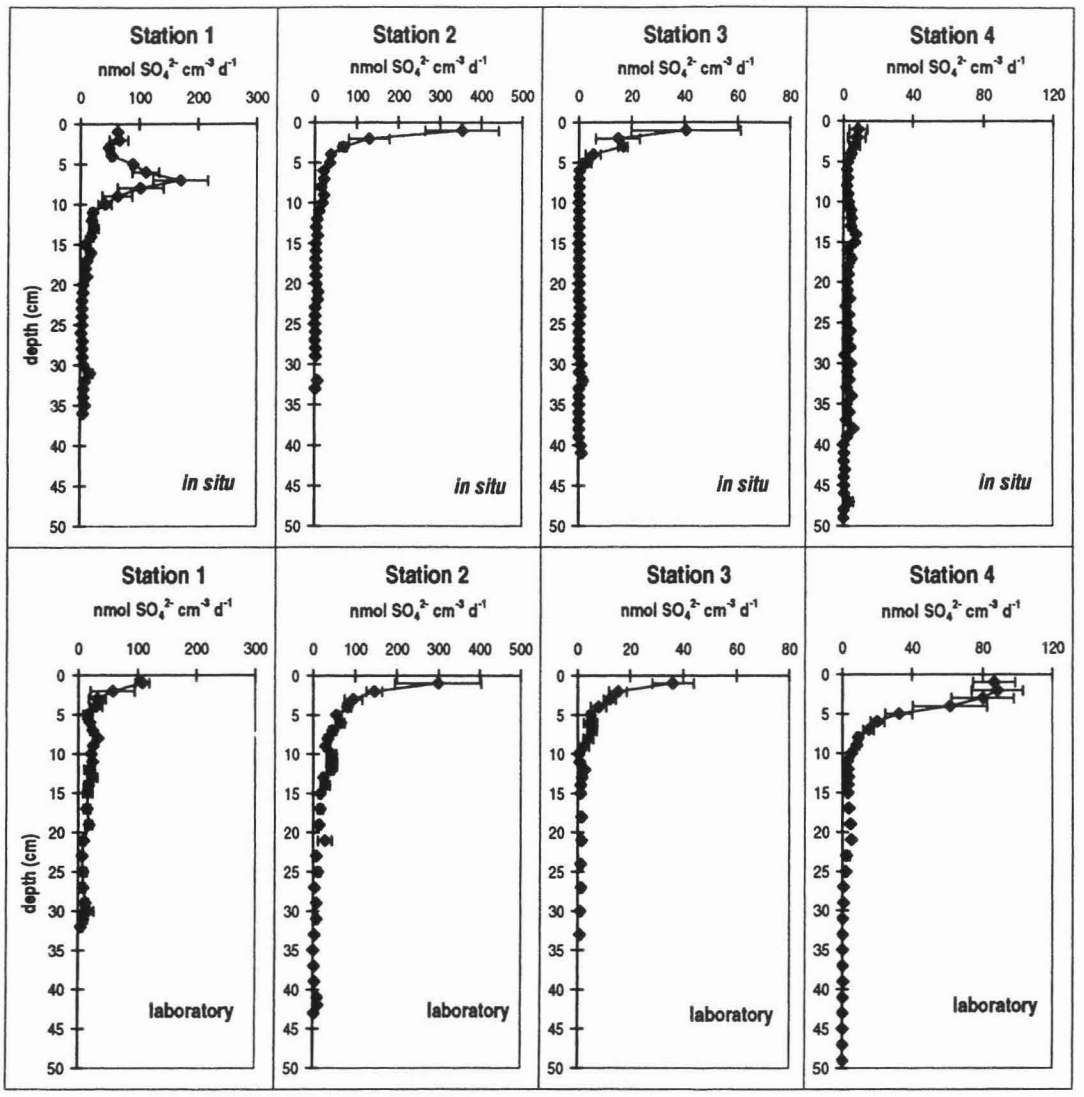

Fig. 3: Sulfate reduction rates of sediments from Gotland Basin. Upper panel shows results from *in situ* incubations, lower panel those from laboratory incubations of all stations. Each data point represents triplicate measurements. The errorbar indicates the standard error of the mean value (= mean value/(SQR(n)). For information on incubation time and calculation method see text.

Table 4: Depth-integrated sulfate reduction rates (SRR; 0 - 15 cm) of Station 1 to 4 as determined by *in situ* and laboratory whole core incubation. Standard deviation (n = 3) given in parentheses.

Station	*in situ* SRR mmol m^{-2} d^{-1}	laboratory SRR mmol m^{-2} d^{-1}
1	8.99 (± 2.36)	4.66 (± 0.82)
2	7.52 (± 1.46)	10.55 (± 1.93)
3	0.80 (± 0.39)	1.01 (± 0.18)
4	0.69 (± 0.15)	4.21 (±0.60)

Discussion

Sulfate reduction

Comparison between *in situ* and laboratory determined O_2 uptake rates for deep sea environments have demonstrated significant overestimation in laboratory incubated cores (Glud et al., 1994). This is typically ascribed to transient heating. However, at shallow water depths such effect seems to be of minor importance (Glud *et al.*, 1994, 1998). In this study laboratory and *in situ* SRR differed significantly at two stations (Tab. 4). At both stations the temperature difference between the bottom water and the surface water was around 15°C. Using Q_{10}-values for sulfate reducing bacteria of approximately 3 (Jørgensen, 1977; Skyring *et al.*, 1983; Wetsrich and Berner, 1988; Isaksen and Jørgensen, 1996), the exposure time of these samples to increased temperature (approx. 1 h) was not sufficient to stimulate fast growth and/or enhanced metabolic activity. It was calculated that only a maximum increase of 11 - 15 % could have taken place. Station 1 showed a subsurface peak in the *in situ* profile that was absent in the laboratory profiles, causing a higher *in situ* depth integrated rate at this site. Station 4 represent the opposite end in the range of SRR, where the integrated *in situ* sulfate reduction rate was only one third of the laboratory value. Because of the fluffy sediment surface at this setting we can not exclude that a bow wave effect disturbed the upper centimetre of the cores. This would apply to both the *in situ* and laboratory measurements. However, sediment heterogeneity and sampling artefacts may add to produce a complex picture, in which the true differences between *in situ* and laboratory measurements are hard to resolve on the basis of 4 stations. Nevertheless, depth integrated SRR determined in this study (Tab. 4) are similar to rates found by Thamdrup *et al.* (1996) in a study on sediments from an anoxic basin in Costa Rica and in shelf sediments from the Skagerrak (Canfield *et al.*, 1993b), whereas anoxic settings off Chile (Thamdrup and Canfield, 1996) exhibited far higher rates. SRR from similar water depth were 6 - 30 times higher than our rates.

Oxygen dynamics

The *in situ* oxygen penetration depth of approx. 1 mm was caused by a rapid consumption of oxygen in the upper sediment layers, through mineralization of organic matter and/or reoxidation of reduced species diffusing upwards from the anoxic zone of the sediment. The profile gradients result in fluxes of 7 - 8 mmol m^{-2} d^{-1} of O_2 into the sediment and are in the range of values reported from coastal environments (Archer and Devol, 1992; Glud *et al.*, 1998). Comparison of the *in situ* DOU and TOU of the stations shows a higher TOU value for Station 1 (+20%), which was most probably caused by fauna related irrigation and respiration (Tab. 3). At the deeper

Station 2 (115 m), where no fauna were found, DOU and TOU measurements agreed closely. Yet at Station 3 TOU was lower by 56 % as compared to DOU measurements; this is probably due to a considerable sediment heterogeneity at the slopes of Gotland Basin. Generally, oxygen uptake rates indicated high uptake rates at the sediment surface, where highest quality and quantity of organic carbon is deposited (Fig. 2E/F). However, at the fauna-rich station 1, the specific oxygen activity was constant indicating efficient sediment mixing (Fig. 2D).

Applying TOU as a measure for the total mineralization rate, assuming low denitrification rates as inferred from other coastal studies (Glud *et al.*, 1998; Canfield, 1993) and accounting for the fact that 2 moles of CO_2 are produced per mole of sulfate reduced (Westrich, 1983), the *in situ* SRR and TOU rates were compared (Tab. 5). At Stations 1 and 2, SRR accounts for almost twice the amount of C degraded as inferred from TOU (Tab. 5). This could be because of spatial heterogeneity of the sediment or non steady state reoxidation of reduced sulfur is occuring. In the case of shallow shelf sediments, the possibility of an incomplete reoxidation of the sulfide produced during sulfate reduction may lead to lower ratios between TOU and SRR (Tab. 5). At Station 3 SRR accounted for 37 % of the total mineralization, while at Station 4 all of the carbon most probably was degraded by SRR.

Table 5: Comparison of carbon oxidation rates as calculated from benthic oxygen uptake (TOU) and integrated *in situ* sulfate reduction rates (SRR; 0 - 15 cm). A ratio of O_2 : TCO_2 of 1 : 1 has been assumed (e.g., Canfield, 1993), while SRR from Tab. 4 were converted to carbon equivalents by multiplication by 2 (Froelich et al., 1979).

Station	Carbon oxidation as measured by (mmol C m^{-2} d^{-1})		Ratio % C degraded by SRR
	TOU	SRR	
1	10.0	17.98	179
2	8.9	15.40	173
3	4.3	1.60	37
4	- [1]	1.38	-

[1] no oxygen in bottom water

The annual primary production in the surface waters above the thermocline at 10 m depth of Central Gotland Basin is estimated at approx. 15 mol C m^{-2} a^{-1} (Lassig *et al.*, 1978; Schulz *et al.*, 1992). Assuming our measurement represent the yearly average, calculated annual benthic

degradation between 2.5 - 4 mol C m^{-2} a^{-1} (Stations 1, 3 and 4) and approx. 8.5 mol C m^{-2} a^{-1} (Station 2) thus accounted for around 16 - 26 % (Stations 1, 3 and 4) and 56 % (Station 4) of the primary production. These values most likely represent an overestimation since our measurements were performed in summer, where the sediment can be assumed to be enriched in organic carbon. A phytoplankton bloom was indeed observed during the cruise period .

Acknowledgements - We wish to thank Bo Thamdrup and Susan Boehme for helpful discussions and valuable comments during the preparation of the manuscript. We are also indebted to Anja Eggers, Gabi Eickert and Vera Hübner for assembling the electrodes used on PROFILUR and ELINOR. The assistance of the crew of R.V. „Professor Albrecht Penck" is greatly appreciated. Earlier versions of this manuscript benefited greatly from the input of three anonymous reviewers.

Chapter 6

Summary and research outlook

The main goal of my thesis was to resolve the impact of biogeochemical processes occurring at the sediment water interface in marine sediments. The importance of the oxygen dynamics in deep sea sediments was investigated as well as the effect of metabolically mediated CO_2 on the calcite dissolution in marine sediments. A third topic was the impact on interface gradients in an extreme environment of a shallow hydrothermal vent site as a result of unique physical processes.

To measure the impact of oxygen on carbon mineralization in oligotrophic deep sea sediments it was necessary to develop a new sensor. Earlier *in situ* measurements of oxygen profiles indicated that oxygen microelectrodes are limited to a certain profiling depth due there fragile glass housing. Recently developed oxygen microoptodes provided another technique for measuring oxygen profiles in sediments. The use of optical fibers as main component of an optode gave us the opportunity to develop an oxygen sensor of 95 cm length and an outer diametre of 1 mm. The optode size allows a vertical resolution of > 2 mm to ensure minimal effects on the physical and chemical surrounding environment. Because oxygen respiration is low in oligotrophic deep sea sediments we chose a vertical resolution of 0.5 cm. The first ever deep penetration *in situ* oxygen profiles in the western South Atlantic indicate that this resolution is adequate to describe the oxygen dynamics in such a sediment. This is not true for measurements across the sediment water interface where a resolution of 0.5 cm is not fine enough to determine the diffusive boundary layer (DBL). Here a finer vertical profiling resolution is absolutely necessary. Not only the step resolution is the important factor but also the sensor dimension can impact on the DBL thickness and therefore on the oxygen uptake of the sediment. In our investigations we combined oxygen microsensors (to define the DBL) together with deep penetration oxygen optodes (measuring the complete oxygen penetration depth) providing an excellent tool to study the oxygen dynamics in oligotrophic deep sea sediments. To quantify the importance of oxygen respiration on organic matter mineralization in oligotrophic sediments more *in situ* measurements are necessary.

To quantify the influence of metabolically produced CO_2 on the dissolution of calcite within marine sediments I used well known O_2 and pH microelectrodes as well as new developed pCO_2 microoptodes and Ca^{2+} microelectrodes. The first ever *in situ* Ca^{2+} microprofiles together with the pH and pCO_2 profiles provided a direct determination of calcite dissolution in marine sediments. At two calcite–poor stations in the eastern South Atlantic, a calcium flux of 0.6 mmol m^{-2} d^{-1} was measured. The Ca^{2+} flux from one station (GeoB 4909) is predicted by using a dissolution rate constant k = 7000 mol kgw^{-1} a^{-1} in the model CoTReM. The study showed that metabolically mediated CO_2 enhanced the amount of calcite dissolution within marine sediments, even in sediments overlain with supersaturated water. Because of the dynamic processes occurring at the sediment surface resulting in steep gradients of solutes, microsensors with high vertical resolution are a good tool for studying the processes. However, even in deep sea sediments with a relative homogeneous sediment structure the study of the carbonate chemistry requires also a low horizontal resolution for measuring the single components (pH, pCO_2 and also Ca^{2+}). The available microsensors and our lander system permit a minimum lateral resolution of 3 cm between the sensors. The newly developed pH microoptode (Kohls et al., 1997a; Kosch et al., 1998) may provide the opportunity to measure two major components of the carbonate system (in our case pH and pCO_2) with a horizontal resolution of < 0.5 cm. But first the pH optode must be adapted to our profiling lander system. To investigate the impact of sediment recovery on the pore water carbonate system profiling measurements of pH, pCO_2 and Ca^{2+} under defined conditions in a pressure chamber are also necessary.

In situ measurements of the importance of oxygen respiration and sulfate reduction with three benthic landers in the Gotland basin (Baltic Sea) were performed. Sulfate reduction was the major pathway in organic carbon degradation, while most of the oxygen consumed within the sediments must be related to reoxidation of hydrogen sulfate.

In situ microprofiles of O_2, pH, H_2S and temperature at a shallow water hydrothermal vent site in Milos together with laboratory O_2 microprofiles resolved a microcirculation of pore water in the inner vent area. A downward transport of oxygenated water created small convective cells which efficiently reoxidise H_2S in the seep fluid. It was also shown that enhanced dissolved inorganic carbon concentrations due to CO_2 release from the seep fluid has no significant effect on the benthic primary production. More studies are needed to quantify the influence of such shallow hydrothermal vent systems on the marine nutrient cycles.

References

Adler, M., Hensen, C., Wenzhöfer, F., Schulz, H.D., in prep. Modeling of subsurface calcite dissolution by oxic respiration in supralysoclinal deep sea sediments.

Aller, R.C., 1990. Bioturbation and manganese cycling in hemipelagic sediments. Phil. Trans. R. Soc. Lond. A 331, 51-68.

Amman, D., 1986. Ion-selective microelectrodes: principles, design and applications. Springer, Berlin.

Ammann, D., Bührer, T., Schefer, U., Müller, M., Simon, W., 1987. Intracellular neutral carrier-based Ca^{2+} microelectrode with subnanomolar detection limit. Plügers Archiv-European Journal of Physiology 409, 223-228.

Archer, D., 1991. Modeling the Calcite Lysocline. Journal of Geophysical Research 96(No. C9), 17,037-17,050.

Archer, D., Maier-Reimer, E., 1994. Effect of deep-sea sedimentary calcite preservation on atmospheric CO_2 concentration. Nature 367, 260-263.

Archer, D., Devol, A., 1992. Benthic oxygen fluxes on the Washington shelf and slope: A comparison of *in situ* microelectrodes and chamber flux measurements. *Limnology and Ocenaography* 37 (3), 614-629.

Archer, D., Emerson, S., Reimers, C., 1989a. Dissolution of calcite in deep-sea sediments: pH and O_2 microelectrode results. Geochimica et Cosmochimica Acta 53, 2831-2845.

Archer, D., Emerson, S., Smith, C.R., 1989b. Direct measurement of the diffusive sublayer at the deep sea floor using oxygen microelectrode. Nature 340, 623-626.

Arrhenius, G., 1988. Rate of production, dissolution, and accumulation of biogenic solids in the ocean. Paleaogeogr. Paleoclimatol. Paleaoecol. 67, 119-146.

Barnett, P.R.O., Watson, J., Connelly, D., 1984. A multiple corer for taking virtually undisturbed samples from shelf, bathyal and abyssal sediments. Oceanologica Acta 7(No. 4), 399-408.

Barranguet, C., Kromkamp, J., Peene, J., 1998. Factors controlling primary production and photosynthetic characteristics of intertidal microphytobenthos. Mar. Ecol. Prog. Ser. 173, 117-126.

Baumgärtl, H., Lübbers, D.W., 1973. Platinum needle electrodes for polarographic measurements of oxygen and hydrogen. In: Kessler, M. (ed.): Oxygen supply. Urban & Schwarzenberg, München, 130-136.

Bender, M.L., Heggie, D.T., 1984. Fate of organic carbon reaching the deep sea floor: a status report. Geochimica et Cosmochimica Acta 48, 977-986.

Berelson, W.M., Hammond, D.E., Cutter, G. 1990. *In situ* measurements of calcium carbonate dissolution in deep-sea sediments. Geochim. Cosmochim. Acta 54, 3013-3020.

Berelson, W.M., Hammond, D.E., McManus, J., Kilgore, T.E., 1994. Dissolution kinetics of calcium carbonate in equatorial Pacific sediments. Global Biogeochemical Cycles 8(No. 2), 219-235.

Berelson, W.M., Hammond, D.E., Smith jr., K.L., Jahnke, R.A., Devol, A.H., Hinga, K.R., Rowe, G.T., Sayles, E., 1987. *In situ* benthic flux measurement devices: bottom lander technology. Marine Technology Society 21, 26-32.

Berelson, W.M., Anderson, R.F., Dymond, J., Demaster, D., Hammond, D.E., Collier, R., Honjo, S., Leinen, M., McManus, J., Pope, R., Smith, C., Stephens, M., 1997. Biogenic budgets of particle rain, benthic remineralization and sediment accumulation in the equatorial Pacific. Deep-Sea Research II 44, 2251-2282.

Berger, W.H., 1989. Global Maps of Ocean Productivity. In: Berger, W.H., Smetacek, V.S., Wefer, G. (Eds.), Productivity of the Ocean: Present and Past. John Wiley & Sons, Dahlem Konferenzen, pp. 429-455.

Berger, W.H., Wefer, G., 1990. Export production: Seasonality and intermittency, and paleoceanographic implications. Paleoceanogr., Paleoclim., Paleoecol. 89, 245-254.

Berger, W.H., Smetacek, V.S., Wefer, G., 1989. Ocean Productivity and Paleoproductivity - An Overview. In: W.H. Berger, V.S. Smetacek, G. Berger (Eds.), Productivity of the Ocean: Present and Past. John Wiley & Sons, Dahlem Konferenzen, pp. 1-34.

Berger, W.H., Fischer, K., Lai, C., Wu, G., 1987. Ocean productivity and organic carbon flux. I. Overview and maps of primary production and export production.- Univ. California, San Diego, SIO Reference 87-30, 67pp.

Berner, R.A., 1989. Biogeochemical cycles of carbon and sulfur and their effect on atmospheric oxygen over Phanerozoic time. Palaeogeogr. Palaeoclimatol. Palaeoecol. 73, 97-122.

Berner, R.A., 1982. Burial of organic carbon and pyrite sulfur in the modern ocean: its geochemical and environmental significance. *American Journal of Science* 282, 451-473.

Berner, R.A., 1980. Early Diagenesis - A Theoretical Approach. Princeton University Press, Princeton, N.J.

Berntsen, J., Ramsing, N.B., (in prep.). A new model for analyzing concentration profiles.

Betzer, P.R., Showers, W.J., Laws, E.A., Winn, C.D., Dituillio, G.R., Kroopnick, P.M., 1984. Primary productivity and particle fluxes on a transect of the Equator at 153° W in the Pacific Ocean. Deep-Sea Research 31, 1-11.

Boudreau, B.P., 1987. A steady-state diagenetic model for dissolved carbonate species and pH in the porewaters of oxic and suboxic sediments. Geochimica et Cosmochimica Acta 51, 1985-1996.

Boudreau, B.P., Canfield, D.E., 1993. A comparison of closed- and open-system models for porewater pH and calcite-saturation state. Geochimica et Cosmochimica Acta 57, 317-334.

Boyle, E.A., 1988. The role of vertical chemical fractionation in controlling late quaternary atmospheric carbon dioxide. J. Geophys. Res. 93, 15,701-15,714.

Brendel, P.J., Luther III, G.W., 1995. Development of a gold amalgam voltametric microelectrode for the determination of dissolved Fe, Mn, O_2, and S(II-) in pore waters of marine and freshwater sediments. Environmental Science and Technology 29, 751-761.

Broecker, W.S., Peng, T.-H., 1987. The role of $CaCO_3$ compensation in the glacial to interglacial atmospheric CO_2 change. Global Biogeochemical Cycles 1(No. 1), 15-29.

Broecker, W.S., Peng, T.H., 1982. Tracers in the Sea. Eldigio Press, Palisades, NY.

Broecker, W.S., Peng, T.H., 1974. Gas exchange rates between air and sea. Tellus, XXVI, 21-35.

Cadee, G.C., Hegeman, J., 1977. Distribution of primary production of the benthic microflora and accumulation of organic matter on a tidal flat area, Balgzand, Dutch Wadden Sea. Neth. J. Sea Res.11 (1), 24-41.

Cadee, G.C., Hegeman, J., 1974. Primary production of the benthic microflora living on tidal flats in the Dutch Wadden Sea. Neth. J. Sea Res. 8, 260-291

Cai, W.-J., Sayles, F.L., 1996. Oxygen penetration depths and fluxes in marine sediments. Marine Chemistry 52, 123-131.

Cai, W.-J., Reimers, C.E., 1993. The development of pH and pCO_2 microelectrodes for studying the carbonate chemistry of pore waters near the sediment-water interface. Limnol. Oceanogr. 38(8), 1762-1773.

Cai, W.-J., Reimers, C.E., Shaw, T., 1995. Microelectrode studies of organic carbon degradation and calcite dissolution at a California Continental rise site. Geochimica et Cosmochimica Acta 59(No. 3), 497-511.

Canfield, D.E., 1993. Organic matter oxidation in marine sediments. In: Wollast, R., Chou, L., Mackenzie, F. (Eds.), Interactions of C, N, P and S. Biogeochemical cycles and global change. Springer Verlag, Berlin Heidelberg, pp. 333-363.

Canfield, D.E., 1989. Sulfate reduction and oxic respiration in marine sediments: implications for organic carbon preservation in euxinic environments. *Deep-Sea Research I* 36 (1), 121-138.

Canfield, D.E., Thamdrup, B., Hansen, J. W., 1993a. The anaerobic degradation of organic matter in Danish coastal sediments: Iron reduction, manganese reduction, and sulfate reduction. *Geochimica et Cosmochimica Acta* 57, 3867-3883.

Canfield, D.E., Jørgensen, B.B., Fossing, H., Glud, R., Gundersen, J., Ramsing, N.B., Thamdrup, B., Hansen, J.W., Nielsen, L.P., Hall, P.O.J., 1993b. Pathways of organic carbon oxidation in three continental margin sediments. *Marine Geology* 113, 27-40.

Cronan, D.S., Varnavas, S.P., 1993. Submarine fumarolic and hydrothermal activity off Milos, Hellenic Volcanic Arc. Terra Abstracts 5, 569.

Cronan, D.S., Varnavas, S., Perissoratis, C., 1995. Hydrothermal sedimentation in the caldera of Santorini, Hellenic Volcanic Arc. Terra Nova 7, 2, 289-293.

Cronenberg, C.C.H., Van Groen, H., De Beer , D., Van den Heuvel, J.C., 1991. Oxygen-independent glucose microsensor based on glucose oxidase. Analytica Cimica Acta 242, 275-278.

Curry, W.B., Lohmann, G.P., 1985. Carbon deposition rates and deep water residence time in the equatorial Atlantic ocean through-out the last 160,000 years. In: Sunquist, E.T., Broecker, W.S. (Eds.), The Carbon Cycle and Atmospheric CO_2: Natural Variations, Archean to Present. Geophys. Mono. Ser. 32, pp.285-302.

Cutter, G.A., Radford-Knoery, J., 1991. Determination of Carbon, Nitogen, Sulfur, and Inorganic Sulfur Species in Marine Particles.

Damgaard, L.R., Revsbech, N.P., 1997. A microscale biosensor for methane. Analytical Chemistry 69, 2262-2267.

Damgaard, L.R., Revsbech, N.P., Reichardt, W., 1998. Use of an oxygen-insensitive microscale biosensor for methane concentration profiles in a rice paddy. Applied and Environmental Microbiology 64, 864-870.

Dando, P.R., Hughes, J.A., Thiermann, F., 1995a. Preliminary observations on biological communities at shallow hydrothermal vents in the Aegean Sea. In: Parson, L.M., Walker, C.L., Dixon, D.L. (Eds.), Hydrothermal Vents and Processes. Spec. Publ. Geol. Soc., London 87, 303-317.

Dando, P.R., Hughes, J.A., Leahy, Y., Niven, S.J., Tayler, L.J., Smith, C., 1995b. Gas venting from submarine hydrothermal areas around the island of Milos in the Hellenic Volcanic Arc. Cont. Shelf Res. 15, 913-929.

DeBaar, J.W., Suess, E., 1993. Ocean Carbon Cycle and Climate Change.- An introduction to the Interdisciplinary Union Symposium.- Global Planet Change 8, VII-XI.

de Beer, D., 1997. Microenvironments and mass transfer phenomena in biofilms and activated sludge studied with microsensors. In: Verachtert, H., Verstraete, W. (Eds.), Proceedings of the International Symposium on Environmental Biotechnology, Oostende.

de Beer D., Sweerts, J.P.R.A., 1989. Measurements of nitrate gradients with an ion-selective microelectrode. Analytica Acta 219, 351-356.

de Beer, D., Van den Heuvel, J.C., 1988. Response of ammonium-selective microelectrodes based on the neutral carrier nonactin. Talanta 35, 728-730.

de Beer, D., Glud, A., Epping, E,.Kühl, M., 1997a. A fast-responding CO_2 microelectrode for profiling sediments, microbial mats, and biofilms. Limnol. Oceanogr. 42(7), 1590-1600.

de Beer, D., Schramm, A., Santegoeds, C.M., Kühl, M., 1997b. A nitrite microsensor for profiling environmental biofilms. Applied and Environmental Microbiology 63, 973-977.

Deming, J.W., Baross, J.A., 1993. The Early Diagenesis of Organic Matter: Bacterial Activity. In: M.H. Engel, S.A. Macko (Eds.), Organic Geochemistry. Plenum Press, New York, pp. 119-144.

Devol, A.H., 1991. Direct measurements of nitrogen gas fluxes from continental shelf sediments. Nature 349, 319-321.

Ebert, A., Brune, A., 1997. Hydrogen concentration profiles at the oxic-anoxic interface: A microsensor study of the hindgut of the wood-feeting lower termite *Reticulitermes flavipes* (Kollar). Applied and Environmental Microbiology 63, 4039-4046.

Emerson, S.R., Archer, D., 1990. Calcium carbonate preservation in the ocean. Phil. Trans. R. Soc. Lond. A, 331: 29-40.

Emerson, S., Bender, M., 1981. Carbon fluxes at the sediment-water interface of the deep-sea: calcium carbonate preservation. Journal of Marine Research 39, 139-162.

Emerson, S., Grundmanis, V. and Graham, D., 1982. Carbonate chemistry in marine pore waters: MANOP sites C and S. Earth and Planetary Science Letters 61, 220-232.

Epping, E.H.G., Helder, W., 1997. Oxygen budgets calculated from *in situ* oxygen microprofiles for Nothern Adriatic sediments. Continental Shelf Research 7(No. 14), 1737-1764.

Farrel, J.W., Prell, W.L., 1989. Climate change and $CaCO_3$ preservation: an 800,00 year bathymetric reconstruction from the central equatorial Pacific Ocean. Paleo. 4, 447-466.

Fischer, G. and Wefer, G., 1996. Long-term Observation of Particle Fluxes in the Eastern Atlantic: Seasonality, Changes of Flux with depth and Comparison with the Sediment Record. In: G. Wefer, W.H. Berger, G. Siedler and D.J. Webb (Eds), The South Atlantic: Present and Past Circulation. Springer-Verlag, Berlin - Heidelberg.

Fitzsimons, M.F., Dando, P.R., Hughe,s J.A., Thiermann, F., Akoumianaki, I. and Pratt, S.M., 1997. Submarine hydrothermal brine seeps off Milos, Greece: Observations and geochemistry. Marine Chemsitry 57, 325-340.

Fossing, H., Jørgensen, B.B., 1989. Measurement of bacterial sulfate reduction in sediments: Evaluation of a single-step chromium reduction method. *Biogeochemistry* 8, 205-222.

Froelich, P.N., Klinkhammer, G.P., Bender, M.L., Luedtke, N.A., Heath, G.R., Cullen, D., Dauphin, P., Hammond, D., Hartman, P., Maynard, V., 1979. Early oxidation of organic matter in pelagic sediments of the eastern equatorial Atlantic: suboxic diagenesis. Geochimica et Cosmochimica Acta 43, 1075-1090.

Gehlen, M., Rabouille, C., Ezat, U., Guidi-Guilvard, L.D., 1997. Drastic changes in deep-sea sediments porewater composition induced by episodic input of organic matter. Limnol. Oceanogr. 42(5), 980-986.

Gilboa-Garber, N., 1971. Direct spectrophotometric determination of inorganic sulphide in biological materials an in other complex mixtures. Anal. Biochem. 43, 129-133.

Glud, R.N., Gundersen, J.K., Holby, O., in press. Benthic *in situ* respiration in the upwelling area off central Chile. Marine Ecology Progress Series.

Glud, R.N., Ramsing, N.B., Revsbech, N.P., 1992. Photosynthesis and photosynthesis-coupled respiration in natural biofilms quantified with oxygen microsensors. J. Phycol. 28, 51-60.

Glud, R.N., Holby, O., Hoffmann, F., Canfield, D.E., 1998. Benthic mineralization and exchange in arctic sediments (Svalbard, Norway). *Marine Ecology Progress Series* 173, 237-251.

Glud, R.N., Ramsing, N.B., Gundersen, J.K., Klimant, I., 1996. Planar optodes: a new tool for fine scale measurements of two-dimensional O_2 distribution in benthic communities. Mar. Ecol. Prog. Ser., 140: 217-226.

Glud, R.N., Gundersen, J.K., Revsbech, N.P., Jørgensen, B.B., Hüttel, M., 1995. Calibration and performance of the stirred flux chamber from the benthic lander ELINOR. *Deep-Sea Research I* 42 (6), 1029-1042.

Glud, R.N., Gundersen, J.K., Jørgensen, B.B., Revsbech, N.P., Schulz, H.D., 1994. Diffusive and total oxygen uptake of deep-sea sediments in the eastern South Atlantic Ocean: *in situ* and laboratory measurements. Deep-Sea Research 41(No. 11/12), 1767-1788.

Glud, R.N., Klimant, I., Holst, G., Kohls, O., Meyer, V., Kühl, M., Gundersen, J., 1999. Adaptation, test and *in situ* measurements with O_2 microopt(r)odes on benthic landers. Deep Sea Research I 46, 171-183.

Grasshoff, K., 1983. Determination of oxygen. In: Grasshoff, K., Ehrhardt, M., Kremling, K. (Eds.), Methods of seawater analysis. Verlag Chemie GmbH, Weinheim, 61-72.

Grasshoff, K., Voipio, A., 1981. Chemical Oceanography. In: Voipio, A. (Ed.), The Baltic Sea. Elsevier, Amsterdam, pp 183-218.

Greeff, O., Glud, R.N., Gundersen, J., Holby, O., Jørgensen, B.B., 1998. A benthic lander for tracer studies in the sea bed: *in situ* measurements of sulfate reduction. Continental Shelf Research 18, 1581-1594.

Gundersen, J.K., Jørgensen, B.B., 1991. Fine-scale *in situ* measurements of oxygen distribution in marine sediments. Kieler Meeresforsch., Sonderh. 8, 376-380.

Gundersen, J.K., Jørgensen, B.B., 1990. Microstructure of diffusive boundary layers and the oxygen uptake of the sea floor. Nature 345, 604-607.

Gundersen, J.K., Ramsing, N.B., Glud, R.N., 1998. Predicting the signal of O_2 microsensors from physical dimensions, temperature, salinity, and O_2 concentration. Limnol. Oceanogr. 43(8), 1932-1937.

Gundersen, J.K., Jørgensen, B.B., Larsen, E., Jannasch, H.W., 1992. Mats of giant sulphur bacteria on deep-sea sediments due to fluctuating hydrothermal flow. Nature 360, 454-455.

Hales, B., 1995. Calcite Dissolution on the Sea Floor: An *In Situ* Study. Doctor of Philosophy Thesis, University of Washington, Washington, 165 pp.

Hales, B., Emerson, S., 1997a. Calcite dissolution in sediments of the Ceara Rise: *In situ* measurements of porewater O_2, pH, and CO_2(aq). Geochimica et Cosmochimica Acta 61(No. 3), 501-514.

Hales, B., Emerson, S., 1997b. Evidence in support of first-order dissolution kinetics of calcite in seawater. Earth and Planetary Science Letters 148, 317-327.

Hales, B., Emerson, S., 1996. Calcite dissolution in sediments of the Ontong-Java Plateau: *In situ* measurements of pore water O_2 and pH. Global Biogeochemical Cycles 10(No. 3), 527-541.

Hales, B., Burgess, L., Emerson, S., 1997. An absorbance-based fiber-optic sensor for CO_2(aq) measurement in porewater of sea floor sediments. Marine Chemistry, 59: 51-62.

Hales, B., Emerson, S., Archer, D., 1994. Respiration and dissolution in the sediments of the western North Atlantic: estimates from models of *in situ* microelectrode measurements of porewater oxygen and pH. Deep-Sea Research 41(No. 4), 695-719.

Hedges, J.I., 1992. Global biogeochemical cycles: progress and problems. Mar. Chem., 39: 67-93.

Hedges, J.I., Keil, R.G., 1995. Sedimentary organic matter preservation: an assessment and speculative synthesis. *Marine Chemistry* 49, 81-115.

Henrichs, S.M., 1992. Early diagenesis of organic matter in marine sediments: progress and perplexity. *Marine Chemistry* 39, 119-149.

Henrichs, S.M., Reeburgh, W.S., 1987. Anaerobic mineralization of marine sediment organic matter: rates and role of anaerobic processes in the oceanic carbon economy. *Geomicrobiology Journal* 5 (3/4), 191-237.

Hensen, C., Landenberger, H., Zabel, M., Gundersen, J.K., Glud, R.N., Schulz, H.D., 1997. Simulation of early diagenetic processes in continental slope sediments off southwest Africa: the computer model CoTAM tested. Marine Geology 144, 191-210.

Hoaki, T., Nishijima, M., Miyashita, H., Maruyama, T., 1995. Dense community of hyperthermophilic sulfur-dependent heterotrophs in a geothermally heated shallow

submarine biotope near Kodakara-Jima Island Kagoshima, Japan. Appl. Environ. Microbiol. 61, 1931-1937.

Holst, G., Klimant, I., Kühl, M., in press. Optical Microsensors and Microprobes. In: Varney, M. (Ed.), Chemical Sensors in Oceanography.

Holst, G., Kühl, M., Klimant, I., Liebsch, G., Kohls, O., 1997. Characterization and application of temperature microoptodes for use in aquatic biology. SPIE Proceedings 2980, 164-171.

Isaksen, M.F., Jørgensen, B.B., 1996. Adaptation of psychrophilic and psychrotrophic sulfate-reducing bacteria to permanently cold marine environments. *Applied and Environmental Microbiology* 62 (2), 408-414.

Jahnke, R.A., 1996. The global ocean flux of particulate organic carbon: Areal distribution and magnitude. Global Biogeochemical Cycle 10, 71-88.

Jahnke, R.A., Jackson, G.A., 1992. The Spatial Distribution of Sea Floor Consumption in the Atlantic and Pacific Oceans. In: Rowe, G.T., Pariente, V. (Eds.), Deep-Sea Food Chains and the Global Carbon Cycle. Kuwer Academic Publishers, Dordrecht/Boston/London, pp. 295-307.

Jahnke, R.A., Christiansen, M.B., 1989. A free-vehicle benthic chamber instrument for sea floor studies. Deep Sea Research 36, 625-637.

Jahnke, R.A., Craven, D.B., Gaillard, J.-F., 1994. The influence of organic matter diagenesis on $CaCO_3$ dissolution at the deep-sea floor. Geochimica et Cosmochimica Acta, 58(No. 13), 2799-2809.

Jahnke, R.A., Reimers, C.E., Craven, D.B., 1990. Intensification of recycling of organic matter at the sea floor near ocean margins. Nature 348, 50-54.

Jahnke, R.A., Craven, D.B., McCorkle, D.C., Reimers, C.E., 1997. $CaCO_3$ dissolution in California continental margin sediments: The influence of organic matter mineralisation. Geochimica et Cosmochimica Acta 61(No. 17), 3587-3604.

Jeroschewski, P., Steuckart, C., Kühl, M., 1996. An Amperometric Microsensor for the Determination of H_2S in Aquatic Environments. Analytical Chemistry 68, 4351-4357.

Joint, I.R., 1978. Microbial production of an estuarine flat. Est. Coast. Mar. Sci. 7, 185-195.

Jørgensen, B.B., 1983. Processes at the Sediment-Water Interface. In: B. Bolin and R.B. Cook (Eds), The Major Biogeochemical Cycles and Their Interactions. SCOPE, pp. 477-509.

Jørgensen, B.B., 1982. Mineralization of organic matter in the sea bed - the role of sulfate reduction. Nature 296, 643-645.

Jørgensen, B.B., 1978. A comparison of methods for the quantification of bacterial sulfate reduction in coastal marine sediments. I Measurement with radiotracer techniques. *Geomicrobiology Journal* 1 (1), 11-27.

Jørgensen, B.B., 1977. The sulfur cycle of a coastal marine sediment (Limfjorden, Denmark). *Limnology and Oceanography* 22 (5), 814-832.

Jørgensen, B.B., Revsbech, N.P., 1985. Diffusive boundary layers and oxygen uptake of sediments and detritus. Limnology and Oceanography 30, 111-122.

Kamenev, G.M., Fadeev, V.I., Selin, N.I., Tarasov, V.G., Malakhov, V.V., 1993. Composition and distribution of macro- and meiobenthos around sublittoral hydrothermal vents in the Bay of Plenty, New Zealand, NZ. J. Mar. Freshwater Res. 27 (4), 407-418.

Keir, R.S., 1980. The dissolution kinetics of biogenic calcium carbonates in seawater. Geochimica et Cosmochimica Acta 44, 241-252.

Klimant, I., Meyer, V., Kühl, M., 1995. Fiber-optic oxygen microsensor, a new tool in aquatic biology. Limnol. Oceanogr. 40(6), 1159-1165.

Klimant, I., Holst, G., Kühl, M., 1997a. A simple fiber-optic sensor to detect the penetration of microsensors into sediments and other biogeochemical systems. Limnol. Oceanogr. 42, 1638-1643.

Klimant, I., Kühl, M., Glud, R.N., Holst, G., 1997b. Optical measurement of oxygen and temperature in microscale: strategies and biological applications. Sensors and Actuators B 38-39, 29-37.

Kohls, O., Klimant, I., Holst, G., Kühl, M., 1997a. Development and comparison of pH microoptodes for use in marine systems. SPIE Proceedings 2978, 82-94.

Kohls, O., Epping, E., Holst, G., Kühl, M., 1997b. Microoptodes for CO_2 measurements in marine systems. SPIE Conference on Chemical, Biochemical and Environmental Fiber Sensors VII, München, Germany.

Komada, T., Reimers, C.E., Boehme, S.E., 1998. Dissolved Inorganic Carbon Profiles and Fluxes Determined Using pH and pCO_2 Microelectrode. Limnology and Oceanography 43(5), 769-781.

Kosch, U., Klimant, I., Werner, T., Wolfbeis, O.S., 1998. Strategies to Design pH Optodes with Luminescence Decay Times in the Microsecond Time Regime. Anal. Chem. 70, 3892-2897.

Kühl, M., Revsbech, N.P., 1999. Microsensors for the study of interfacial biogeochemical processes. In: Boudreau, B.P., Jørgensen, B.B. (Eds.): The Benthic Boundary Layer. Oxford University Press, Oxford. in press.

Kühl, M., Jørgensen, B.B., 1994. The light field of microbenthic communities: radiance distribution and microscale optics of sandy coastal sediments. Limnol. Oceanogr. 39, 136-1398.

Kühl, M., Steuckart, C., Eickert, G., Jeroschewski, P., 1998. A H_2S microsensor for profiling biofilms and sediments: Application in an acidic lake sediment. Aquatic Microbial Ecology, 201-209.

Kullenberg, G., 1981. Physical Oceanography. In: Voipio, A. (Ed.), The Baltic Sea. Elsevier, Amsterdam, pp 135-182.

Lassig, J., Leppäner, J.-M., Niemi, A., Tamelander, G., 1978. Phytoplankton primary production in the Gulf of Bothnia 1972-1975 as compared with other parts of the Baltic Sea. *Finnish Marine Research* 244, 101-115.

Larsen, L.H., Kjaer, T., Revsbech, N.P., 1997. A microscale NO_3^- biosensor for environmental applications. Analytical Chemistry 69, 3527-3531.

Lassen, C., Jørgensen, B.B., 1994. A fiber-optic irradiance microsensor (cosine collector): application for *in situ* measurements of absorption coefficients in sediments and microbial mats. FEMS Microbiology Ecology 15, 321-336.

Lee, C., Murray, D.W., Barber, R.T., Buessler, K.O., Dymond, J., Hedges, J.I., Honjo, S., Manganini, S.J., Marra, J., Moser, C. Peterson, M.L., Prell, W.L., Wakeham, S.G., 1998. Particulate organic carbon fluxes: compliation of results from the 1995 US JGOFS Arabian Sea process study. Deep Sea Res. 45, 2489-2501.

Li, Y.-H., Gregory, S., 1974. Diffusion of ions in sea water and in deep-sae sediments. Geochimica et Cosmochimica Acta 38, 703-714.

Lyle, M., Murray, D.W., Finney, B.P., Dymond, J., Robbins, J.M., Brooksforce, K., 1988. The record of late pleistocene biogenic sedimentation in the eastern tropical Pacific Ocean. Paleo 3, 39-59.

Martin, W.R.., Sayles, F.L., 1996. $CaCO_3$ dissolution in sediments of the Ceara Rise, western equatorial Atlantic. Geochimica et Cosmochimica Acta 60(No. 2), 243-263.

Martin, J.H., Knauer, G.A., Karl, D.M., Broenkow, W.W., 1987. VERTEX: Carbon cycling in the Northeast Pacific. Deep Sea Res. 34, 267-285.

Morse, J.W., 1978. Dissolution kinetics of calcium carbonate in sea water: VI. The near-equilibrium dissolution kinetics of calcium carbonate-rich deep sea sediments. Am. J. Sci. 278, 344-353.

Morse, J.W., Mackenzie, F.T. (Eds), 1990. Geochemistry of Sedimentary Carbonate. Elsevier, Amsterdam - Oxford - New York - Tokyo, 707 pp.

Muller-Karger, F.E., McCain, C.R., Richardson, P.L., 1988. The dispersal of the Amazon's water. Nature 333, 56-59.

Murray, J.W., Grundmanis, V., 1980. Oxygen Consumption in Pelagic Marine Sediments. Science 209, 1527-1530.

Neudörfer, F., Meyer-Reil, L.A., 1997. A microbial biosensor for the microscale measurement of bioavailable organic carbon in oxic sediments. Marine Ecology Progress series 147, 295-300.

Nielsen, L.P., Christensen, P.B., Revsbech, N.P. Sørensen, J., 1990. Denitrification and oxygen respiration in biofilms studied with a microsensor for nitrous oxide and oxygen. Microbial Ecology 19, 63-72.

Parkhurst, D,L., 1995. PHREEQC - User's guide to PHREEQC - A computer program for speciation, reaction-path, advective-transport, and inverse geochemical calculations. U.S. Geol. Survey Water Resource Invest. Rept. 95-4227, Lakewood, 143pp.

Pedersen, T.F., Pickering, M., Vogel, J.S., Southon, J.N., Nelson, D.E., 1988. The response of benthic foraminifera to productivity cycles in the eastern equatorial Pacific: faunal and geochemical constraints on bottom water oxygen levels. Paleo 3, 157-168.

Rasmussen, H., Jørgensen, B.B., 1992. Microelectrode studies of seasonal oxygen uptake in a coastal sediment: role of molecular diffusion. Mar. Ecol. Prog. Ser. 81, 289-303.

Reimers, C.E., 1987. An *in situ* microprofiling instrument for measuring interfacial pore water gradients: methods and oxygen profiles from the North Pacific Ocean. Deep-Sea Research 34(No. 12), 2019- 2035.

Reimers, C.E., Jahnke, R.A. and McCorkle, 1992. Carbon fluxes and burial rates over the continental slope and rise off central California with implications for the global carbon cycle. Global Biogeochemical Cycles 6(No. 2), 199-224.

Reimers, C.E., Fischer, K.M., Merewether, R., Smith jr., K.L., Jahnke, R.A., 1986. Oxygen microprofiles measured *in situ* in deep ocean sediments. Nature 320, 741-744.

Revsbech, N.P., 1989a. An oxygen microsensor with a guard cathode. *Limnology and Oceanography* 34 (2), 474-478.

Revsbech, N.P., 1989b. Diffusion characteristics of microbial communities determined by use of oxygen microsensors. *Journal of Microbial Methods* 9, 111-122.

Revsbech, N.P., Jørgensen, B.B., 1986. Microelctrodes: Their use in microbial ecology. In: Marschall, K.C. (Ed.), Advances in microbial ecology, Vol. 9, Plenum Publishing Corporation, pp. 293-352.

Revsbech, N.P., Nielsen, L.P., Christensen, P.B., Sørensen, J., 1988. A combined oxygen and nitrous oxide microsensor for denitrification studies. Appl. Environ. Microbiol. 45, 2245-2249.

Revsbech, N.P., Jørgensen, B.B., Blackburn, T.H., Cohen, Y., 1983. Microelectrode studies of the photosynthesis and O_2, H_2S, and pH profiles of a microbial mat. Limnol. Oceanogr. 28(6), 1062-1074.

Robinson, C. (in prep.). Plankton gross production and respiration in the shallow water hydrothermal systems of Milos, Agean Sea.

Rowe, G.T., Boland, G.S., Phoel, W.C., Anderson, R.F., Biscaye, P.E., 1994. Deep sea-floor respiration as an indication of lateral input of biogenic detritus from continental margins. Deep Sea Research 41, 657-668.

Roy, R.N., Roy, L.N., Vogel, K.M., Porter-Moore, C., Pearson, T.,Good, C.E., Millero, F.J., Campbell, D.M., 1993. The dissociation contants of carbonic acid in seawater at salinities 5 to 45 and tempertaures 0 to 45°C. Marine Chemistry 44, 249-267.

Rutgers van der Loeff, M.M., 1990. Oxygen in pore waters of deep-sea sediments. Phil. Trans. R. Soc. Lond. A 331, 69-84.

Santschi, P., Höhener, P., Benoit, G., Buchholtz-ten Brink, M., 1990. Chemical processes at the sediment-water interface. Marine Chemistry 30, 269-315.

Sayles, F.L., Livingston, H.D., 1987. The Distribution of $^{239,240}Pu$, ^{137}Cs, and ^{55}Fe in Continental Margin sediments: Relation to sedimentary Redox Environment. In: O´Connor,T.P., Burt,W.V., Duedall, I.W. (Eds.), Oceanic Processes in Marine Pollution. Robert E. Krieger Publishing Company, Malabar, Florida, pp. 175-195.

Schulz, S., Kaiser, W., Breuel, G., 1992. A comparison of biological data from 1976-1990 and 1991 - the influence of a warm winter. *Biological and Oceanographic Committee* L:19, 1-5.

Siegenthaler, U., Sarmiento, J.L., 1993. Atmospheric carbon dioxide and the ocean. Nature 365, 119-125.

Skyring, G.W., Chambers, L.A., Bauld, J., 1983. Sulfate reduction in sediments colonized by cyanobacteria, Spencer Gulf, South Australia. *Australian Journal of Marine and Freshwater Research* 34, 359-374.

Smith, P.A., Cronan, D.S., 1983. The geochemistry of metalliferous sediments and waters associated with shallow submarine hydrothermal activity (Santorini, Aegean Sea). Chem. Geol. 39, 241-262.

Smith, K.L. jr., Hinga, K.R., 1983. Sediment community respiration in the deep sea. In: Rowe, G.T. (Ed.), The sea - Vol.8. John Wiley & Sons, New York, pp 331-370.

Smith jr., K.L., Baldwin, R.J., Edelman, J.L., 1989. Supply of and demand for organic matter by sediment communities on two central North Pcific seamounts. Deep Sea Research 36, 1917-1932.

Smith jr., K.L., Clifford, C.H., Eliason, A.H., Walden, B., Rowe, G.T., Teal, J.M., 1976. A free vehicle for measuring benthic community metabolism. Limnol. Oceanogr. 21, 164-170.

Smith jr., K.L., Glatts, R.C., Baldwin, R.J., Beaulieu, S.E., Uhlmann, A.H., Horn, R.C., Reimers, C.E., 1997. An autonomous, bottom-transecting vehicle for making long time-series measurements of sediment community oxygen consumption to abyssal depths. Limnol. Oceanogr. 42(7), 1601-1612.

Stein, J.L., 1984. Subtidal gastropods consume sulphur-oxidising bacteria: Evidence from coastal hydrothermal vents. Science 223, 696-698.

Stern, O., Volmer, M., 1919. Über die Abklingzeit der Fluoreszenz. Physikalische Zeitschrift 20, 183-188.

Stigebrandt, A., Wulff, F., 1987. A model for the dynamics of nutrients and oxygen in the Baltic proper Europe. *Journal of Marine Research* 45, 729-760.

Strotmann, B., Ferdelman, T.G., Schubert, K., Zabel, M., Schulz, H.D., Jørgensen, B.B., in prep. Latitudinal distribution of sulfate reduction rates along the continental slope of the North Angola Basin.

Sweerts, J.-P.R.A., St. Louis, V., Cappenberg, T.E., 1989. Oxygen concentration profiles and exchange in sediment cores with circulated overlying water. Freshwater Biology 21, 401-409.

Suess, R., 1980. Particulate organic carbon flux in the oceans. - Surface productivity and oxygen utilization. Nature 228, 260-263.

Sunquist, E.T., 1993. The Global Carbon Dioxide Budget. Science 259, 934-941.

Tarasov, V.G., Propp, M.V., Propp, L.N., Zhirmunsky, A.V., Namsaraev, B.B., Gorlenko, V.M., Starynin, D.A., 1990. Shallow-water gashydrothermal vents of Ushishir Volcano and the ecosystem of Kraternaya Bight (The Kurile Islands). Mar. Ecol. 11, 1-23.

Thiermann, F., Akoumanianaki, I., Hughes, J.A., Giere, O., 1997. Benthic fauna of a shallow-water gaseohydrothermal vent area in the Aegean Sea (Milos, Greece). Marine Biology 128, 149-159.

Tengberg, A., De Bovee, F., Hall, P., Berelson, W., Chadwick, D., Ciceri, G., Crassous, P., Devol, A., Emerson, S., Gage, J., Glud, R., Graziotini, F., Gundersen, J., Hammond, D., Helder, W., Hinga, K., Holby, O., Jahnke, R., Khripounoff, A., Liebermann, S., Nuppenau, V., Pfannkuche, O., reimers, C., Rowe, G., Sahami, A., Sayles, F., Schurter, M. Smallmann, D., Wehrli, B., De Wilde, P., 1995. Benthic chamber and profiling landers in oceanography - A review of design, technical solutions and functioning. Prog. Oceanog. 35, 253-294.

Thamdrup, B., Canfield, D.E., 1996. Pathways of carbon oxidation in continental margin sediments off central Chile. Limnol. Oceanogr. 41(8), 1629-1650.

Thamdrup, B, Canfield, D., Ferdelman, T., Glud, R.N., Gundersen, J.K., 1996. A biogeochemical survey of the anoxic basin Golfo Dulche, Costa Rica. *Rev. Biol. Trop.* 44, 19-33.

Thomas, R.C., 1978. Ion-sensitive intracellular microelectrodes, how to make and use them. Academic Press.

Turley, C.M., Lochte, K., Patterson, D.J., 1988. A barophilic flagellate isolated from 4500 m in the mid-North Atlantic. Deep-Sea Research 35, 1079-1092.

Ullmann, W.J., Aller, R.C., 1982. Diffusion coefficients in nearshore marine sediments. Limnol. Oceanogr. 27(3), 552-556.

Varnavas, S.P., 1989. Submarine hydrothermal metallogenesis associated with the collision of two plates: The Southern Aegean Sea region. Geochim et Cosmochim. Acta 53, 43-57.

Varnavas, S.P., Cronan, D.S., 1991. Hydrothermal metallogenic processes off the islands of Nisiros and Kos in the Hellenic Volcanic Arc. Marine Geology 99, 109-133.

Von Damn, K.L., Edmond, J.M., Grant, B., Measures, C.I., Walden, B., Weiss, R.F., 1985. Chemistry of hydrothermal solutions at 21°N East Pacific Rise. Geochim. Cosmochim. Acta 49, 2220-2221.

Van Capellen, P., Wang, Y., 1996. Cycling of iron and manganese in surface sediments: a general theory for the coupeld transport and reaction of carbon, oxygen, nitrogen, sulfur, iron and manganese. Amer. J. Sci. 296, 197-243.

Van Den Heuvel, J.C., De Beer, D., Cronenberg, C.C.H., 1992. Microelectrodes: A versatile tool in biofilm research. In: Melo, L.F. et al. (Ed.), Biofilms - Science and Technology. Kluwer, The Netherlands, pp. 631-644.

VanHoudt, P., Lewandowski, Z., Little, B., 1992. Iridium oxide pH microelectrode. Biotechnology and Bioengineering 40, 601-608.

Walsh, J.J., 1991. Importance of continental margins in the marine biogeochemical cycling of carbon and nitrogen. Geochimica et Cosmochimica Acta 52, 1557-1569.

Walsh, J., Rowe, G.T., Iverson, R.L., McRoy, C.P., 1981. Biological export of shelf carbon: a neglected sink of the global CO_2 cycle. Nature 291, 196-201.

Walter, L., Morse, J.W., 1985. The dissolution kinetics of shallow marine carbonate in seawater: A laboratory study. Geochimica et Cosmochimica Acta 49, 1503-1513.

Wefer, G., Fischer, G., 1993. Seasonal patterns of vertical patical flux in equatorial and costal upwelling areas of the eastern Atlantic. Deep-Sea Research I 40(No. 8), 1613-1645.

Weiss, R.F., 1974. Carbon dioxide in water and seawater: the solubility of non-ideal gas. Marine Chemistry 2, 203-215Wolfbeis, O.S., 1991. Fiber Optic Chemical Sensors and Biosensors. CRC Press, Boca Raton.

Wenzhöfer, F., Holby, O., Kohls, O., subm. Deep penetrating oxygen profiles measured *in situ* by oxygen optodes. Deep Sea Research.

Westcott, C.C., 1978. pH Measurements. Academic press, San Diego.

Westrich, J.T., 1983. The consequences and controls of bacterial sulfate reduction in marine sediments. Ph.D., Yale University, New Haven, Connecticut.

Westrich, J.T., Berner, R.A., 1988. The effect of temperature on rates of sulfate reduction in marine sediments. *Geomicrobiology Journal* 6, 99-117.

Winterhalter, B., Flodén, T., Ignatius, H., Axberg, S., Niemistö, L., 1981. Geology of the Baltic Sea. In: Voipio, A. (Ed.), The Baltic Sea. Elsevier, Amsterdam, pp 1-122.

Wolfbeis, O.S., 1991. Fiber Optic Chemical Sensors and Biosensors. CRC Press, Boca Raton.

Wollast, R., Mackenzie, F., Chou, L., 1993. Interactions of C, N, P, and S in Biogeochemical Cycles. NATO Series, Vol. 4, Springer Verlag, Heidelberg Berlin.

Wollast, R., Mackenzie, F.T., Chou, L., 1990. Interactions of C, N, P, and S in Biogeochemical cycles and Global Change. NATO Series, Vol. 4, Springer Verlag, Berlin Heidelberg.

Yayanos, A.A., Dietz, A.S., 1982. Thermal inactivation of a deep-sea barophilic bacterium, isolate CNPT-3. Applied and Environmental Biology 43, 1481-1489.

Zhao P., Cai, W.-J., 1997. An improved potentiometric pCO_2 microelectrode. Analytical Chemistry 69, 5052-5058.

Danksagung

Ich möchte mich bei Herrn Prof. Dr. Bo B. Jørgensen und Herrn Prof. Dr. Horst D. Schulz recht herzlich für die Vergabe der vorliegenden Dissertation und deren Begutachtung bedanken. Die finanzielle Unterstützung sowohl meiner Stelle als auch zum Bau des Landers erfolgte durch die DFG, im Rahmen des Sonderforschungsbereiches 261 "Der Südatlantik im Spätquartär: Rekonstruktion von Stoffhaushalt und Stromsystemen".

Meine Untersuchungen wären ohne den unermüdlichen Bau von Sensoren (die ich dann oftmals im Feldeinsatz zerbrochen habe) durch Gaby, Anja und Vera nicht möglich gewesen, und daher gilt Ihnen mein besonderer Dank. Ebenso möchte ich mich bei unseren beiden Lander-Technikern Stephan und Axel bedanken, die mich bei meiner Arbeit am Lander und den Fahrtvorbereitungen jederzeit unterstützt haben. Georg und Gerd möchte ich ebenfalls danken für die gute Zusammenarbeit bei Bau und Reparatur von Landerteilen. Mein spezieller Dank gilt Volker für die vielen Arbeiten und Modifikationen an den Lander-Elektroniken.

Bei Ola, Ronnie, Susan und Ursula als direkte Mitglieder der Landergruppe möchte ich mich bedanken für die immer währende Bereitschaft zur wissenschaftlichen Diskussion. Dies gilt besonders für Ola und Ronnie, die während der Endphase, trotz räumlicher Distanz immer Zeit zur Diskussion hatten. Ein besonderer Dank gilt Susan, da sie die Aufgabe übernommen hatte, die Manuskripte auf gutes Englisch zu überprüfen. Bedanken möchten mich auch bei allen Mitgliedern der Arbeitsgruppe Mikrosensoren, besonders jedoch bei Eric, Oliver und Gerhard für die zahlreiche Unterstützung bei der Anpassung der Optoden an die Lander. Mein Dank gilt ebenso den Mitarbeitern der Arbeitsgruppe Geochemie im Fachbereich Geologie der Universität Bremen Matthias Zabel, Christian Hensen, Sabine Kasten, Martin Kölling sowie Matthias Adler und allen anderen Mitarbeitern, die immer ein offenes Ohr für Fragen hatten.

Für das gute Arbeitsklima und die stetige Hilfsbereitschaft nicht nur die Arbeit betreffend möchte ich mich bei meinen Doktorandenkollegen und Freunden Wolfgang und Andreas ganz herzlich bedanken. Ich glaube wir haben alle eine ereignisreiche Zeit durchlebt.

Bei meiner Freundin Anita möchte ich mich für die Unterstützung und das Verständnis, auch in etwas schwierigeren Zeiten, recht herzlich bedanken. Zu guter letzt gilt mein Dank meinen Eltern, die mich jederzeit in all meinen Entscheidungen unterstützt haben.

Publications of this series:

No. 1	**Wefer, G., E. Suess and cruise participants** Bericht über die POLARSTERN-Fahrt ANT IV/2, Rio de Janeiro - Punta Arenas, 6.11. - 1.12.1985. 60 pages, Bremen, 1986.
No. 2	**Hoffmann, G.** Holozänstratigraphie und Küstenlinienverlagerung an der andalusischen Mittelmeerküste. 173 pages, Bremen, 1988. (out of print)
No. 3	**Wefer, G. and cruise participants** Bericht über die METEOR-Fahrt M 6/6, Libreville - Las Palmas, 18.2. - 23.3.1988. 97 pages, Bremen, 1988.
No. 4	**Wefer, G., G.F. Lutze, T.J. Müller, O. Pfannkuche, W. Schenke, G. Siedler, W. Zenk** Kurzbericht über die METEOR-Expedition No. 6, Hamburg - Hamburg, 28.10.1987 - 19.5.1988. 29 pages, Bremen, 1988. (out of print)
No. 5	**Fischer, G.** Stabile Kohlenstoff-Isotope in partikulärer organischer Substanz aus dem Südpolarmeer (Atlantischer Sektor). 161 pages, Bremen, 1989.
No. 6	**Berger, W.H. and G. Wefer** Partikelfluß und Kohlenstoffkreislauf im Ozean. Bericht und Kurzfassungen über den Workshop vom 3.-4. Juli 1989 in Bremen. 57 pages, Bremen, 1989.
No. 7	**Wefer, G. and cruise participants** Bericht über die METEOR - Fahrt M 9/4, Dakar - Santa Cruz, 19.2. - 16.3.1989. 103 pages, Bremen, 1989.
No. 8	**Kölling, M.** Modellierung geochemischer Prozesse im Sickerwasser und Grundwasser. 135 pages, Bremen, 1990.
No. 9	**Heinze, P.-M.** Das Auftriebsgeschehen vor Peru im Spätquartär. 204 pages, Bremen, 1990. (out of print)
No. 10	**Willems, H., G. Wefer, M. Rinski, B. Donner, H.-J. Bellmann, L. Eißmann, A. Müller, B.W. Flemming, H.-C. Höfle, J. Merkt, H. Streif, G. Hertweck, H. Kuntze, J. Schwaar, W. Schäfer, M.-G. Schulz, F. Grube, B. Menke** Beiträge zur Geologie und Paläontologie Norddeutschlands: Exkursionsführer. 202 pages, Bremen, 1990.
No. 11	**Wefer, G. and cruise participants** Bericht über die METEOR-Fahrt M 12/1, Kapstadt - Funchal, 13.3.1990 - 14.4.1990. 66 pages, Bremen, 1990.
No. 12	**Dahmke, A., H.D. Schulz, A. Kölling, F. Kracht, A. Lücke** Schwermetallspuren und geochemische Gleichgewichte zwischen Porenlösung und Sediment im Wesermündungsgebiet. BMFT-Projekt MFU 0562, Abschlußbericht. 121 pages, Bremen, 1991.
No. 13	**Rostek, F.** Physikalische Strukturen von Tiefseesedimenten des Südatlantiks und ihre Erfassung in Echolotregistrierungen. 209 pages, Bremen, 1991.
No. 14	**Baumann, M.** Die Ablagerung von Tschernobyl-Radiocäsium in der Norwegischen See und in der Nordsee. 133 pages, Bremen, 1991. (out of print)
No. 15	**Kölling, A.** Frühdiagenetische Prozesse und Stoff-Flüsse in marinen und ästuarinen Sedimenten. 140 pages, Bremen, 1991.
No. 16	**SFB 261 (ed.)** 1. Kolloquium des Sonderforschungsbereichs 261 der Universität Bremen (14.Juni 1991): Der Südatlantik im Spätquartär: Rekonstruktion von Stoffhaushalt und Stromsystemen. Kurzfassungen der Vorträge und Poster. 66 pages, Bremen, 1991.
No. 17	**Pätzold, J. and cruise participants** Bericht und erste Ergebnisse über die METEOR-Fahrt M 15/2, Rio de Janeiro - Vitoria, 18.1. - 7.2.1991. 46 pages, Bremen, 1993.
No. 18	**Wefer, G. and cruise participants** Bericht und erste Ergebnisse über die METEOR-Fahrt M 16/1, Pointe Noire - Recife, 27.3. - 25.4.1991. 120 pages, Bremen, 1991.
No. 19	**Schulz, H.D. and cruise participants** Bericht und erste Ergebnisse über die METEOR-Fahrt M 16/2, Recife - Belem, 28.4. - 20.5.1991. 149 pages, Bremen, 1991.

No. 20 **Berner, H.**
Mechanismen der Sedimentbildung in der Fram-Straße, im Arktischen Ozean und in der Norwegischen See. 167 pages, Bremen, 1991.

No. 21 **Schneider, R.**
Spätquartäre Produktivitätsänderungen im östlichen Angola-Becken: Reaktion auf Variationen im Passat-Monsun-Windsystem und in der Advektion des Benguela-Küstenstroms. 198 pages, Bremen, 1991. (out of print)

No. 22 **Hebbeln, D.**
Spätquartäre Stratigraphie und Paläozeanographie in der Fram-Straße. 174 pages, Bremen, 1991.

No. 23 **Lücke, A.**
Umsetzungsprozesse organischer Substanz während der Frühdiagenese in ästuarinen Sedimenten. 137 pages, Bremen, 1991.

No. 24 **Wefer, G. and cruise participants**
Bericht und erste Ergebnisse der METEOR-Fahrt M 20/1, Bremen - Abidjan, 18.11.- 22.12.1991. 74 pages, Bremen, 1992.

No. 25 **Schulz, H.D. and cruise participants**
Bericht und erste Ergebnisse der METEOR-Fahrt M 20/2, Abidjan - Dakar, 27.12.1991 - 3.2.1992. 173 pages, Bremen, 1992.

No. 26 **Gingele, F.**
Zur klimaabhängigen Bildung biogener und terrigener Sedimente und ihrer Veränderung durch die Frühdiagenese im zentralen und östlichen Südatlantik. 202 pages, Bremen, 1992.

No. 27 **Bickert, T.**
Rekonstruktion der spätquartären Bodenwasserzirkulation im östlichen Südatlantik über stabile Isotope benthischer Foraminiferen. 205 pages, Bremen, 1992. (out of print)

No. 28 **Schmidt, H.**
Der Benguela-Strom im Bereich des Walfisch-Rückens im Spätquartär. 172 pages, Bremen, 1992.

No. 29 **Meinecke, G.**
Spätquartäre Oberflächenwassertemperaturen im östlichen äquatorialen Atlantik. 181 pages, Bremen, 1992.

No. 30 **Bathmann, U., U. Bleil, A. Dahmke, P. Müller, A. Nehrkorn, E.-M. Nöthig, M. Olesch, J. Pätzold, H.D. Schulz, V. Smetacek, V. Spieß, G. Wefer, H. Willems**
Bericht des Graduierten Kollegs. Stoff-Flüsse in marinen Geosystemen. Berichtszeitraum Oktober 1990 - Dezember 1992. 396 pages, Bremen, 1992.

No. 31 **Damm, E.**
Frühdiagenetische Verteilung von Schwermetallen in Schlicksedimenten der westlichen Ostsee. 115 pages, Bremen, 1992.

No. 32 **Antia, E.E.**
Sedimentology, Morphodynamics and Facies Association of a mesotidal Barrier Island Shoreface (Spiekeroog, Southern North Sea). 370 pages, Bremen, 1993.

No. 33 **Duinker, J. and G. Wefer (ed.)**
Bericht über den 1. JGOFS-Workshop. 1./2. Dezember 1992 in Bremen. 83 pages, Bremen, 1993.

No. 34 **Kasten, S.**
Die Verteilung von Schwermetallen in den Sedimenten eines stadtbremischen Hafenbeckens. 103 pages, Bremen, 1993.

No. 35 **Spieß, V.**
Digitale Sedimentographie. Neue Wege zu einer hochauflösenden Akustostratigraphie. 199 pages, Bremen, 1993.

No. 36 **Schinzel, U.**
Laborversuche zu frühdiagenetischen Reaktionen von Eisen (III) - Oxidhydraten in marinen Sedimenten.189 pages, Bremen, 1993.

No. 37 **Sieger, R.**
CoTAM - ein Modell zur Modellierung des Schwermetalltransports in Grundwasserleitern. 56 pages, Bremen, 1993. (out of print)

No. 38 **Willems, H. (ed.)**
Geoscientific Investigations in the Tethyan Himalayas. 183 pages, Bremen, 1993.

No. 39 **Hamer, K.**
Entwicklung von Laborversuchen als Grundlage für die Modellierung des Transportverhaltens von Arsenat, Blei, Cadmium und Kupfer in wassergesättigten Säulen. 147 pages, Bremen, 1993.

No. 40 **Sieger, R.**
Modellierung des Stofftransports in porösen Medien unter Ankopplung kinetisch gesteuerter Sorptions- und Redoxprozesse sowie thermischer Gleichgewichte. 158 pages, Bremen, 1993.

No. 41 **Thießen, W.**
Magnetische Eigenschaften von Sedimenten des östlichen Südatlantiks und ihre paläozeanographische Relevanz. 170 pages, Bremen, 1993.

No. 42 **Spieß, V. and cruise participants**
Report and preliminary results of METEOR-Cruise M 23/1, Kapstadt - Rio de Janeiro, 4.-25.2.1993. 139 pages, Bremen, 1994.

No. 43 **Bleil, U. and cruise participants**
Report and preliminary results of METEOR-Cruise M 23/2, Rio de Janeiro - Recife, 27.2.-19.3.1993 133 pages, Bremen, 1994.

No. 44 **Wefer, G. and cruise participants**
Report and preliminary results of METEOR-Cruise M 23/3, Recife - Las Palmas, 21.3. - 12.4.1993 71 pages, Bremen, 1994.

No. 45 **Giese, M. and G. Wefer (ed.)**
Bericht über den 2. JGOFS-Workshop. 18../19. November 1993 in Bremen.
93 pages, Bremen, 1994.

No. 46 **Balzer, W. and cruise participants**
Report and preliminary results of METEOR-Cruise M 22/1, Hamburg - Recife, 22.9. - 21.10.1992. 24 pages, Bremen, 1994.

No. 47 **Stax, R.**
Zyklische Sedimentation von organischem Kohlenstoff in der Japan See: Anzeiger für Änderungen von Paläoozeanographie und Paläoklima im Spätkänozoikum.
150 pages, Bremen, 1994.

No. 48 **Skowronek, F.**
Frühdiagenetische Stoff-Flüsse gelöster Schwermetalle an der Oberfläche von Sedimenten des Weser Ästuares. 107 pages, Bremen, 1994.

No. 49 **Dersch-Hansmann, M.**
Zur Klimaentwicklung in Ostasien während der letzten 5 Millionen Jahre:
Terrigener Sedimenteintrag in die Japan See (ODP Ausfahrt 128). 149 pages, Bremen, 1994.

No. 50 **Zabel, M.**
Frühdiagenetische Stoff-Flüsse in Oberflächen-Sedimenten des äquatorialen und östlichen Südatlantik. 129 pages, Bremen, 1994.

No. 51 **Bleil, U. and cruise participants**
Report and preliminary results of SONNE-Cruise SO 86, Buenos Aires - Capetown, 22.4. - 31.5.93 116 pages, Bremen, 1994.

No. 52 **Symposium: The South Atlantic: Present and Past Circulation.**
Bremen, Germany, 15 - 19 August 1994. Abstracts. 167 pages, Bremen, 1994.

No. 53 **Kretzmann, U.B.**
^{57}Fe-Mössbauer-Spektroskopie an Sedimenten - Möglichkeiten und Grenzen.
183 pages, Bremen, 1994.

No. 54 **Bachmann, M.**
Die Karbonatrampe von Organyà im oberen Oberapt und unteren Unteralb (NE-Spanien, Prov. Lerida): Fazies, Zyklo- und Sequenzstratigraphie. 147 pages, Bremen, 1994. (out of print)

No. 55 **Kemle-von Mücke, S.**
Oberflächenwasserstruktur und -zirkulation des Südostatlantiks im Spätquartär.
151 pages, Bremen, 1994.

No. 56 **Petermann, H.**
Magnetotaktische Bakterien und ihre Magnetosome in Oberflächensedimenten des Südatlantiks.
134 pages, Bremen, 1994.

No. 57 **Mulitza, S.**
Spätquartäre Variationen der oberflächennahen Hydrographie im westlichen äquatorialen Atlantik.
97 pages, Bremen, 1994.

No. 58 **Segl, M. and cruise participants**
Report and preliminary results of METEOR-Cruise M 29/1, Buenos-Aires - Montevideo, 17.6. - 13.7.1994
94 pages, Bremen, 1994.

No. 59 **Bleil, U. and cruise participants**
Report and preliminary results of METEOR-Cruise M 29/2, Montevideo - Rio de Janiero 15.7. - 8.8.1994. 153 pages, Bremen, 1994.

No. 60 **Henrich, R. and cruise participants**
Report and preliminary results of METEOR-Cruise M 29/3, Rio de Janeiro - Las Palmas 11.8. - 5.9.1994. Bremen, 1994 (not published). (out of print)

No. 61 **Sagemann, J.**
Saisonale Variationen von Porenwasserprofilen, Nährstoff-Flüssen und Reaktionen in intertidalen Sedimenten des Weser-Ästuars. 110 pages, Bremen, 1994. (out of print)

No. 62 **Giese, M. and G. Wefer**
Bericht über den 3. JGOFS-Workshop. 5./6. Dezember 1994 in Bremen.
84 pages, Bremen, 1995.

No. 63 **Mann, U.**
Genese kretazischer Schwarzschiefer in Kolumbien: Globale vs. regionale/lokale Prozesse.
153 pages, Bremen, 1995. (out of print)

No. 64 **Willems, H., Wan X., Yin J., Dongdui L., Liu G., S. Dürr, K.-U. Gräfe**
The Mesozoic development of the N-Indian passive margin and of the Xigaze Forearc Basin in southern Tibet, China. – Excursion Guide to IGCP 362 Working-Group Meeting "Integrated Stratigraphy". 113 pages, Bremen, 1995. (out of print)

No. 65 **Hünken, U.**
Liefergebiets - Charakterisierung proterozoischer Goldseifen in Ghana anhand von Fluideinschluß - Untersuchungen. 270 pages, Bremen, 1995.

No. 66 **Nyandwi, N.**
The Nature of the Sediment Distribution Patterns in ther Spiekeroog Backbarrier Area, the East Frisian Islands. 162 pages, Bremen, 1995.

No. 67 **Isenbeck-Schröter, M.**
Transportverhalten von Schwermetallkationen und Oxoanionen in wassergesättigten Sanden. - Laborversuche in Säulen und ihre Modellierung -. 182 pages, Bremen, 1995.

No. 68 **Hebbeln, D. and cruise participants**
Report and preliminary results of SONNE-Cruise SO 102, Valparaiso - Valparaiso, 95
134 pages, Bremen, 1995.

No. 69 **Willems, H. (Sprecher), U.Bathmann, U. Bleil, T. v. Dobeneck, K. Herterich, B.B. Jorgensen, E.-M. Nöthig, M. Olesch, J. Pätzold, H.D. Schulz, V. Smetacek, V. Speiß. G. Wefer**
Bericht des Graduierten-Kollegs Stoff-Flüsse in marine Geosystemen.
Berichtszeitraum Januar 1993 - Dezember 1995.
45 & 468 pages, Bremen, 1995.

No. 70 **Giese, M. and G. Wefer**
Bericht über den 4. JGOFS-Workshop. 20./21. November 1995 in Bremen. 60 pages, Bremen, 1996. (out of print)

No. 71 **Meggers, H.**
Pliozän-quartäre Karbonatsedimentation und Paläozeanographie des Nordatlantiks und des Europäischen Nordmeeres - Hinweise aus planktischen Foraminiferengemeinschaften.
143 pages, Bremen, 1996. (out of print)

No. 72 **Teske, A.**
Phylogenetische und ökologische Untersuchungen an Bakterien des oxidativen und reduktiven marinen Schwefelkreislaufs mittels ribosomaler RNA. 220 pages, Bremen, 1996. (out of print)

No. 73 **Andersen, N.**
Biogeochemische Charakterisierung von Sinkstoffen und Sedimenten aus ostatlantischen Produktions-Systemen mit Hilfe von Biomarkern. 215 pages, Bremen, 1996.

No. 74 **Treppke, U.**
Saisonalität im Diatomeen- und Silikoflagellatenfluß im östlichen tropischen und subtropischen Atlantik. 200 pages, Bremen, 1996.

No. 75 **Schüring, J.**
Die Verwendung von Steinkohlebergematerialien im Deponiebau im Hinblick auf die Pyritverwitterung und die Eignung als geochemische Barriere. 110 pages, Bremen, 1996.

No. 76 **Pätzold, J. and cruise participants**
Report and preliminary results of VICTOR HENSEN cruise JOPS II, Leg 6,
Fortaleza - Recife, 10.3. - 26.3. 1995 and Leg 8, Vitoria - Vitoria, 10.4. - 23.4.1995.
87 pages, Bremen, 1996.

No. 77 **Bleil, U. and cruise participants**
Report and preliminary results of METEOR-Cruise M 34/1, Cape Town - Walvis Bay, 3.-26.1.1996.
129 pages, Bremen, 1996.

No. 78 **Schulz, H.D. and cruise participants**
Report and preliminary results of METEOR-Cruise M 34/2, Walvis Bay - Walvis Bay, 29.1.-18.2.96
133 pages, Bremen, 1996.

No. 79 **Wefer, G. and cruise participants**
Report and preliminary results of METEOR-Cruise M 34/3, Walvis Bay - Recife, 21.2.-17.3.1996.
168 pages, Bremen, 1996.

No. 80 **Fischer, G. and cruise participants**
Report and preliminary results of METEOR-Cruise M 34/4, Recife - Bridgetown, 19.3.-15.4.1996. 105 pages, Bremen, 1996.

No. 81 **Kulbrok, F.**
Biostratigraphie, Fazies und Sequenzstratigraphie einer Karbonatrampe in den Schichten der Oberkreide und des Alttertiärs Nordost-Ägyptens (Eastern Desert, N'Golf von Suez, Sinai). 153 pages, Bremen, 1996.

No. 82 **Kasten, S.**
Early Diagenetic Metal Enrichments in Marine Sediments as Documents of Nonsteady-State Depositional Conditions. Bremen, 1996.

No. 83 **Holmes, M.E.**
Reconstruction of Surface Ocean Nitrate Utilization in the Southeast Atlantic Ocean Based on Stable Nitrogen Isotopes. 113 pages, Bremen, 1996.

No. 84 **Rühlemann, C.**
Akkumulation von Carbonat und organischem Kohlenstoff im tropischen Atlantik: Spätquartäre Produktivitäts-Variationen und ihre Steuerungsmechanismen. 139 pages, Bremen, 1996.

No. 85 **Ratmeyer, V.**
Untersuchungen zum Eintrag und Transport lithogener und organischer partikulärer Substanz im östlichen subtropischen Nordatlantik. 154 pages, Bremen, 1996.

No. 86 **Cepek, M.**
Zeitliche und räumliche Variationen von Coccolithophoriden-Gemeinschaften im subtropischen Ost-Atlantik: Untersuchungen an Plankton, Sinkstoffen und Sedimenten. 156 pages, Bremen, 1996.

No. 87 **Otto, S.**
Die Bedeutung von gelöstem organischen Kohlenstoff (DOC) für den Kohlenstoffffluß im Ozean. 150 pages, Bremen, 1996.

No. 88 **Hensen, C.**
Frühdiagenetische Prozesse und Quantifizierung benthischer Stoff-Flüsse in Oberflächensedimenten des Südatlantiks. 132 pages, Bremen, 1996.

No. 89 **Giese, M. and G. Wefer**
Bericht über den 5. JGOFS-Workshop. 27./28. November 1996 in Bremen. 73 pages, Bremen, 1997.

No. 90 **Wefer, G. and cruise participants**
Report and preliminary results of METEOR-Cruise M 37/1, Lisbon - Las Palmas, 4.-23.12.1996. 79 pages, Bremen, 1997.

No. 91 **Isenbeck-Schröter, M., E. Bedbur, M. Kofod, B. König, T. Schramm & G. Mattheß**
Occurrence of Pesticide Residues in Water - Assessment of the Current Situation in Selected EU Countries. 65 pages, Bremen 1997.

No. 92 **Kühn, M.**
Geochemische Folgereaktionen bei der hydrogeothermalen Energiegewinnung. 129 pages, Bremen 1997.

No. 93 **Determann, S. & K. Herterich**
JGOFS-A6 „Daten und Modelle": Sammlung JGOFS-relevanter Modelle in Deutschland. 26 pages, Bremen, 1997.

No. 94 **Fischer, G. and cruise participants**
Report and preliminary results of METEOR-Cruise M 38/1, Las Palmas - Recife, 25.1.-1.3.1997, with Appendix: Core Descriptions from METEOR Cruise M 37/1. Bremen, 1997.

No. 95 **Bleil, U. and cruise participants**
Report and preliminary results of METEOR-Cruise M 38/2, Recife - Las Palmas, 4.3.-14.4.1997. 126 pages, Bremen, 1997.

No. 96 **Neuer, S. and cruise participants**
Report and preliminary results of VICTOR HENSEN-Cruise 96/1. Bremen, 1997.

No. 97 **Villinger, H. and cruise participants**
Fahrtbericht SO 111, 20.8. - 16.9.1996. 115 pages, Bremen, 1997.

No. 98 **Lüning, S.**
Late Cretaceous - Early Tertiary sequence stratigraphy, paleoecology and geodynamics of Eastern Sinai, Egypt. 218 pages, Bremen, 1997.

No. 99 **Haese, R.R.**
Beschreibung und Quantifizierung frühdiagenetischer Reaktionen des Eisens in Sedimenten des Südatlantiks. 118 pages, Bremen, 1997.

No. 100 **Lührte, R. von**
Verwertung von Bremer Baggergut als Material zur Oberflächenabdichtung von Deponien - Geochemisches Langzeitverhalten und Schwermetall-Mobilität (Cd, Cu, Ni, Pb, Zn). Bremen, 1997.

No. 101 **Ebert, M.**
Der Einfluß des Redoxmilieus auf die Mobilität von Chrom im durchströmten Aquifer. 135 pages, Bremen, 1997.

No. 102 **Krögel, F.**
Einfluß von Viskosität und Dichte des Seewassers auf Transport und Ablagerung von Wattsedimenten (Langeooger Rückseitenwatt, südliche Nordsee). 168 pages, Bremen, 1997.

No. 103 **Kerntopf, B.**
Dinoflagellate Distribution Patterns and Preservation in the Equatorial Atlantic and Offshore North-West Africa. 137 pages, Bremen, 1997.

No. 104 **Breitzke, M.**
Elastische Wellenausbreitung in marinen Sedimenten - Neue Entwicklungen der Ultraschall Sedimentphysik und Sedimentechographie. 298 pages, Bremen, 1997.

No. 105 **Marchant, M.**
Rezente und spätquartäre Sedimentation planktischer Foraminiferen im Peru-Chile Strom. 115 pages, Bremen, 1997.

No. 106 **Habicht, K.S.**
Sulfur isotope fractionation in marine sediments and bacterial cultures. 125 pages, Bremen, 1997.

No. 107 **Hamer, K., R.v. Lührte, G. Becker, T. Felis, S. Keffel, B. Strotmann, C. Waschkowitz, M. Kölling, M. Isenbeck-Schröter, H.D. Schulz**
Endbericht zum Forschungsvorhaben 060 des Landes Bremen: Baggergut der Hafengruppe Bremen-Stadt: Modelluntersuchungen zur Schwermetallmobilität und Möglichkeiten der Verwertung von Hafenschlick aus Bremischen Häfen. 98 pages, Bremen, 1997.

No. 108 **Greeff, O.W.**
Entwicklung und Erprobung eines benthischen Landersystemes zur *in situ*-Bestimmung von Sulfatreduktionsraten mariner Sedimente. 121 pages, Bremen, 1997.

No. 109 **Pätzold, M. und G. Wefer**
Bericht über den 6. JGOFS-Workshop am 4./5.12.1997 in Bremen. Im Anhang: Publikationen zum deutschen Beitrag zur Joint Global Ocean Flux Study (JGOFS), Stand 1/1998. 122 pages, Bremen, 1998.

No. 110 **Landenberger, H.**
CoTReM, ein Multi-Komponenten Transport- und Reaktions-Modell. 142 pages, Bremen, 1998.

No. 111 **Villinger, H. und Fahrtteilnehmer**
Fahrtbericht SO 124, 4.10. - 16.10.199. 90 pages, Bremen, 1997.

No. 112 **Gietl, R.**
Biostratigraphie und Sedimentationsmuster einer nordostägyptischen Karbonatrampe unter Berücksichtigung der Alveolinen-Faunen. 142 pages, Bremen, 1998.

No. 113 **Ziebis, W.**
The Impact of the Thalassinidean Shrimp *Callianassa truncata* on the Geochemistry of permeable, coastal Sediments. 158 pages, Bremen 1998.

No. 114 **Schulz, H.D. and cruise participants**
Report and preliminary results of METEOR-Cruise M 41/1, Málaga - Libreville, 13.2.-15.3.1998. Bremen, 1998.

No. 115 **Völker, D.J.**
Untersuchungen an strömungsbeeinflußten Sedimentationsmustern im Südozean. Interpretation sedimentechographischer Daten und numerische Modellierung. 152 pages, Bremen, 1998.

No. 116 **Schlünz, B.**
Riverine Organic Carbon Input into the Ocean in Relation to Late Quaternary Climate Change. 136 pages, Bremen, 1998.

No. 117 **Kuhnert, H.**
Aufzeichnug des Klimas vor Westaustralien in stabilen Isotopen in Korallenskeletten. 109 pages, Bremen, 1998.

No. 118 **Kirst, G.**
Rekonstruktion von Oberflächenwassertemperaturen im östlichen Südatlantik anhand von Alkenonen. 130 pages, Bremen, 1998.

No. 119 **Dürkoop, A.**
Der Brasil-Strom im Spätquartär: Rekonstruktion der oberflächennahen Hydrographie während der letzten 400 000 Jahre. 121 pages, Bremen, 1998.

No. 120 **Lamy, F.**
Spätquartäre Variationen des terrigenen Sedimenteintrags entlang des chilenischen Kontinentalhangs als Abbild von Klimavariabilität im Milanković- und Sub-Milanković-Zeitbereich. 141 pages, Bremen, 1998.

No. 121 **Neuer, S. and cruise participants**
Report and preliminary results of POSEIDON-Cruise Pos 237/2, Vigo – Las Palmas, 18.3.-31.3.1998. 39 pages, Bremen, 1998

No. 122 **Romero, O.E.**
Marine planktonic diatoms from the tropical and equatorial Atlantic: temporal flux patterns and the sediment record. 205 pages, Bremen, 1998.

No. 123 **Spiess, V. und Fahrtteilnehmer**
Report and preliminary results of RV SONNE Cruise 125, Cochin – Chittagong, 17.10.-17.11.1997. 128 pages, Bremen, 1998.

No. 124 **Arz, H.W.**
Dokumentation von kurzfristigen Klimaschwankungen des Spätquartärs in Sedimenten des westlichen äquatorialen Atlantiks. 96 pages, Bremen, 1998.

No. 125 **Wolff, T.**
Mixed layer characteristics in the equatorial Atlantic during the late Quaternary as deduced from planktonic foraminifera. 132 pages, Bremen, 1998.

No. 126 **Dittert, N.**
Late Quaternary Planktic Foraminifera Assemblages in the South Atlantic Ocean: Quantitative Determination and Preservational Aspects. 165 pages, Bremen, 1998.

No. 127 **Höll, C.**
Kalkige und organisch-wandige Dinoflagellaten-Zysten in Spätquartären Sedimenten des tropischen Atlantiks und ihre palökologische Auswertbarkeit. 121 pages, Bremen, 1998.

No. 128 **Hencke, J.**
Redoxreaktionen im Grundwasser: Etablierung und Verlagerung von Reaktionsfronten und ihre Bedeutung für die Spurenelement-Mobilität. 122 pages, Bremen 1998.

No. 129 **Pätzold, J. und Fahrtteilnehmer**
Report and preliminary results of METEOR-Cruise M 41/3, Vitoria, Brasilien – Salvador de Bahia, Brasilien, 18.4. - 15.5.1998. Bremen, 1999.

No. 130 **Fischer, G. und Fahrtteilnehmer**
Report and preliminary results of METEOR-Cruise M 41/4, Salvador de Bahia, Brasilien – Las Palmas, Spanien, 18.5. – 13.6.1998. Bremen, 1999.

No. 131 **Schlünz, B. und G. Wefer**
Bericht über den 7. JGOFS-Workshop am 3. und 4.12.1998 in Bremen. Im Anhang: Publikationen zum deutschen Beitrag zur Joint Global Ocean Flux Study (JGOFS), Stand 1/ 1999. 100 pages, Bremen, 1999.

No. 132 **Wefer, G. and cruise participants**
Report and preliminary results of METEOR-Cruise M 42/4, Las Palmas - Las Palmas - Viena do Castelo; 26.09.1998 - 26.10.1998. 104 pages, Bremen, 1999.

No. 133 **Felis, T.**
Climate and ocean variability reconstructed from stable isotope records of modern subtropical corals (Northern Red Sea). 111 pages, Bremen, 1999.

No. 134 **Draschba , S.**
North Atlantic climate variability recorded in reef corals from Bermuda. 108 pages, Bremen, 1999.

No. 135 **Schmieder, F.**
Magnetic Cyclostratigraphy of South Atlantic Sediments. 82 pages, Bremen, 1999.

No. 136 **Rieß, W.**
In situ measurements of respiration and mineralisation processes – Interaction between fauna and geochemical fluxes at active interfaces. 68 pages, Bremen, 1999.

No. 137 **Devey, C.W. and cruise participants**
Report and shipboard results from METEOR-cruise M 41/2, Libreville – Vitoria, 18.3. – 15.4.98. 59 pages, Bremen, 1999.